Advanced Transmission Solutions for High-Data-Rate Wireless Communications

Mohammad-Ali Khalighi

▶ **To cite this version:**

Mohammad-Ali Khalighi. Advanced Transmission Solutions for High-Data-Rate Wireless Communications. Signal and Image processing. Aix-Marseille Université, 2014. tel-02502045

HAL Id: tel-02502045
https://hal.science/tel-02502045

Submitted on 8 Mar 2020

HAL is a multi-disciplinary open access archive for the deposit and dissemination of scientific research documents, whether they are published or not. The documents may come from teaching and research institutions in France or abroad, or from public or private research centers.

L'archive ouverte pluridisciplinaire **HAL**, est destinée au dépôt et à la diffusion de documents scientifiques de niveau recherche, publiés ou non, émanant des établissements d'enseignement et de recherche français ou étrangers, des laboratoires publics ou privés.

AIX-MARSEILLE UNIVERSITÉ

TITRE:

Solutions Avancées de Transmission de Données pour les Communications Sans-fil Haut-débit

Habilitation à Diriger des Recherches

AIX-MARSEILLE UNIVERSITÉ

École Doctorale : Physique et Sciences de la Matière
Mention : Optique, Photonique et Traitement d'Image

Présentée et soutenue publiquement par:

Mohammad-Ali KHALIGHI

le 28 Novembre 2014

JURY :

M. Jean-François DIOURIS	Professeur, Polytech Nantes	Président
Mme. Anne JULIEN-VERGONJANNE	Professeur, ENSIL, Limoges	Rapporteur
M. Alain SIBILLE	Professeur, Télécom ParisTech	Rapporteur
M. Eric Moreau	Professeur, Université de Toulon	Rapporteur
M. Pascal LARZABAL	Professeur, IUT Cachan	Examinateur
M. Zabih GHASSEMLOOY	Professeur, Northumbria University	Examinateur
M. Salah BOURENNANE	Professeur, École Centrale Marseille	Examinateur

ANNEE : 2014

AIX-MARSEILLE UNIVERSITY

TITLE:

Advanced Transmission Solutions for High-Data-Rate Wireless Communications

Accreditation for Research Supervision
AIX-MARSEILLE UNIVERSITY

Doctoral school: Physics and Material Sciences
Discipline: Optics, Photonics and Image Processing

Presented and defended publicly by:

Mohammad-Ali KHALIGHI

on November 28, 2014

COMMITTEE :

Prof. Jean-François DIOURIS	Polytech Nantes	Chairman
Prof. Anne JULIEN-VERGONJANNE	ENSIL, Limoges	Reviewer
Prof. Alain SIBILLE	Télécom ParisTech	Reviewer
Prof. Eric Moreau	Université de Toulon	Reviewer
Prof. Pascal LARZABAL	IUT Cachan	Examiner
Prof. Zabih GHASSEMLOOY	Northumbria University, UK	Examiner
Prof. Salah BOURENNANE	École Centrale Marseille	Examiner

YEAR : 2014

to my family

Acknowledgments

I would like to express my sincere gratitude to the members of the panel for agreeing to take part of the committee and for their evaluation of my work, namely, *Jean-François Diouris, Fary Ghassemlooy*, *Anne Julien-Vergonjanne*, *Pascal Larzabal*, *Eric Moreau*, and *Alain Sibille*.

The principal part of the research works presented in this report have been realized in Institut Fresnel, for which I wish to thank the former and current lab directors. I would also express my appreciation to the head of my research team, *Salah Bourennane*, for all his support during the past years, for giving me the liberty to work on the research topics I have been interested in, and for encouraging me all along these years.

I am also very grateful to the people with whom I have been working during my PhD thesis and my post-docs, especially the late *Geneviève Jourdain*, *Karim Abed-Meraim*, *Joseph Jean Boutros*, and *Jean-François Hélard*. It has been a great pleasure working with them, from whom I learned a lot and to whom I owe so much. Also, I should not forget the immense support of my previous advisors in LIS lab (currently Gipsa-lab), *Jean-Marc Chassery* and *Christian Jutten*, as well as that of LTCI lab, *Henri Maître*. I would like also to acknowledge my former advisors at Sharif University for their encouragements and support, in particular, *Mohammad-Mehdi Nayebi*, the late *Kasra Barkeshli*, and *Forouhar Farzaneh*.

My sincere thanks go also to the French COST office for their confidence. Undoubtedly, my involvement in the Opticwise COST Action IC1101 opened to me many doors for fruitful collaborations and discussions with the top-level European laboratories and researchers. I should at the same time thank my COST colleagues with whom I could have the opportunity to collaborate and exchange knowledge: *Murat Uysal*, *Fary Ghassemlooy*, *Stanislav Zvanovec*, *Bruno Fracasso*, *Anne Julien-Vergonjeanne*, *Yahya Kemal Baykal*, *Mike Wolf*, *George Karagiannidis*, and many others. My special thanks go to *Fary Ghassemlooy* and the other members of the OCRG lab at Northumbria University with whom I have had the pleasure to collaborate.

Obviously, the contribution of my PhD and master students has been very decisive in my career. In particular, I would cordially acknowledge my past and current PhD students: *Fang Xu*, *Yi Zhang*, *Chadi Gabriel*, *Guowei Yang*, *Shihe Long*, *Tasnim Hamza*, and *Norhanis Aida Nor*, as well as the PhD students of the OCRG lab that I had the pleasure to work with, *It-Ee Lee*, *Dehao Wu*, and *Mojtaba Mansour Abadi*.

I would like also to mention my appreciation to all colleagues I have been delighted to work with during the past years: *Jean-Marc Brossier*, *Kosai Raoof*, *Laurent Ros*, *Eric Simon*, *Noah Schwartz*, *Frédéric Chazallet*, *Pierre Léon*, *Vincent Rigaud*, *Anne Julien-Vergonjanne*, *Bruno Fracasso*, *Sajad Sadough*, *Steve Hranilovic*, *Kostas Yiannopoulos*, *Kostas Peppas*, *Hoa Le Minh*, and *Theodoros Tsiftsis*. I am also very grateful to my IFREMER colleagues for their availability and for the countless help and support and fruitful discussions. My particular thanks also go to Institut Fresnel colleagues, in particular: *Hassan Akhouayri*, *Anabela Dasilva*, *Philippe Réfrégier*, *Michel Lequime*, *Frédéric Lemarquis*, *Fabien Lemarchand*, and *Jérôme Wenger*, without forgetting *Alexan-*

dre Hatchikian and *Jean Cayzac* and many other colleagues, as well as my friends of GSM and Phyti teams: *Mouloud Adel*, *Caroline Fossati*, *Stéphane Derrode*, *Julien Marot*, *Nicolas Bertaux*, and *Muriel Roche*, for providing a calming and enjoyable work environment.

I should not forget my ECM colleagues, especially my director, *Férédic Fotiadu*, for his support for the preparation of my HDR.

Lastly, I am deeply indebted to my family for their constant support and encouragement and their understanding of my frequent unavailabilities during the past years, as well as to my parents for the sacrifices they have made for me. And to One who made this all possible, I give my ultimate thanks.

Table of contents

List of Notations

$\mathrm{E}\{.\}$	Expected value
$(.)^*$	Complex conjugate
$(.)^t$	Vector or matrix transpose
$(.)^\dagger$	Vector or matrix Hermitian transpose
$\det[.]$	Matrix determinant
$\prod$	Interleaving operator
C_{erg}	Ergodic capacity
C_{out}	Outage capacity
E_b	Averaged received energy per information bit
$\boldsymbol{I}_R$	Identity matrix of dimension $R \times R$
$K_i(.)$	Modified Bessel function of second kind and i-order
N_0	Noise unilateral power spectral density
P_{out}	Outage probability
r_0	Fried parameter
λ	Optical wavelength
L	Link span
ρ_0	Spatial coherence radius

List of Acronyms

4MORE project	4G MC-CDMA Multiple Antenna System On Chip for Radio Enhancements
5G PPP	5th-Generation (telecommunicaion systems) Public and Private Partnership
ADC	Analog-to-Digital Converter
AF	Amplify-and-Forward
APD	Avalanche Photo-Diode
ARQ	Automatic Repeat reQuest
AUV	Automated Underwater Vehicle
AWG	Arbitrary Waveform Generator
AWGN	Additive White Gaussian Noise
BCID	Binary Convolutional encoding with Iterative Detection
BER	Bit-Error-Rate
BICM	Bit-Interleaved Coded Modulation
BLAST	Bell Labs Layered Space-Time Architecture
BPF	Band-Pass Filter
CAP	Carrier-less Amplitude and Phase modulation
CFAR	Constant False Alarm Rate
CIR	Channel Impulse Response
CNRS	Centre National de la Recherche Scientifique
CSI	Channel State Information
DAC	Digital-to-Analog Converter
DD	Decision Directed
DEA	Diplôme des Études Approfondies (MSc equivalent)
DemAF	Demodulate-And-Forward
DetF	Detect-and-Forward
DF	Decode-and-Forward
DPIM	Digital Pulse Interval Modulation
DSTBC	Distributed Space-Time Block Coding
ECM school	École Centrale Marseille
EGC	Equal-Gain Combining
EM	Expectation Maximization
ENSTA	École Nationale Supérieure des Techniques Avancées
ESM	Electronic Support Measures

EXIT	EXtrinsic Information Transfer
FSO	Free Space Optics
FOV	Field Of View
Gbps	Giga-bits per second
GIPSA-lab	laboratoire Grenoble Images Parole Signal Automatique
GLD	Golden ST code
GS	Guard Slot
GSM team	Groupe des Signaux Multidimensionnel
HARQ	Hybrid ARQ
ICP lab	Institut de la Communication Parlée
IEMN lab	Institut d'Electronique, Microélectronique et de Nanotechnologies
IETR lab	Institut d'Électronique et de Télécommunications de Rennes
IFREMER institute	Institut Français de Recherche pour l'Exploitation de la MER
IM/DD	Intensity-Modulation Direct-Detection
INPG	Institut National Polytechnique de Grenoble
IR	Infra-Red
IOP	Inherent Optical Properties
ISI	Inter-Symbol Interference
LAN	Local Area Network
LD	Laser Diode
LDPC	Low-Density Parity Check code
LED	Light Emitting Diode
LIS lab	Laboratoire des Images et des Signaux
LLR	Log-Likelihood Ratio
LOHM	Liaison Optique Haut débit avec un élément Mobile
LOS	Line Of Sight
LPF	Low-Pass Filter
LS	Least Squares
LSS lab	Laboratoire des Signaux et des Systèmes
LTCI lab	Laboratoire Traitement et Communication de l'Information
MAC	Media Access Control
MAP	Maximum *A Posteriori*
Mbps	Mega-bits per second
MGF	Moment Generating Function
MI	Mutual Information
MIMO	Multiple-Input Multiple-Output
MISO	Multiple-Input Single-Output
ML	Maximum Likelihood
MLD	Maximum Likelihood Detection
MMSE	Minimum Mean-Square-Error

MMW	Milli-Meter Wave
MPPM	Multipulse PPM
MRC	Maximal-Ratio Combining
NRNSC	Non-Recursive Non-Systematic Convolutional
NRZ	Non Return-to-Zero
OCRG lab	Optical Communication Research Group
OFDM	Orthogonal Frequency Division Multiplexing
OLED	Organic LED
ONERA institute	Office National d'Études et de Recherches Aérospatiales
OOK	On-Off Keying
OP	Overlay Pilots
OSM	Optical Spatial Modulation
OSTBC	Orthogonal ST Block Code
OWC	Optical Wireless Communication
PAM	Pulse Amplitude Modulation
PAPR	Peak-to-Average Power Ratio
PD	Photo-Diode
PDF	Probability Density Function
PHY	PHYsical layer
PIC	Parallel Interference Cancelation
PO	Pilot Only
PPM	Pulse Position Modulation
PSAM	Pilot Symbol-Assisted Modulation
PU	Primary User
PWM	Pulse Width Modulation
QoS	Quality of Service
R&D	Research and Development
RC	Repetition Coding
RF	Radio-Frequency
RGB	Red-Green-Blue
RIN	Relative Intensity Noise
RMS	Root Mean Square
RoF	Radio over Fiber
RoFSO	Radio over Free Space Optics
ROV	Remotely Operated Vehicle
RS	Reed Solomon code
RTE	Radiative Transfer Equation
RV	Random Variable
Rx	Receiver
SB	Semi-Blind

SI	Scintillation Index
SIM	Subcarrier Intensity Modulation
SIMO	Single-Input Multiple-Output
SISO	Single-Input Single-Output
SMux	Spatial Multiplexing
SNR	Signal-to-Noise Ratio
SP	Set-Partition
ST	Space-Time
SU	Secondary User
Th-HD	Thresholded Hard-Decisions
TDMA	Time Division Multiplexing Access
TIZ	Trans-Impedance amplifier
TTHG	Two Term Henyey Greenstein
Tx	Transmitter
UWB	Ultra Wide-Band
UWOC	Underwater Wireless Optical Communication
VLC	Visible Light Communication
VSF	Volume Scattering Function
WBAN	Wireless Body Area Network
WHOI	Woods Hole Oceanographic Institution
WLAN	Wireless Local Area Network
WRN	Wireless Relay Network
WSN	Wireless Sensor Network

Résumé étendu

Contents

0.1 Contexte

Une des caractéristiques essentielles des futurs systèmes de télécommunications sans-fil est l'évolution vers des débits très élevés tout en envisageant des mobilités de plus en plus importantes des usagers. En même temps ces évolutions sont affectées par les tendances et recommandations pour baisser la consommation d'énergie; on parle alors des techniques de communication "vertes". Ces besoins nécessitent de nouvelles techniques de traitement du signal pour augmenter la capacité du canal de transmission et l'autonomie des terminaux et gérer des utilisateurs à forte mobilité, mais aussi de nouvelles technologies de transmission pour pallier au problème de la *saturation* du spectre électromagnétique dans la bande radio-fréquence (RF) auquel nous faisons face aujourd'hui.

Pour ces raisons, j'ai contribué au développement de techniques efficaces de traitement de signal dans les domaines de transmissions sans-fil RF et optiques qui sont considérées comme des technologies complémentaires.

Dans ce qui suit, je décris brièvement et dans l'ordre chronologique mes travaux de recherche dans les domaines RF et optique, avant de détailler ces activités de recherche et présenter quelques perspectives pour des travaux que je souhaite réaliser à court et à moyen terme. Il est à noter qu'une présentation plus détaillée du déroulement de ma carrière et de mes activités de recherche se trouve dans la partie principale de ce manuscrit, rédigée en anglais.

0.2 Parcours Professionnel

CONFIDENTIELLE

0.3 Activités de Recherche

0.3.1 Systèmes de communication MIMO RF

Face aux évanouissements du canal dans un milieu sans-fil, l'usage des réseaux d'antennes et des techniques de traitement d'antennes s'avère très efficace pour préserver la qualité de transmission des données. En particulier, les structures MIMO qui utilisent des antennes multiples à la fois à l'émission et à la réception, permettent d'atteindre des taux de transmission très élevés dans un milieu de transmission riche en diffuseurs. Ceci est typiquement le cas des milieux de propagation intra-bâtiment mais aussi, la plupart du temps, des milieux urbains. Ces systèmes ont été au cours des années 2000 l'un des thèmes de recherche les plus dynamiques au niveau national et international. Ils sont notamment utilisés aujourd'hui dans les systèmes de communications mobiles de la quatrième génération.

J'ai commencé mes recherches sur les systèmes MIMO par l'étude des aspects de théorie de l'information, de codage correcteur d'erreur, d'optimisation du débit et de détection des données. Un de mes objectifs a été de développer des détecteurs performants et de complexité raisonnable. En effet, la question de complexité est primordiale quand il s'agit de l'implémentation du récepteur dans les terminaux mobiles, par exemple. Je me suis particulièrement intéressé aux techniques de détection itérative. En fait, en présence du codage canal, un tel détecteur permet de profiter de la redondance introduite par le codage canal afin d'améliorer la détection de données au fil des itérations. J'ai étudié le détecteur quasi-optimal basé sur le maximum *a posteriori* (MAP) mais aussi un détecteur sous-optimal basé sur l'annulation d'interférences qui a l'avantage d'avoir une complexité calculatoire réduite par rapport au détecteur MAP. Un autre aspect pratique que j'ai étudié a été celui de l'estimation du canal MIMO à la réception. Cette tâche est indispensable quand on effectue une détection cohérente au récepteur. J'ai en particulier travaillé sur les techniques d'estimation semi-aveugle qui préservent l'efficacité spectrale au prix d'une augmen-

tation de la complexité du récepteur. Pour les deux cas de séquences pilotes multiplexées en temps et superposées aux symboles de données, nous avons proposé des solutions d'estimation semi-aveugles basées sur l'algorithme EM (Expectation Maximization), permettant une amélioration considérable de l'estimation du canal tout en restant de complexité raisonnable. Nous avons également proposé des solutions sous-optimales de complexité réduite pour faciliter une implémentation en temps-réel, ou au moins pour permettre une implémentation moins coûteuse. Nous avons étudié la convergence de ces récepteurs itératifs à l'aide notamment des diagrammes EXIT (EXtrinsic-Information Transfer).
Étant donné que le récepteur dispose en pratique d'une estimation imparfaite des coefficients du canal, un autre axe de recherche a été de développer des techniques optimisées de détection de données pour prendre en compte ces erreurs d'estimation du canal et ainsi améliorer les performances du système par rapport à l'approche classique. Supposant connaître la distribution de ces erreurs, nous avons proposé de moyenner la fonction de coût (sur laquelle est basé le récepteur) par rapport à la distribution des coefficients du canal conditionnée à leur estimation. Cette solution permet d'obtenir des gains de performance intéressants sans pour autant augmenter considérablement la complexité du récepteur.

Outre le codage canal, utilisé classiquement pour réduire l'effet du bruit et interférences, un certain codage peut être effectué au niveau de la transmission des données sur les antennes émettrices, il s'agit du codage dit espace-temps. Une autre partie de mes travaux de recherche a été consacrée au codage et décodage espace-temps. Une des questions à laquelle j'ai essayé de répondre a été le choix approprié d'un schéma espace-temps pour une efficacité spectrale souhaitée. Il s'agit en fait de trouver la solution la plus adéquate pour fixer le codage canal, le schéma espace-temps et la constellation du signal. Nous avons montré qu'un schéma espace-temps non-orthogonal est préférable à un schéma orthogonal si on admet une complexité de détection légèrement plus importante au niveau du récepteur. Il s'agit en fait d'un détecteur itératif simple, basé sur l'annulation d'interférences qui constitue un bon compromis entre complexité et performance. Ceci est vrai également quand les erreurs d'estimation du canal sont prises en compte.

0.3.2 Réseaux de capteurs sans-fil RF

Nous avons étudié les problèmes liés à la mise en œuvre des réseaux de capteurs qui concernent notamment les contraintes fortes sur les ressources spectrale, énergétique et de calcul numérique au niveau de chaque nœud du réseau. En particulier, pour réduire l'effet des évanouissements du canal, les techniques classiques de diversité ne peuvent pas être utilisées en raisons des contraintes sur la taille et le coût des nœuds; il faudrait donc privilégier les techniques de diversité dites coopératives. Dans ce contexte des réseaux coopératifs, nous nous sommes particulièrement intéressés aux réseaux de relais et avons étudié les aspects de détection du signal et d'estimation du canal en prenant en compte le codage espace-temps effectué au niveau de relais.

En ce qui concerne l'estimation du canal dans les réseaux de relais, nous avons travaillé sur

les techniques semi-aveugles afin de réduire la consommation énergétique des nœuds en minimisant le nombre des symboles pilotes. Également, nous avons étudié les techniques optimales de détection de données pour prendre en compte les erreurs d'estimation du canal. L'utilisation de ces techniques est justifiée quand nous avons moins de contraintes sur la capacité de calcul et les ressources énergétiques au nœud de destination.

0.3.3 Radio cognitive

L'objectif du récent concept de radio cognitive est de permettre à un réseau secondaire d'utiliser de manière opportuniste les ressources spectrales d'un réseau primaire. Nous travaillons actuellement sur les solutions efficaces d'estimation du canal adaptées à ces systèmes. Plus particulièrement, nous étudions le cas d'un réseau de capteurs qui souhaite bénéficier des ressources spectrales d'un réseau primaire sans toutefois perturber le fonctionnement de ce dernier.

0.3.4 Communications optiques aériennes

Dans un contexte "outdoor", on peut utiliser des faisceaux optiques dans la bande infrarouge pour établir une transmission haut-débit entre deux points en vis-à-vis. La technologie FSO convient *a priori* aux applications à mobilité réduite. Les avantages de la technologie FSO par rapport aux communications RF sont nombreux. Notamment, du fait de la grande largeur de bande spectrale disponible, le débit atteignable avec les liens FSO est très élevé, et peut dépasser le Gbps. Néanmoins, les performances de ces systèmes sont limitées par des erreurs d'alignement entre l'émetteur et le récepteur, les phénomènes météorologiques, et les turbulences atmosphériques qui causent des fluctuations dans l'intensité du signal reçu. Nos travaux de recherche ont principalement porté sur la modélisation du canal de propagation, notamment dans le cas des systèmes utilisant la diversité spatiale en employant des faisceaux multiples à l'émission et/ou des lentilles multiples à la réception. Nous avons étudié le problème des évanouissements corrélés qui sont à l'origine de la perte d'efficacité des systèmes à diversité spatiale. Nous avons évalué cette corrélation à l'aide de la méthode des écrans de phase et étudié l'impact des différents paramètres du système et l'influence des conditions de turbulence sur cette dernière. Aussi, nous avons proposé des méthodes pour évaluer les performances du système à l'aide des simulations de Monte Carlo ou avec des expressions analytiques.

Nous avons également considéré les techniques efficaces de codage et modulation pour les systèmes FSO et aussi proposé des solutions efficaces pour réduire l'effet de l'éclairement ambiant. Réduire l'effet de désalignement entre l'émetteur et le récepteur en optimisant les paramètres du faisceau laser et le codage espace-temps pour les structures MIMO sont considérés dans nos récents travaux. Un autre sujet sur lequel nous avons travaillé est celui des liens de transmission hybride RF/FSO. L'intérêt de cette approche est qu'elle permet de conserver la liaison en cas de conditions de brouillard relativement dense qui a pour effet d'atténuer fortement le faisceau laser.

Quand il n'y a pas de trajet direct (LOS pour Line-Of-Sight) entre l'émetteur et le récepteur, ce qui arrive souvent dans les métropoles denses d'immeubles hauts, ou lorsque la transmission est faite sur de très longues distances, une solution adéquate pour mettre en place un lien FSO consiste à utiliser des relais pour contourner les obstacles et/ou amplifier le signal. Nous avons récemment étudié l'intérêt de mettre en place un réseau FSO coopératif dans le but de réduire l'effet des turbulences atmosphériques.

0.3.5 Communications optiques sous-marines

Dans un milieu aquatique, les transmissions optiques point-à-point ont l'avantage de bénéficier d'un débit très élevé, un faible niveau d'interférences et une vitesse de propagation très grande (donc une faible latence). Elles s'avèrent également intéressantes des points de vue de la taille des modules et de la consommation d'énergie. Nous avons travaillé sur la modélisation du canal de propagation en prenant en compte les caractéristiques du milieu mais aussi les imperfections des composants optiques. Nous avons aussi mené une étude sur le choix de schéma de modulation du signal en prenant en compte les contraintes pratiques telles que la synchronisation du récepteur et la vitesse limitée liée à l'électronique de ce dernier. Nous travaillons actuellement sur les techniques de codage correcteur d'erreur adéquates pour ces systèmes et aussi sur les solutions efficaces pour s'affranchir des erreurs de désalignement de l'émetteur-récepteur.

0.3.6 Communications infrarouges ou VLC

Dans un contexte "indoor", les systèmes de communications optiques permettent de réduire les interférences électromagnétiques en remplaçant les systèmes RF habituels tels que les technologies Bluetooth et WiFi. En particulier, les communications VLC constituent un candidat très intéressant pour les connexions haut-débit en utilisant les éclairages LED pour la transmission de données. Cette technique est aussi appelée Li-Fi (L pour Lumière) en analogie avec le WiFi. Nous avons travaillé sur la caractérisation du canal en utilisant des simulations basées sur la technique de lancer de rayons. Nous travaillons actuellement sur des méthodes efficaces de transmission pour réduire l'effet des interférences-entre-symboles qui se manifestent lors de la transmission à de très hauts débits. En fait, étant donnée la bande passante limitée des LEDs, il y a tout intérêt à utiliser les techniques avancées de communications numériques afin d'augmenter le débit de transmission. Parmi elles, on peut parler de la technique MIMO, de l'OFDM, de pré- ou post-égalisation, etc.

0.4 Résumé des Travaux

Un résumé des travaux de recherche effectués et des résultats obtenus jusqu'à présent est présenté dans la suite. Les références les plus importantes sont citées également.

0.4.1 Systèmes MIMO

- Codage et décodage espace-temps
  - Détection itérative pour les codes espace-temps non-orthogonaux.
  - Investigation de la combinaison appropriée du codage canal et du codage espace-temps pour un débit de transmission donné [1].
- Estimation du canal
  - Estimation semi-aveugle du canal pour les pilotes multiplexés en temps ou superposés avec les données [2–4].
  - Optimisation des détecteurs basés sur les critères du maximum *a posteriori* et de l'annulation d'interférences en tenant compte des erreurs d'estimation du canal [5].
- Techniques avancées de codage canal (turbo-codes et codes LDPC) pour les réseaux LTE et WiMAX.
- Estimation du canal pour les canaux MIMO-OFDM soumis aux évanouissements rapides [6].

0.4.2 Réseaux de capteurs coopératifs

- Réseaux de relais
  - Étude des codages espace-temps "distribués", adaptés à ces réseaux.
  - Estimation semi-aveugle du canal et détection itérative à la destination [7, 8].
  - Détection optimale du signal en présence des erreurs d'estimation du canal [9].

0.4.3 Systèmes FSO [10]

- Modélisation mathématique des turbulences atmosphériques
- Réduction des effets de turbulence
  - Techniques de diversité temporelle utilisant le codage canal et entrelacement [11].
  - Analyse de l'efficacité de l'approche "aperture averaging" [12].
  - Exploitation de la diversité spatiale en utilisant des faisceaux ou/et des lentilles multiples.
  - Etude des conditions d'évanouissements corrélés, modélisation statistique et évaluation des performances du système [13–16].
  - Codage espace-temps pour les systèmes MIMO-FSO.

  - Etude expérimentale pour la quantification des turbulences atmosphériques et l'évaluation des performances d'un lien FSO dans différents régimes de turbulence avec une maquette de laboratoire (au laboratoire OCRG de Newcastle) .
  - Etude des performances d'un réseau FSO coopératif (assisté par des relais).

- Optimisation des paramètres de l'émetteur pour réduire l'impact des erreurs d'alignement d'émetteur-récepteur [17].
- Transmission différentielle pour supprimer le bruit ambiant au récepteur [18].
- Techniques de modulations adéquates pour les systèmes FSO.
  - Modulations PPM et MPPM et solutions de codage canal adaptées; codage convolutif et détection itérative [19].

0.4.4 Transmissions optiques sous-marines [20]

- Caractérisation et modélisation mathématique du canal de propagation aquatique [21].
- Investigation de l'impact réel de la diffusion du faisceau dans l'eau sur le débit de transmission.
- Etude des techniques de modulation appropriées.
- Etude de l'effet de désalignement d'émetteur-récepteur sur les performances du système.
- Réalisation d'une maquette de transmission (à l'IFREMER de La-Seyne-sur-Mer).

0.4.5 Communications optiques intra-bâtiment

- Optimisation du profil d'intensité d'un émetteur infrarouge pour maximiser la capacité du canal [22].
- Compréhension des principes de la technologie VLC.
  - Étude expérimentale de plusieurs maquettes de transmission VLC (au laboratoire OCRG de Newcastle).
  - Investigation d'une méthode précise et efficace pour simuler le canal de transmission.

0.5 Perspectives

CONFIDENTIELLE

Chapter 1

General Introduction

Contents

1.1 Context

The proliferation of wireless communication systems can be considered as one of the most remarkable changes in human life over the past thirty years. Wireless devices and technologies have become pervasive very quickly and are among the most integral elements of modern society. The term “wireless” is usually used synonymously with radio-frequency (RF) technologies as a result of the wide-scale deployment of wireless RF devices and systems. However, the RF band of the electromagnetic spectrum is fundamentally limited in capacity due to the fact that most of the sub-bands are exclusively licensed and strictly regulated by the local and international authorities today. While very high data-rate wireless system are receiving an ever-growing popularity, the demand for RF spectrum is outstripping the available resources, what is commonly called “spectrum famine.” This has appealed for new and efficient techniques and technologies in order to increase the spectral efficiency of RF wireless systems or to use the upper parts of the electromagnetic spectrum.

The MIMO technology can be considered as one of milestones of the end of last century that opened the door to a new concept of data transmission, i.e., exploiting multipath propagation, which was previously-considered as an impairment to reliable communication, to multiplex data over multiple transmitting antennas and to obtain data rates until then unattainable. Another solution to deal with the congested spectrum problem has been the ultra wide-band (UWB) transmission which is based on transmitting the signal on a very large frequency band while using a very low power spectral density in order not to interfere with other existing systems. A more re-

cent technique for circumventing the limited spectral resources is cognitive radio, which consists in using the spectral resources of a primary user in an opportunistic manner, for example. At the same time, new needs for global networks were at the origin of developing wireless sensor networks at the beginning of the 21st century. Considered as a key technology of the century, they provide exceptional opportunities for monitoring and controlling homes, cities, and the environment, for instance. Cooperative networks, in particular, allow reliable data transmission through the efficient use of spectral and energy resources.

On the other hand, there has been a trend to shift toward higher carrier frequencies where a substantial frequency bandwidth is available. An example is the use of the millimeter waves (e.g. around 60 GHz) but these frequencies have limited applications due to the high propagation loss that limits the link span seriously. A dramatically different approach is that of optical wireless communications (OWC) which can enable wireless connectivity using infrared (IR), visible or ultraviolet bands. OWC has powerful features such as high bandwidth, low cost, robustness to electromagnetic interference, operation in an unregulated spectrum, high degree of spatial confinement, and inherent physical security. Due to these reasons, OWC can be a powerful alternative to the wireless RF technology for some applications. It has recently become one of the most dynamic areas of research with significant potential for impacting considerably the wireless market that has been mostly dominated by the RF technology since a long time. Variations of OWC can be employed in a diverse range of communication applications ranging from very short-range (on the order of millimeters) optical interconnects within integrated circuits to satellite links (larger than 10,000 kilometers).

Today, a relatively mature technology related to OWC is that of outdoor terrestrial OWC links, operating in near IR band, which are widely referred to as free space optical (FSO) communication. FSO systems are typically used for high rate communication between two fixed points over distances up to several kilometers. They are appealing for a wide range of applications such as metropolitan area network extension, local area network (LAN)-to-LAN connectivity, fiber backup, backhaul for wireless cellular networks, disaster recovery, high definition TV transmission, etc. The use of OWC has also been considered in underwater communications recently. This has been especially motivated by the need to high-speed and reliable transmission links due to the increasing use of robotics in underwater missions and the need to communicate with remotely-operated vehicles, for instance. Underwater wireless optical communication (UWOC) in the visible part of the spectrum can provide very high data transmission rates (on the order of Mbps to Gbps) over short to moderate ranges (typically up to one hundred meters or so). In addition to its ability to provide unprecedentedly high data rates, this technology is highly energy efficient, as compared to the traditional technique of acoustic communication, and also has much less impact on the marine animal life; in particular, it is harmless to the cetaceans and coral.
Another interesting and very recent application area of OWC is in indoor environments where it is estimated that more than 70% of the wireless traffic takes place. The visible light communication (VLC), aims at using the incoherent solid-state lighting elements such as LEDs for data transmis-

sion and promises very high data rates up to several Gbps. By exploiting the illumination facilities for data transmission, the VLC technology provides a unique opportunity to get rid of electromagnetic radiations in restrictive areas (such as hospitals or within aircrafts) and at the same time permits a significant reduction in power consumption of the users. It can be seen as an example of "green communication" because in addition to exploiting a part of lighting energy consumption for data transmission, we avoid the need to power-hungry alternative solutions such as WiFi networks.

1.2 Research Itinerary and Related Topics

CONFIDENTIAL

1.3 Document Outline

After this general introduction, I will describe separately in Chapters 3 and 4 my research activities on the two general domains of RF and optical wireless communications, respectively. Therein, for the different corresponding research topics, I will systematically present a review of the technology and the related considerations before specifying my contributions and proposed solutions. The research works on the RF domain, concern the three main topics of MIMO technology, wireless sensor networks, and cognitive radio. Those corresponding to OWC, concern FSO, UWOC, and VLC technologies. I have tried to provide a succinct description of the most important contributions and to refer the reader to the corresponding publications for more detail. At the same time, to make the discussions more understandable, I have presented some main results in form of illustrations and performance figures. Also, I have specified the laboratories or research teams I have been collaborating with on different research subjects. Undoubtedly, without these fruitful collaborations, the help and support of my colleagues in Institut Fresnel (especially my advisor Prof. Bourennane), and the precious work of the students that I have had the pleasure to supervise, I could not accomplish these achievements.

Finally, the main conclusions of my research works as well as some perspectives for future research will be presented in Chapter 5.

Chapter 2

Career Summary

CONFIDENTIAL

Chapter 3

Research Works on RF Wireless Communication Systems

Contents

3.1 Introduction

In this chapter, I present the research topics on which I have been working in the field of RF wireless communications since my PhD. They mainly concern MIMO systems, wireless sensor networks, and cognitive radio. For each topic, I will first present a brief technology overview before specifying my general contributions.

3.2 MIMO Technology

3.2.1 Technology overview and related topics

At the end of the 1990s, pioneering works in Bell Labs showed for the first time that the use of multiple antennas at both sides of the transmission link can result in tremendous channel capacities, provided that the propagation medium is rich scattering [23–26]. This increase in capacity is obtained without any need to extra bandwidth nor to extra transmission power. This way, it was shown that multipath propagation, previously regarded as an impediment to reliable communication, can be exploited in order to increase the throughput.

3.2.1.1 MIMO systems, information theoretical aspects

- Capacity of a fading channel
  Let us first recall the definition of the capacity for a fading channel. For a time-varying channel, the capacity C is a random variable whose instantaneous value depends on the channel realization [27]. The two mostly used definitions for the channel capacity are *ergodic* and *outage* capacities. The ergodic capacity C_{erg}, which is the expected value of C, is suitable for fast varying channels. The outage capacity C_{out} is usually used when considering packet-based transmission systems where the block-fading model properly describes the channel. If the pre-assumed channel capacity is too optimistic, i.e., larger than the instantaneous capacity, a channel outage occurs. The outage capacity, or to say more correctly, the capacity-versus-outage, as its name indicates, is the channel capacity conditioned to an outage probability P_{out}. Obviously, there is a trade-off between the data throughput and the outage probability.

- MIMO capacity
  Consider the global scheme of a MIMO transmission link as shown in Fig. 3.1. We denote

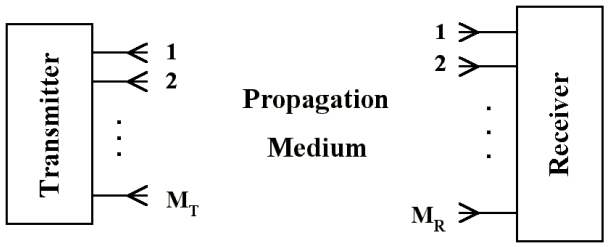

Figure 3.1 — Global scheme of a MIMO communication structure.

by M_T and M_R the number of antennas at the transmitter (Tx) and the receiver (Rx), respectively. The communication channel includes the effect of transmit/receive antennas and the propagation medium. We consider the simple case of frequency non-selective (flat) fading channel that is typically valid for narrow-band communications. The global MIMO channel is described by a channel matrix $\boldsymbol{H}$ of dimension $(M_R \times M_T)$. For instance, the entry H_{ij} of $\boldsymbol{H}$, characterizes the subchannel between the i^{th} receive and the j^{th} transmit antenna. We assume that the total transmit power at each channel-use is constrained to P_T.
If the channel is known (e.g. perfectly estimated) at the Rx but unknown to the Tx, we distribute the available power uniformly on the transmit antennas. Lets denote by ρ_T the total average received signal-to-noise ratio (SNR) at the Rx array: $\rho_T = P_T/\sigma_n^2$, where σ_n^2 is the variance of the additive white Gaussian complex noise. The MIMO channel capacity in units of bps/Hz is then given by the following famous equation:

$$C = \log_2 \det\left[\boldsymbol{I}_{M_R} + \frac{\rho_T}{M_T}\,\boldsymbol{H}\boldsymbol{H}^{\dagger}\right]. \tag{3.1}$$

Here $\boldsymbol{I}_{M_R}$ is the $(M_R \times M_R)$ Identity matrix, and det[.] and $(.)^{\dagger}$ denote matrix determinant and transpose-conjugate, respectively.
Figure 3.2 contrasts the outage capacities C_{out} of MIMO, single-input multiple-output (SIMO), and multiple-input single-output (MISO) systems under the conditions of uncorrelated Rayleigh flat fading and $P_{\text{out}} = 0.01$ [28, 29]. SNR stands in fact for ρ_T. For the MIMO system, we have $M_T = M_R = M$. We notice that the MIMO capacity increases almost linearly with M and is much more considerable than those of MISO and SIMO structures.

3.2.1.2 Space-time coding and decoding

An important aspect in the implementation of MIMO systems is to appropriately distribute redundancy in space and in time at the Tx, what is called space-time (ST) coding [30]. There has been a considerable amount of work on this subject and a variety of ST schemes were proposed. The key criteria in the design of ST codes are the ST coding rate (or the multiplexing gain) and the diversity gain. The first one aims at achieving a high transmission rate by capitalizing on the MIMO capacity, whereas the latter aims at exploiting the space diversity to reduce fading at the Rx. The most popular ST schemes include orthogonal space-time block codes (OSTBC) [31, 32] which aim

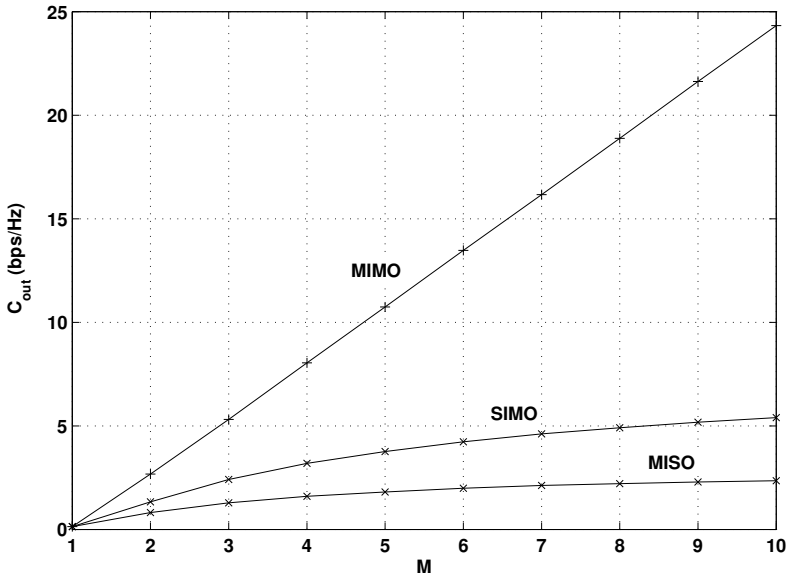

Figure 3.2 — Contrasting outage capacities of MIMO, SIMO, and MISO structures. Uncorrelated Rayleigh flat fading, SNR = 10 dB, $P_{\text{out}} = 0.01$. CSI known at the Rx only.

at diversity gain and some coding rate, spatial multiplexing (SMux) or the V-BLAST architecture that maximizes the coding rate [26], and the general family of linear dispersion codes [33] that maximize the mutual information between the Tx and the Rx, allowing a flexible rate-diversity trade-off.

Apart from the problem of code construction, one important criterion in the choice of the appropriate ST scheme may be its decoding complexity. OSTBCs can offer full diversity while they can be decoded using an optimal decoder with linear complexity. However, these schemes suffer from low rate, especially for a large number of transmit antennas. Non-orthogonal schemes, on the other hand, offer higher coding rates but their optimal decoder becomes prohibitively complex for a large number of transmit antennas and large signal constellation sets.

3.2.1.3 Channel estimation for MIMO systems

When coherent signal detection is to be performed, channel state information (CSI) is required at the Rx, for which a channel estimation step is necessary. Channel estimation plays a critical role in the Rx performance and is a real challenge in practical MIMO systems where the quality of data recovery is as important as attaining a high data throughput. In order to obtain the CSI, usually some known training (also called pilot) symbols are sent from the Tx, based on which the Rx estimates the channel prior to the detection of data symbols.

- Time-multiplexed pilots
  The classical approach consists in time-multiplexing pilot and data symbols, usually referred

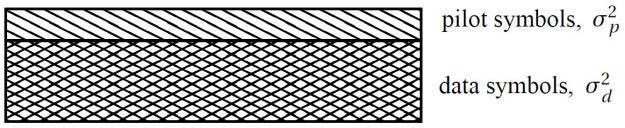

Figure 3.3 — Overlay pilot scheme. σ_p^2 and σ_d^2 denote the variances of pilot and data symbols, respectively.

to as pilot symbol-assisted modulation (PSAM). By this approach, we have a trade-off between the channel estimation quality and the data throughput. With an increased number of pilots, a better channel estimate can be obtained, but at the same time, the spectral efficiency is sacrificed more. Note that there is a minimum number of channel-uses that should be devoted to the transmission of pilots in order that the MIMO channel be identifiable at the Rx. For the case of a flat channel, the number of pilot channel-uses N_p should satisfy $N_p \geq M_T$ [34]. Furthermore, the best channel estimate is obtained with mutually orthogonal training sequences, which result in uncorrelated estimation errors. In such a case, we can model the channel estimation errors by an independent Gaussian random variable [34].

- Semi-blind estimation
  Instead of the classical channel estimation based only on pilot symbols, we can perform semi-blind (SB) estimation, where in addition to pilot symbols, we make use of data symbols in channel estimation. This way, a considerable performance improvement can be achieved at the price of increased Rx complexity. Usually, SB approaches are implemented in an iterative scheme. When channel coding is used, channel estimation is performed iteratively together with signal detection and channel decoding.

- Overlay pilots
  The main drawback of the PSAM approach is that, for finite-length blocks, if channel estimation is to be done on each block of symbols, the periodic insertion of pilot symbols can result in a considerable reduction of the achievable data rate. This loss in the data rate becomes important, especially for large number of transmit antennas, at low SNR, and when the channel undergoes relatively fast variations [35]. As an alternative, we can use overlay pilots (OP), also called superimposed or embedded pilots, for channel estimation [36]. By this approach, a pilot sequence is superimposed on the data sequence before transmission, as shown in Fig. 3.3; thus, no separate time slot is dedicated to pilot transmission. This way, we prevent the loss in the data throughput but we experience a degradation in the quality of the channel estimate due to the unknown data symbols. As a matter of fact, here also there is a trade-off between the quality of channel estimation and the channel capacity: To obtain a better channel estimate, we should increase the percentage of the power dedicated to pilot symbols; this, however, reduces the SNR for the detection of data symbols.

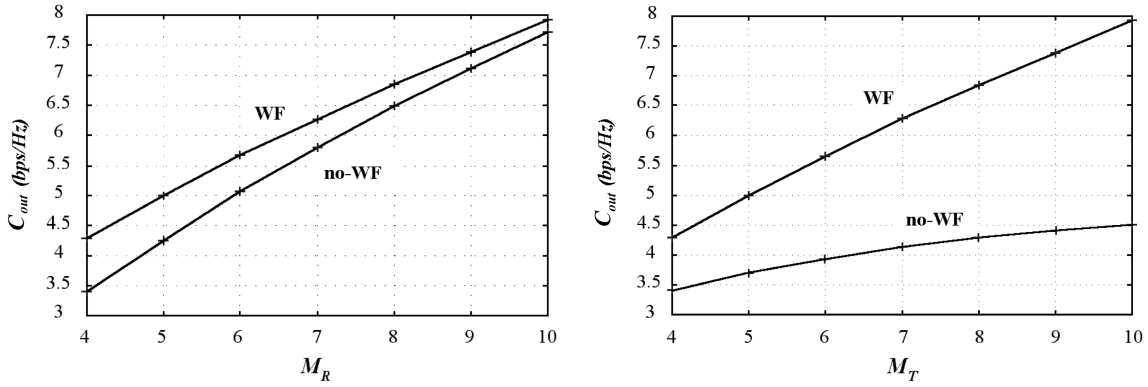

Figure 3.4 — WF and no-WF capacities of a MIMO system with $M_R > M_T = 4$ (left) and $M_T > M_R = 4$ (right). Uncorrelated Rayleigh flat fading, SNR = 3 dB, $P_{\text{out}} = 0.01$.

3.2.2 Contributions

3.2.2.1 MIMO capacity under special conditions

My first works on MIMO systems concerned the information theoretical bounds on the transmission rates for MIMO systems. These works correspond to my PhD dissertation at INPG and shortly after that. Here I provide a brief review of the works I accomplished during this period.

- Water-filling capacity
  The first special case is when CSI is known to both Tx and Rx, which is the case when the estimated CSI at the Rx is provided for the Tx. This is practically feasible when the channel varies slowly in time. Providing the CSI for the Tx can be done using a feedback channel or via the reverse link when the communication takes place in a duplex mode. Assuming that CSI is provided perfectly and without any delay to the Tx, it can allot the available power on the antennas in an optimal manner in order to achieve the maximum capacity [37]. This capacity is often called *known-CSI* or *water-filling* (WF) capacity.
  For $M_R \geq M_T$, the improvement in capacity by performing WF, that we call the *WF gain*, is considerable for low SNR and a large number of transmit antennas [37]. But this gain is much more considerable when $M_T > M_R$. For example, Fig. 3.4 shows curves of no-WF and WF capacities for two cases of $M_R > M_T = 4$ and $M_T > M_R = 4$. Notice that the WF-capacity of an (M_T, M_R) system is equal to that of an (M_R, M_T) system [38].

- Capacity for Ricean fading channels
  Ricean fading conditions hold when there is a dominant non-fading signal component present, such as a line-of-sight (LOS) between the Tx and the Rx. It is also the case when fixed scatterers/signal reflectors exist in addition to random main scatterers. Concerning the Ricean MIMO channel capacity, we have shown that there is a compromise between the diversity gain and fading reduction [39]. Let us define the Ricean factor as the percentage of power received from the LOS with respect to the total received average power. At relatively

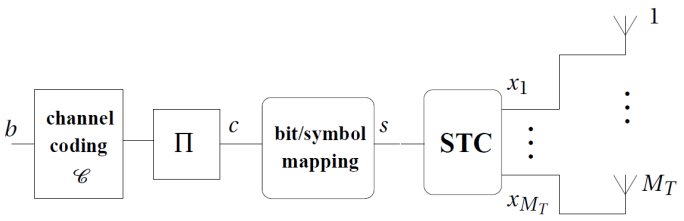

Figure 3.5 — Block diagram of the BICM transmission scheme. STC stands for space-time coding.

high SNR, since an increase in the Ricean factor increases the correlation between the channel coefficients, the MIMO capacity decreases as a result of decreased diversity gain. Meanwhile, the increase in capacity by increase in the number of antennas is still considerable for Ricean factors smaller than 70%. At low SNR, on the other hand, fading is more destructive, and so, an increase in the Ricean factor may result in an increase in the MIMO channel capacity. In other words, fading reduction affects more the channel capacity than the diversity gain [39].

We have also studied the MIMO capacity under the conditions of Ricean fading when CSI is available at the Tx. We have shown that the gain in capacity by WF is specially interesting for the case of correlated channels. In fact, with increased Ricean factor, the WF gain increases and becomes much more considerable, as compared to Rayleigh fading case [38].

3.2.2.2 Iterative MIMO detection

For the case of non-orthogonal ST schemes, instead of performing complex optimal ST decoding, we may use sub-optimal decoding based on sphere decoding [40] or simple linear-algebraic techniques such as interference-canceling-based decoding [41]. For either solution, the Rx performance can be improved considerably by performing iterative detection when channel coding is performed at the Tx, which is usually the case in practical systems. Indeed, by benefiting in this way from the channel coding gain, we can obtain a good performance after only a few iterations and approach the optimal "ST + channel" decoder performance. We have considered iterative ST decoding and channel decoding based on the bit-interleaved coded modulation (BICM) [42] for which a typical scheme is shown in Fig. 3.5. The advantage of the BICM is its flexibility regarding the choice of the code and the bit-symbol mapping, as well as its conformity to iterative detection. In Fig. 3.5, the binary data b are encoded by a channel code $\mathscr{C}$, before being interleaved (the block Π). The output bits c are then mapped to symbols according to a given constellation set. The block diagram of the iterative Rx is shown in Fig. 3.6 where soft-input soft-output signal detection (i.e., ST decoding) and channel decoding are performed. Hereafter, we always consider convolutional coding at the Tx and soft channel decoding based on the Max-Log-MAP algorithm at the Rx [43]. We have studied the Rx performance for MIMO signal detection based on the optimal maximum *a posteriori* (MAP)[1] and the sub-optimal soft parallel interference canceling (soft-PIC). We will

[1]The optimality of MAP detection is in the sense of minimizing the symbol error probability.

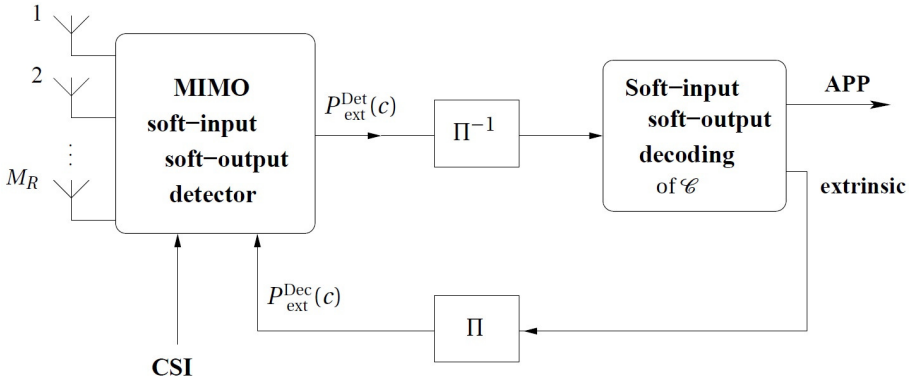

Figure 3.6 — Block diagram of the iterative Rx. $P_{\text{ext}}^{\text{Det}}$ and $P_{\text{ext}}^{\text{Dec}}$ denote the extrinsic probabilities on bits at the output of the MIMO detector and channel decoder, respectively. Also, APP stands for *a posteriori* probabilities.

sometimes refer to these approaches as turbo-MAP and turbo-PIC receivers. In fact, the optimal MAP detector becomes too complex to implement for large number of transmit antennas or large signal constellation sizes. In such cases the latter approach becomes particularly interesting.

As case study, consider the simple SMux ST scheme and a four-transmit antenna system, i.e., $M_T = 4$ with M_R taken between 1 and 4. We perform Gray bit/symbol mapping and pseudo-random interleaving, and consider the Rayleigh flat quasi-static channel model. The rate-1/2 non-recursive non-systematic convolutional (NRNSC) channel code $(5,7)_8$ (in octal representation) is used. SNR is considered in the form of E_b/N_0, where E_b is the average received energy per information bit and N_0 is the unilateral noise power spectral density; E_b/N_0 includes the Rx array gain, M_R. We have presented plots of bit-error-rate (BER) versus E_b/N_0 in Fig. 3.7. We notice that the performance of turbo-PIC and turbo-MAP are relatively close to each other for $M_R = M_T$ (it is also the case for $M_R \geq M_T$). Turbo-PIC can still be used for certain values of $M_R < M_T$, roughly for $M_R > M_T/2$ [2]. So, for these M_R values where turbo-PIC converges properly, it would be preferred to turbo-MAP due to its considerably lower complexity.

3.2.2.3 Choice of appropriate ST schemes

In practice, to attain a desired spectral efficiency, we should adopt the most appropriate transmission scheme by fixing the degrees of freedom of the system, that is, the signal constellation, the channel coding rate, and the ST coding scheme. We have tried to answer to the question “what is the most suitable combination?” Indeed, if a low spectral efficiency is required, an OSTBC scheme together with a powerful channel code would be a suitable solution. To attain high spectral efficiencies with OSTBC schemes, however, we have to use large signal constellations and to increase the channel coding rate by puncturing the encoder output bits. Use of larger signal constellations complicates signal detection at the Rx and results in a higher SNR required to attain a target BER. On the other hand, puncturing results in a reduced channel code robustness against noise. Higher ST coding rates are offered by non-orthogonal schemes, hence, relaxing the conditions on signal

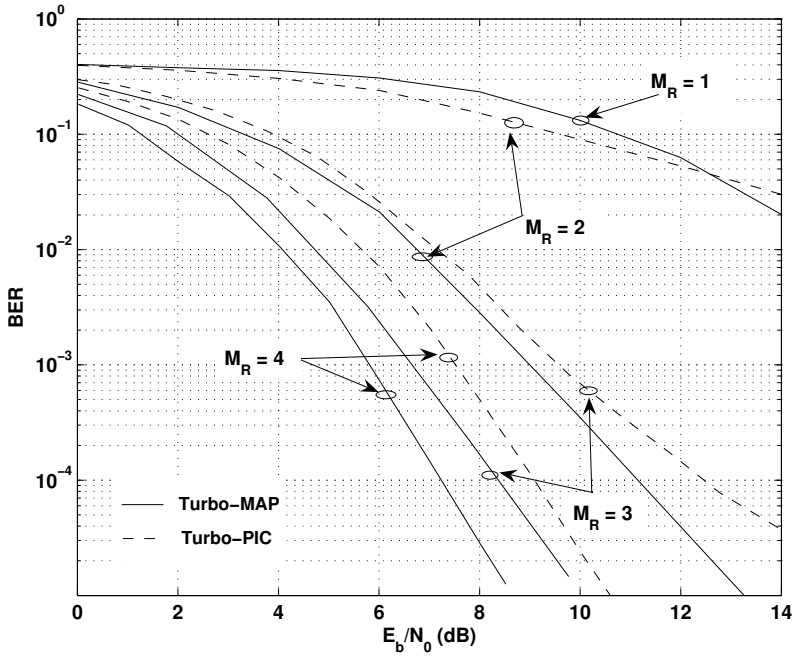

Figure 3.7 — Performance comparison of turbo-PIC and turbo-MAP receivers, $M_T = 4$, $(5,7)_8$ channel code, Gray-mapped QPSK modulation, uncorrelated flat Rayleigh fading, 64 channel-uses per frame. Perfect CSI at Rx is assumed.

constellation and channel coding. For this case, we considered the simple sub-optimal iterative soft-PIC detector for ST decoding. Nevertheless, the detector remains more complex, as compared to the OSTBC case. However, we have shown that this increased Rx complexity is quite justified: by using an appropriate non-orthogonal ST scheme and iterative detection, we obtain a considerable performance improvement with respect to the OSTBC choice [44–46]. Our results in [45, 46] have also confirmed that the gain obtained by using non-orthogonal with respect to orthogonal schemes is even more important when channel estimation errors are taken into account.

For example, consider the case study of a (2×2) MIMO system, Gray bit/symbol mapping, pseudo-random interleaving, and a Rayleigh flat block-fading channel. We use the rate-1/2 NRNSC channel code $(133, 171)_8$. To obtain a spectral efficiency of $\eta = 2$ bps/Hz, we consider three options of Alamouti OSTBC with 16-QAM modulation, and SMux and Golden (GLD) ST coding[2] with QPSK modulation. The corresponding performance curves are shown in Fig. 3.8, assuming perfect CSI at the Rx. For SMux and GLD schemes, BER plots are shown for the second and the fourth iterations where almost full Rx convergence is attained. We notice that, compared to Alamouti ST coding, by using the SMux scheme we gain about 3.3 and 3.75 dB in SNR at BER= 10^{-4} after two and four iterations, respectively. The corresponding gains when using the GLD ST code are about 3.5 and 4.3 dB, respectively. We note that even when, for the reasons of complexity and/or

[2]GLD is an optimized scheme proposed in [47] that offers full-rate and full-diversity with the property of non-vanishing determinant.

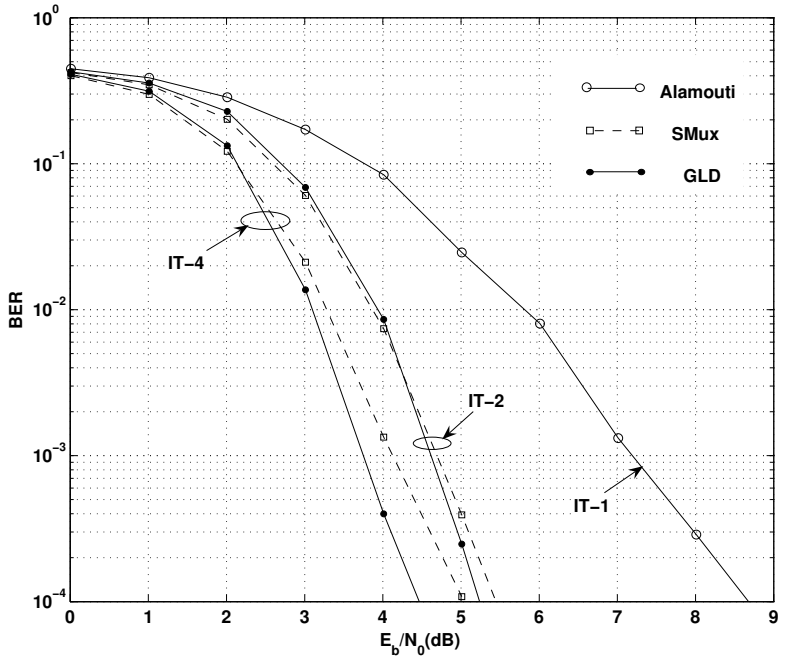

Figure 3.8 — Performance comparison of different ST schemes for a (2×2) MIMO system. Turbo-PIC detection for SMux and GLD, $(133,171)_8$ channel code, block fading channel with $N_c = 32$ independent fades and 768 channel-uses per frame , $\eta = 2$ bps/Hz, perfect CSI at Rx. IT denotes iteration number.

latency, only two iterations are processed at the Rx, a substantial SNR gain is obtained, compared to the Alamouti scheme.

3.2.2.4 Channel estimation for MIMO systems

During my post-docs at LTCI and IETR labs, I have been working on SB MIMO channel estimation using time-multiplexed pilots (i.e., the PSAM scheme). We have proposed a number of solutions for this purpose, including SB estimation based on the expectation maximization (EM) algorithm [2, 3, 48, 49] as well as some simplified schemes such as the *thresholded hard-decision* (Th-HD) method [3]. Note that the interest of the EM algorithm is that it is guaranteed to be stable and to converge to the maximum likelihood (ML) estimate [50]. All these SB estimation techniques have been implemented in an iterative Rx.

- EM-based SB channel estimation
  I do not present here the details on the formulation of the EM-based estimators and refer the reader to [2, 3, 34], for instance. We have mainly considered two formulations for the SB estimator. The classical formulation consists in using data and pilot symbols in the same way in channel estimation. We have shown that substantial performance improvement can be obtained by using this SB estimation method. We have further optimized the estimator

formulation by considering separately the channel estimates obtained using pilot and data symbols and by combining them appropriately in order to obtain a better estimate. Indeed, by this approach, we optimized the EM implementation to provide an unbiased channel estimate which leads to a better convergence of the iterative detector. For the case of MAP signal detection, we showed that considerable improvement in the Rx performance can be obtained by using our proposed method, especially for a large number of transmit antennas and short training sequences. We also showed that when MIMO channel is strongly asymmetric in the sense that we have too few receive antennas, the EM-based channel estimation can be of little interest [3].
We further applied these ideas to the case of soft-PIC signal detection in [2,49].

- Simple Th-HD SB channel estimation
  In the Th-HD method, in addition to pilot symbols, we use in channel estimation the symbols detected with sufficiently high reliability at each iteration. For this, we compare the *a posteriori* probabilities on the transmitted bits P_i at the decoder output and compare them with a threshold $0.5 < P_{\mathrm{TH}} < 1$. If $\mathrm{P}_i > P_{\mathrm{TH}}$, we make the hard decision 1 on the corresponding bit; otherwise, if $\mathrm{P}_i < (1 - P_{\mathrm{TH}})$, we make the hard decision 0 on it; and if none of these conditions are verified, we give up the channel-use corresponding to that bit and do not consider it in channel estimation. If a hard decision is made on all BM_T constituting bits of a channel-use, where B is the number of bits per symbol corresponding to the underlying modulation scheme, we use the resulting hard-detected symbol vector in channel estimation in the same way as pilot symbols. We have investigated the efficacy of this SB estimator and shown that the estimator performance depends highly on the choice of the threshold P_{TH}. The optimum threshold value depends on the MIMO structure, i.e., the number of transmit and receive antennas, as well as on the actual SNR [3].

3.2.2.5 Overlaid pilots and data

We have firstly investigated the interest of OP over the PSAM scheme, given that for both schemes we have a trade-off between the quality of channel estimate and the throughput or BER. We have shown that, in general, OP may be preferred to PSAM for high SNR, not too short channel coherence times, and larger number of receive than transmit antennas [51]. We have also investigated the problem of error floors in the system performance when using OP. In fact, the main problem in the estimation of channel coefficients concerns the interference due to the unknown data symbols. Indeed, although data and pilot sequences are *statistically* uncorrelated, the cross-correlation of data and pilot sequences is calculated over a block of symbols of limited length over which the channel coefficients are supposed to remain unchanged. The smaller is the block length (i.e., the faster the channel variations), the more important this cross-correlation is. This results in an error floor in the Rx BER performance, especially at high SNR, and makes the OP scheme lose its interest [51].
We have studied the interest of iterative data detection and channel estimation to resolve the prob-

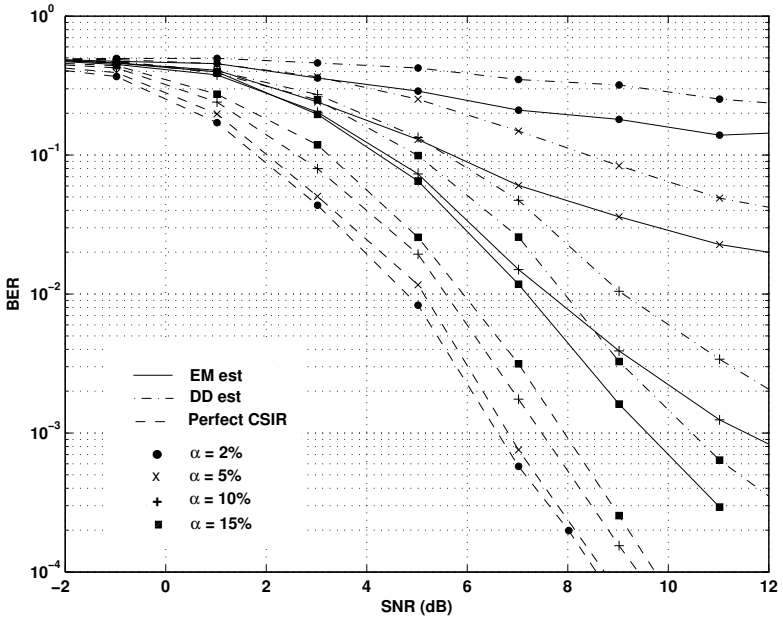

Figure 3.9 — BER after five Rx iterations for EM-based SB, DD, and perfect channel estimation for a (2×4) MIMO system using OP scheme. Uncorrelated Rayleigh quasi-static flat fading, QPSK-modulated pilot and data, $(133,171)_8$ NRNSC rate-1/2 channel code, $N_s = 100$.

lem of error floor by considering two approaches of pilot-only-based decision-directed (DD) estimation [51] and EM-based SB estimation [4, 52]. By the DD method, we proposed to use in each iteration, the soft-estimates of transmitted data symbols using *a posteriori* soft values at the channel decoder output, and to cancel their effect in the channel estimate. The second approach, i.e., EM-based SB estimation provides a better performance at the price of increased Rx complexity [4].

As a case study, let us consider a (2×4) MIMO system using QPSK modulation and iterative soft-PIC detection. We denote by α the ratio of the power of pilot symbols to the total transmit power at a symbol time, i.e., $\alpha = \sigma_p^2/(\sigma_p^2 + \sigma_d^2)$. We have presented in Fig. 3.9, plots of BER versus SNR for DD, EM-based, and perfect channel estimation, and different values of α. Here, SNR stands for the *actual average* received SNR, i.e., $M_R(\sigma_d^2 + \sigma_p^2)/\sigma_n^2$, with σ_n^2 being the Rx noise variance. Pilot sequences for M_T antennas are QPSK-modulated and chosen according to the Walsh-Hadamard series to ensure their orthogonality. For both SB estimation methods, we notice an error floor at high SNR for $\alpha < 15\%$ which is especially visible for $\alpha = 2\%$ and $\alpha = 5\%$. On the other hand, by increasing α, better channel estimates are obtained, but at the same time, less power is dedicated to data symbols. So, increasing α too much, will result in an overall performance degradation. Comparing the performance curves of the EM-based and DD estimators, we see that the performance improvement by the former is quite considerable. This improvement is more important for smaller α values.

3.2.2.6 Improved detection under imperfect channel estimation

Whatever the channel estimation technique, in practice, the Rx can only obtain an *imperfect* estimate of the CSI. Classically, for signal detection, the estimated channel is considered as perfect. This sub-optimal approach is usually called *mismatched* detection. Its sub-optimality is due to the fact that the Rx does not take into account the channel estimation errors [5, 53]. A more appropriate approach is to take into account these estimation inaccuracies in the formulation of the detector. For this purpose, in collaboration with the researchers at LSS lab of Supélec, we have proposed a Bayesian framework based on the *a posteriori* probability density function (PDF) of the perfect channel, conditioned on its estimate. This general framework can be used to formulate any detector by considering the average, over the channel uncertainty, of the detector's cost function that would be applied in the case of perfect channel knowledge.

Assume a channel estimator in which the statistics of the estimation errors are known. This is the case, for instance in the case of pilot-only-based PSAM channel estimation. Let us denote by $\boldsymbol{J}$ the cost function that is used at the detector to decide on the transmitted bits. The improved detection is based on the minimization of a new cost function $\overline{\boldsymbol{J}}$ defined as:

$$\overline{\boldsymbol{J}} = \mathrm{E}_{\boldsymbol{H}|\hat{\boldsymbol{H}}}\{\boldsymbol{J}|\hat{\boldsymbol{H}}\} \tag{3.2}$$

where by using the posterior distribution $p(\boldsymbol{H}|\hat{\boldsymbol{H}})$, we have averaged the cost function $\boldsymbol{J}$ over all realizations of the unknown channel $\boldsymbol{H}$ conditioned on its available estimate $\hat{\boldsymbol{H}}$. Using the metric $\overline{\boldsymbol{J}}$ differs from the mismatched detection on the conditional expectation $\mathrm{E}_{\boldsymbol{H}|\hat{\boldsymbol{H}}}\{.\}$ which provides a robust design by averaging the cost function $\boldsymbol{J}$ over all channel realizations.

We have applied this detection design rule to the cases of iterative MAP and soft-PIC detectors in [5, 53], and showed that significant improvements can be obtained as compared to mismatched detection. The improvement is more important when fewer pilots are used for channel estimation. Thus, the proposed improved detectors are of particular interest under relatively fast-fading conditions, where it is important to reduce the number of pilots to avoid a significant pilot overhead. It is worth mentioning that adopting the improved detection scheme increases only moderately the Rx complexity as it requires just a few more matrix additions and multiplications, compared to the mismatched detector.

As an example, we have shown in Fig. 3.10 plots of BER for mismatched and improved receivers for the case of Gray-mapped QPSK modulation, a (2×2) MIMO system, and iterative soft-PIC detection at the Rx. The number of channel uses for pilot transmission is denoted by N_p. As reference, we have also presented the BER plot for the case of perfect CSI. The SNR gain by using the improved detector for a target BER of 10^{-5} is about 1.4, 0.5, and 0.2 dB, for $N_p = 2$, 4, and 8, respectively. The interesting point is that the two detectors have almost the same convergence trend and the most part of the improvement is obtained after the second iteration for both detectors. We have verified this fact by investigating the extrinsic-information transfer (EXIT) charts of the receivers, which are simple efficient tools for the convergence analysis of iterative receivers [54]. So, if for the reasons of complexity reduction, we only process two receiver iterations, we still have

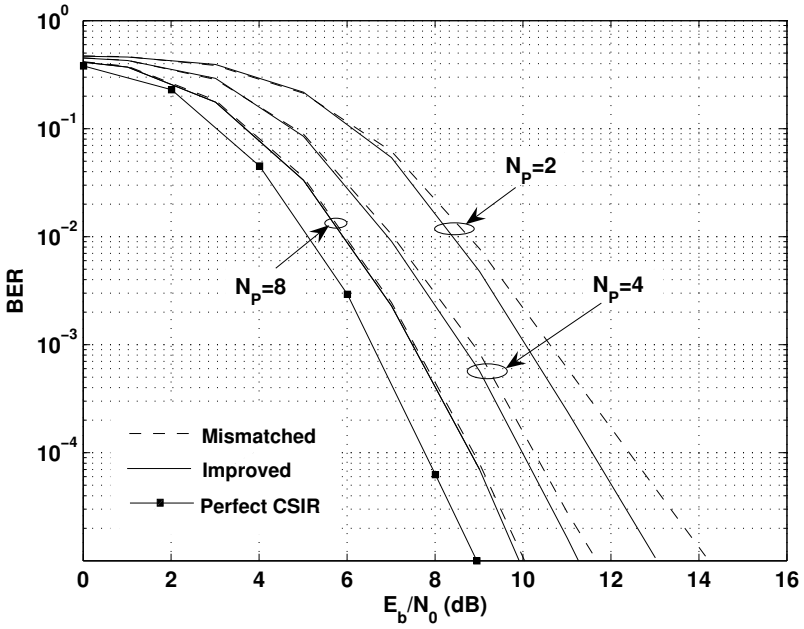

Figure 3.10 — BER performance of improved and mismatched iterative soft-PIC for a (2×2) MIMO with SMux ST scheme. Uncorrelated Rayleigh quasi-static flat fading with $N_c = 4$ fades per frame, QPSK modulation, training sequence length $N_p = 2,\ 4,\ 8$ channel-uses, 5th receiver iteration.

a considerable performance gain by using the improved detector.

3.2.2.7 Multi-carrier modulation for MIMO

Orthogonal frequency-division multiplexing (OFDM) is a spectrally efficient technique for achieving high data-rate wireless transmission over frequency-selective fading channels. This multi-carrier transmission technique offers a simple way to divide the entire channel into a number of narrow-band sub-channels and to multiplex the data over them, thereby allowing an increase in the symbol duration and a reduction of the inter-symbol interference (ISI). In fact, due to the need to very high data rates, most of today's wireless communication systems are faced to ISI and OFDM has become a popular technique to simplify the channel equalization task at the Rx. The combination of OFDM with MIMO technology offers the advantage of high transmission rates and receivers of reasonable complexity by circumventing the need to computationally complex channel equalization. I have been working on the application of multi-carrier techniques to MIMO systems since my post-doc at IETR lab where we were involved in the FP6-IST-4MORE European project on the 4th generation of cellular communication systems. In most of my related research works, I have assumed an uncorrelated channel by assuming perfect interleaving over the sub-channels. Under this assumption, an N_c-carrier OFDM system could be considered as equivalent to a flat MIMO block-fading channel with N_c channel fades per frame of symbols. All of the proposed solutions for single-carrier MIMO systems can then be applied to MIMO-OFDM systems.

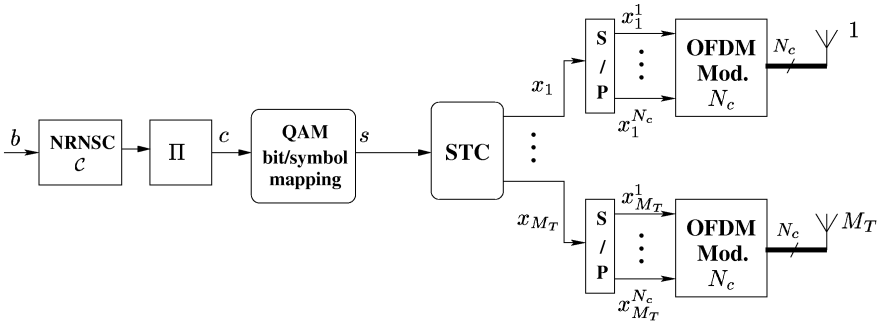

Figure 3.11 — Block diagram of the Tx for a MIMO-OFDM system. N_c denotes the number of sub-carriers, S/P stands for serial-to-parallel conversion.

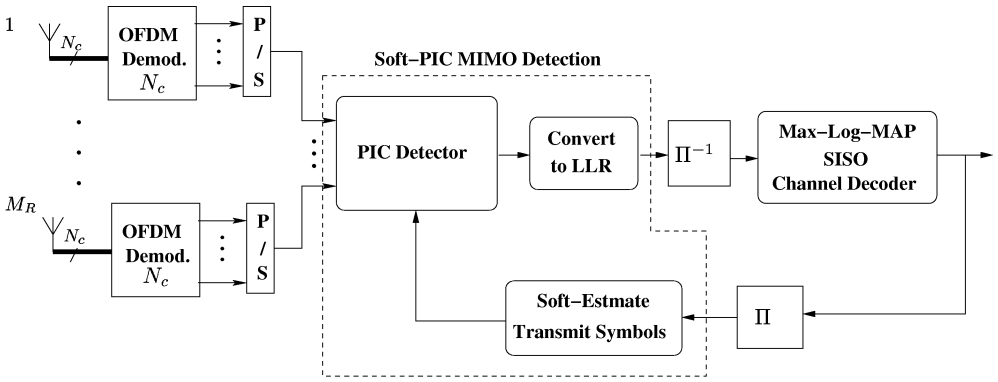

Figure 3.12 — Block diagram of the turbo-PIC Rx for a MIMO-OFDM system. P/S stands for parallel-to-serial conversion and LLR for logarithmic likelihood ratio.

For the sake of clarity, we have provided in Figs. 3.11 and 3.12 the block diagrams of the Tx and the Rx for the case of BICM signaling with turbo-PIC detection.

3.3 Wireless Sensor Networks

3.3.1 Technology overview

Wireless sensor networks (WSNs) are considered as one of the key technologies of the 21st century as they provide exceptional opportunities for monitoring and controlling homes, cities, and the environment [55,56]. A WSN combines inexpensive, yet, smart devices that are usually deployed in large numbers. These devices, called “sensor nodes,” include multiple on-board sensors and computation and communication units, and are networked through wireless links and probably the Internet. Thanks to the recent advances in microelectronics, micro-mechanics, and wireless communications, it is now possible to deploy multi-functional, low cost, low power consumption, and small size sensors. Potential applications of WSNs include environmental and structure monitoring, natural disaster prediction, homeland and physical security, healthcare, traffic surveillance,

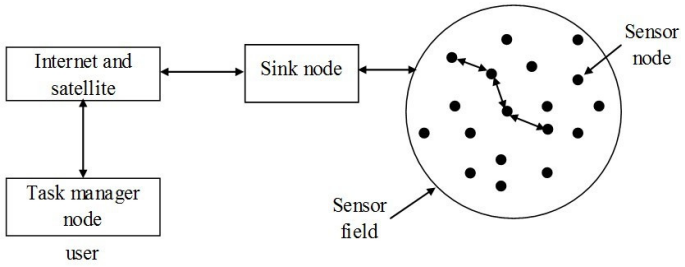

Figure 3.13 — General scheme of a WSN.

industrial and manufacturing automation, video surveillance, military sensing, home appliances and entertainment, etc.

The main advantages of wireless over wired sensor networks are the reduced deployment cost, ubiquity, and the possibility of self-reconfiguration. Also, WSNs use low-cost embedded devices for a wide range of applications and do not rely on any pre-existing infrastructure [57]. This is in contrast to the existing cell phone, WiMAX or WiFi networks, which rely on the pre-deployment of extensive infrastructure support.

In general, the sensor nodes in a WSN are distributed randomly, and there is no need to determine or correct their position. Sometimes, they are deployed in inaccessible areas or on relief for studying the meteorological conditions, for example. This necessitates the automatic self-organization of the sensor nodes to collect information and to transmit it to the data fusion points [56, 58]. This is done thanks to the networking capability that fundamentally differentiates a WSN from a mere collection of sensors, by enabling cooperation, coordination, and collaboration among the nodes [55, 59]. In some WSNs, the nodes do not communicate with a nearby base station, but rather communicate with their local peers, which needs efficient algorithms for data aggregation, ad hoc routing, and distributed signal processing [57, 60]. The general scheme of a WSN is depicted in Fig. 3.13.

Due to size, cost, and energy limitations, WSNs are subject to tight communication and computation constraints. Especially, for battery-operated sensors, energy consumption is an important design parameter because in many applications, replacing batteries may be difficult or impossible. Therefore, the network lifetime should be extended through the design of efficient networking, communication, and signal processing methods.

3.3.1.1 Cooperative diversity

The classical diversity techniques cannot be employed in a WSN due to the stringent constraints on the nodes' size and cost. In particular, it is usually impractical to use multiple antennas at each sensor node. As a result, *cooperative* or *distributed* diversity techniques are mostly employed in WSNs where nodes cooperate among each other to exploit some amount of spatial diversity [61, 62]. In other words, by cooperative diversity, a virtual multi-antenna communication link is

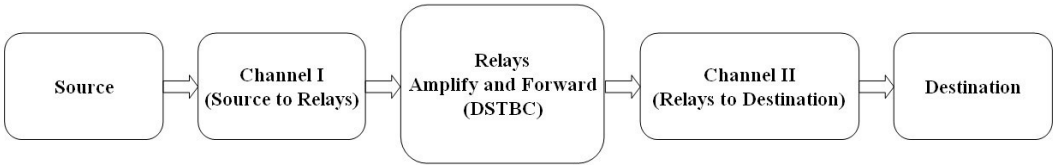

Figure 3.14 — Data transmission block diagram in a typical dual-hop AF WRN.

established between the source and the destination nodes.

3.3.1.2 Wireless relay networks

A simple form of cooperative diversity networks is a wireless relay network (WRN) where some nodes have the role of relaying the signal transmitted from a source node towards a destination node [63, 64]. In such networks, data transmission usually takes place in a multi-hop manner. When "parallel" relays participate in signal transmission, the relay nodes cooperate with each other through the use of some kind of space-time coding in order to benefit from distributed diversity. The use of *distributed* space-time block coding (DSTBC) has extensively been studied in the literature [62,65–67]). Depending on whether the destination knows the CSI or not, there are three main types of DSTBC that can be employed: non-coherent, differential, and coherent schemes.

On the other hand, there are three main cooperation strategies regarding the data processing performed at the relays: amplify-and-forward (AF) [68], decode-and-forward (DF) [69] and demodulate-and-forward (DemAF) [70]. In the AF mode, the relay nodes just amplify the (noisy) received signal from the source node (or the previous relay or a superior level cluster head) and then simply convey it to the destination node (or the next relay or another cluster head). The advantage of the AF strategy is that the relays have no requirement to know the CSI. So, this scheme is interesting regarding power consumption and transmission delay considerations. On the other hand, in the DF mode, the relay nodes firstly decode the received signal and then re-encode, amplify, and forward it to the destination. This way, the noise can be greatly reduced at the expense of complexity and power consumption at the relays. Also, by the DF scheme, CSI is required for signal detection at the relays. Lastly, by DemAF, the received signals at the relays are first demodulated, and then remodulated to reconstruct the transmitted symbols before being sent to the destination. This way, we can effectively eliminate the influence of noise amplification at the relays at the expense of increased network's energy consumption. The general block diagram of a typical dual-hop AF WRN is shown in Fig. 3.14.

3.3.2 Contributions

3.3.2.1 Signal detection in WRN with channel coding

In order to perform node cooperation, we have considered the use of coherent DSTBC at the relays that allows a better system performance [71]. For the case of coherent detection, we have to

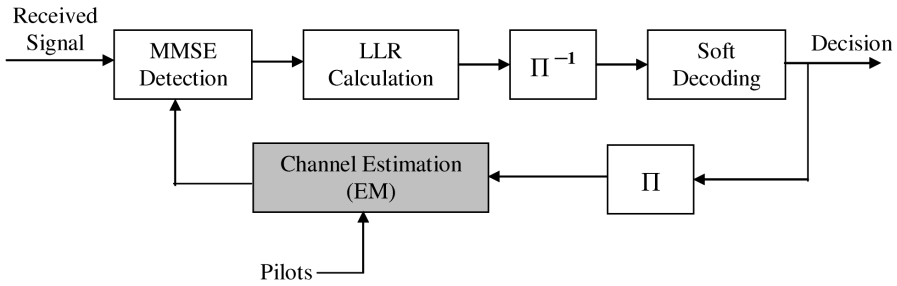

Figure 3.15 — Block diagram of the iterative receiver at the destination node with EM-based SB channel estimation.

estimate the CSI at the destination based on some pilot sequences.

We firstly studied the performance of different DSTBC schemes considering the BICM scheme at the source based on a classical convolutional code. At the destination, we considered soft signal demodulation followed by soft channel decoding. For space-time decoding and signal demodulation, as shown in Fig. 3.15, we first perform minimum mean-square-error (MMSE) detection and then convert the detected symbols to Log-likelihood ratios (LLRs) [38]. These LLRs are next passed to the Max-Log-MAP channel decoder after being de-interleaved.

Consider the general scheme of a WRN with R relay nodes, as shown in Fig. 3.16. When using orthogonal DSTBCs e.g. the Alamouti code for the case of $R = 2$, we can perform signal detection based on the so-called partial channel knowledge, i.e. the product of $f_i g_i$, instead of requiring all fading coefficients separately (see Fig. 3.16). This simplifies considerably the channel estimation task and reduces the overall pilot overhead. On the other hand, at the relays, we perform DSTBC on the pilots, which allows to obtain a better channel estimate. In other words, we suffer from less data-rate loss for the same quality of channel estimate, compared to the time-division multiple-access (TDMA) approach, proposed in [72]. We have shown that for the case of orthogonal DSTBCs at the relays, partial CSI knowledge is practically sufficient for optimal signal detection. When a non-orthogonal DSTBC is employed, however, the performance difference between the two cases of full CSI and partial CSI knowledge becomes more considerable. Nevertheless, the performance degradation due to the use of partial CSI remains acceptable, given the increased network complexity to acquire the full CSI [71].

3.3.2.2 Channel estimation in WRNs

Since power consumption is a critical issue in sensor networks [73, 74], we should minimize the number of pilots in order to reduce power consumption at the source and the relays. Inspired by the main ideas that we presented previously for the case of classical MIMO systems, we have investigated SB channel estimation based on the EM algorithm to address this requirement [75]. We have shown that with this approach, we can considerably reduce the pilot overhead while obtaining a channel estimate of good quality. We have also proposed a modification to the clas-

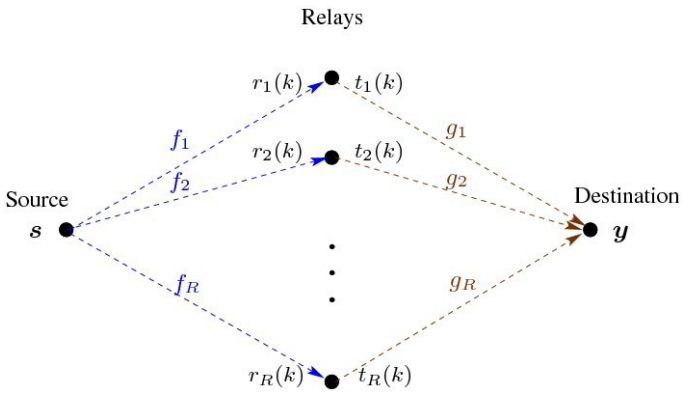

Figure 3.16 — General scheme of the studied WRN: f_i and g_i represent fading coefficients corresponding to the source-relay and relay-destination sub-channels, respectively.

sical formulation of EM, via appropriate combination of the channel estimates obtained using pilots and data symbols separately, in order to further improve the quality of channel estimate. We showed that this approach is particularly interesting for modulations of relatively large constellation sizes [8]. Also, the obtained performance improvement is more significant for a larger number of relays, where we can benefit from more distributed diversity and the contribution of the detected data symbols to channel estimation becomes more beneficial [71].

Figure 3.15 shows the block diagram of the proposed Rx. At the first iteration, we use a primary pilot-only-based channel estimate for signal detection. In the succeeding iterations, iterative channel estimation, signal demodulation, and channel decoding are performed, where we take into account DSTBC at the relays in the estimator formulation. It is worth mentioning that the computational complexity of SB estimation can be justified when we have less stringent constraints on the energy and computational resources of the destination node (where the main computations are done), compared to the source and the relay nodes.

We have further generalized the iterative SB channel estimation scheme to the case of non-orthogonal DSTBCs, where we have proposed to perform iterative DSTBC decoding through iterations. Note that non-orthogonal DSTBCs generally offer higher rates and diversity gains but suffer from high Rx complexity if optimal decoding has to be performed. We have proposed in [76] to perform iterative soft-PIC detection at the Rx together with soft channel decoding and channel estimation, as shown in Fig. 3.17.

3.3.2.3 Improved signal detection with imperfect channel estimate

Due to the relatively high computational complexity of SB methods, in relatively fast fading conditions, the real-time implementation of the Rx may not be an easy task. As an alternative solution, similar to the idea explained for MIMO systems, we have proposed to modify the signal detector at the destination node in order to take into account the imperfect channel estimation. We have used this improved detection method in an iterative Rx, and shown that it allows a signifi-

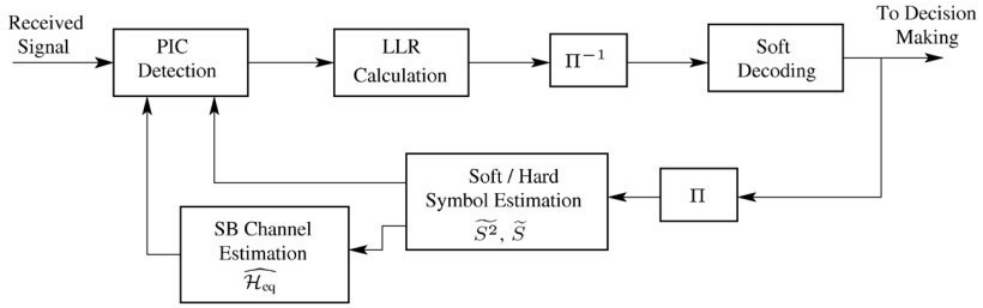

Figure 3.17 — Block diagram of the Rx performing iterative soft-PIC detection and channel estimation. Blocks Π^{-1} and Π represent de-interleaver and interleaver, respectively. Also, $\widehat{\mathcal{H}_{eq}}$ is the estimated equivalent channel matrix, and $\widetilde{S}$ and $\widetilde{S^2}$ denote the soft estimates of the transmitted symbols and their square.

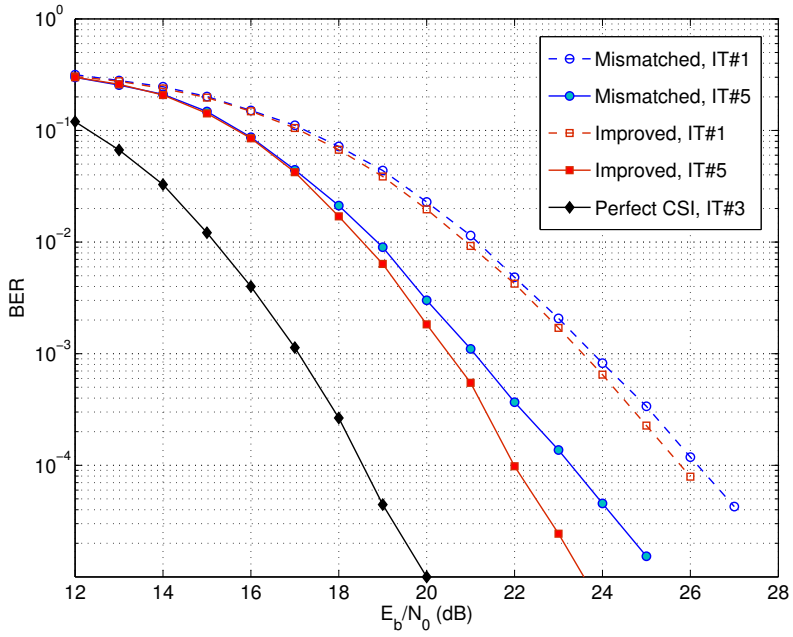

Figure 3.18 — BER performance of the improved and mismatched detectors. $R = 2$ with Alamouti DSTBC; Number of channel-uses per frame for data and pilot symbols is 128 and 1, respectively; 16-QAM modulation with SP bit-symbol mapping; Channel code 1/2-rate NRNSC $(5,7)_8$; Pseudo-random interleaving; IT denotes iteration number.

cant performance improvement while increasing only slightly the Rx's complexity. This improved detection is of special interest for non-constant modulus signal constellations of relatively large size, as well as for relatively low pilot powers [9, 71, 77]. For instance, we have shown in Fig. 3.18 plots of BER versus SNR per bit for a WRN with two relay nodes using 16-QAM modulation with set-partition (SP) [78] bit/symbol mapping. We notice an interesting performance improvement by the improved detector over the mismatched one.

3.4 Cognitive Radio

3.4.1 Technology overview

Cognitive radio (CR) has recently attracted a great attention in order to alleviate inefficient utilization of scarce spectrum resources [79]. In *opportunistic* CR, whenever a primary user (PU) is not present in the radio environment, secondary users (SUs) are allowed to use the frequency band [80]. For this, SUs should perform spectrum sensing to sense and estimate the presence of the PU. In the so-called *underlay* mode, cognitive users are allowed to share the frequency band allocated to a PU as long as no harmful interference is imposed on the PU [80]. Hence, to address the challenge of stringent interference temperature constraint, very low transmit power level is permitted for the SUs, and this can significantly degrade the quality of service (QoS) of the SUs and reduce the coverage of CR networks.

3.4.2 Contributions

3.4.2.1 Signal detection for cognitive WRNs

We have been working on the Rx design for a CR system operating in the underlay mode. Here, we should take into account two fundamental aspects: the low transmit power of SUs and the imposed interference from PU signal transmission. As a matter of fact, the immense potential of cooperative communication to solve the problem of low power transmission and short coverage in underlay paradigm has attracted a great deal of attention [80–82]. As we explained in the previous section, an advantage of WRNs lies in reducing the overall path loss achieved by using one (or a number of) relay(s) between a source and a destination node. So, we have proposed to exploit this potential of WRNs in a CR transmission scenario with the aim of lowering the interference from the secondary network to the PU Rx. This way, benefiting from our research experience on WRNs, we aim to propose efficient transmission solutions in this context.

We are interested particularly in channel estimation issues in such a network. In fact, in a coherent cognitive Rx, besides the additive noise that degrades the channel estimation process, the interference imposed from PU signal transmission degrades the accuracy of channel estimates. Inspired by similar problematics in MIMO and WRNs, described previously, we are currently working on the development of efficient channel estimation and signal detection solutions to deal with these limitations.

3.5 Concluding Remarks

As I explained in the introduction and in the second chapter, before joining Ecole Centrale Marseille and Institut Fresnel in September 2005, I have been mainly working on several topics in RF wireless communications that I briefly described in this chapter. Thereafter, in order to better fit

in the research activities of Institut Fresnel, I started working on OWC to which I have devoted the next chapter. Meanwhile, I continued working on RF communications in parallel with my new research activities, and in particular, considered WSNs and had the opportunity to co-supervise a PhD thesis on this topic. Moreover, I established new collaborations with other research teams whose activities were close to my area of expertise. My continuous participation in the GDR-ISIS seminars in Télécom Paris-Tech (thanks to the support of CNRS) has also been decisive to stay up-to-date about the new evolutions and research topics in the field of RF communications, mainly in areas of cooperative communications, green Radio, MIMO systems, ultra-wideband systems, etc.

While I am highly interested in OWC and am currently devoting an important part of my research activities to this topic, I admit that RF communication is really fascinating to me and I hope I will have the opportunity not to leave totally this field. RF communication is still very promising and offers lots of benefits especially for the new applications and emerging telecommunication technologies. What motivate me further are the new applications and the increasing needs for wireless data transmission. Indeed, the requirement for wireless data transmission in near future will be quite outlandish. For instance, mobile wireless operators are currently witnessing a very fast increase in mobile data traffic due to mobile broadband and mobile Internet; by 2015, there would be a need to about 6 Exabytes of wireless data per month by 2015 [83]; the number of IP mobile connected devices by 2020 is expected to exceed 10 billion [84]; the wireless world research forum (WWRF) envisions about seven trillion wireless devices serving seven billion people by 2020 [85]; and other similar forecasts which appeal for a "revolution" in the wireless data transmission technology where the key question will be spectrum usage. In some special applications, OWC appears to be very promising, but in most of them, such requirements call for new RF communication technologies. As a matter of fact, wireless data transmission is changing its classical from of communication between a single Tx and a single Rx. New applications call for interconnecting machines, vehicles, homes, and health and wellness devices. What's more, the growth of inter-machine communications is expected to be much faster than communications between humans [85]. Interconnecting such heterogeneous wireless devices that can be regarded as a new generation of WSNs is commonly referred to as wireless Internet-of-Things (IoT) [84], which implies different traffic patterns and will load the whole network differently from a "conventional" transmission link. Some key application concepts are smart cities, wireless body networks, software-defined networking, cloud services, and 5G mobile communications. In this view, some fascinating research areas to me are massive MIMO[3], CR, cooperative communication, and network-aware PHY layer design.

[3]Massive MIMO, also known as large-scale antenna systems, very large MIMO, or hyper MIMO, concerns mainly the use of a large number of antenna elements in the base stations for 5G mobile networks. Extra antennas help improve the network coverage, throughput, and energy efficiency by focusing energy into ever-smaller regions of space by using inexpensive low-power components [86]. For this, the base station needs the CSI in both uplink and downlink.

Chapter 4

Research Works on Optical Wireless Communications

Contents

4.1 Introduction

Globally, I have been working on three different technologies related to wireless optical communications, which are free-space optical (FSO) communications, underwater wireless optical communications (UWOC), and visible light communications (VLC). In the following, I will firstly provide an overview of each technology and the related most important challenges before specifying my contributions.

4.2 Free-Space Optical Communications

4.2.1 Technology overview

FSO systems are usually used for high-rate communication between two fixed points over distances up to several kilometers. In comparison to RF counterparts, FSO links have a very large optical bandwidth available, allowing much higher data rates. Today, terrestrial FSO products with transmission rates of 10 Gbps are already in the market [87] and the speeds of recent experimental FSO systems are competing with optical fiber. Because FSO systems use very narrow laser beams, this spatial confinement provides a high reuse factor, an inherent security, and robustness to electromagnetic interference. Furthermore, the frequency in use by the FSO technology is unlicensed worldwide (at least, at the present time), releasing the need for license fees. FSO systems are also easily deployable and can be reinstalled without the cost of dedicated fiber optic connections.

FSO systems have initially attracted attention as an efficient solution for the “last mile” problem to bridge the gap between the end-user and the fiber optic infrastructure already in place.

Other applications of the FSO technology include enterprise/campus connectivity, video surveillance and monitoring, back-haul for cellular systems, redundant link and disaster recovery, etc. [88, 89].

4.2.1.1 Channel modeling for FSO systems

The optical power launched from the Tx is affected by various factors before arriving at the Rx. These include system loss, geometric loss, misalignment loss, atmospheric loss, atmospheric turbulence, and background noise. System loss highly depends on the design specifications and is usually specified by the manufacturers. We provide here a brief description of the other factors.

- Atmospheric loss
  The particles affecting the visibility such as rain, snow, fog, but also pollution, dust, aerosols, smoke, etc., absorb to some degree the laser light energy, causing an attenuation of the optical power. These particles further cause light scattering, which is the deflection of incident light from its initial direction, causing spatial, angular, and temporal spread. When the particle diameter is on the order of the wavelength, the resulting scattering coefficient is very high. That is why the most detrimental environmental conditions are fog and haze as they are composed of small particles with radii close to the near-IR wavelengths. Even modest fog conditions can highly attenuate IR signals over shorter distances. Experimental tests have reported about 90% loss in the transmit power over a distance of 50 m in moderate fog [90, 91]. It should be noted that, given the typical data rates of FSO links, the channel delay spread as a result of beam scattering due to fog or rain is practically negligible. For instance, it is shown in [92] that the channel root mean square (RMS) delay spread under moderate and dense fog is typically limited to 50 picoseconds for a 1 km link. Consequently, the channel can effectively be considered as frequency non-selective, introducing no ISI.

- Atmospheric turbulence
  Under clear atmosphere conditions, we are faced to another adverse effect known as scintillation or atmospheric turbulence. Inhomogeneities in the temperature and the pressure of the atmosphere, caused by solar heating and wind, lead to the variations of the air refractive index along the transmission path [93] (see Fig. 4.1). The resulting atmospheric turbulence causes random fluctuations in both amplitude and phase of the received signal, i.e., channel fading. This results in a considerable degradation of the system performance, especially in long-distance transmissions of about several kilometers [93, 94]. To illustrate the effect of the atmospheric turbulence on the received optical intensity, we have shown in Fig. 4.2 the irradiance on the observation plane for transmission through vacuum and turbulent atmosphere that we have obtained via wave-optics simulations [95].

  To quantify the fluctuations resulting from atmospheric turbulence, the scintillation index

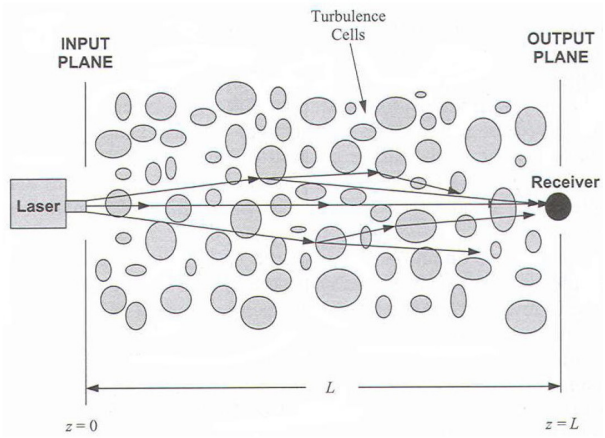

Figure 4.1 — An example of optical wave propagation through atmosphere (Reproduced from [93]).

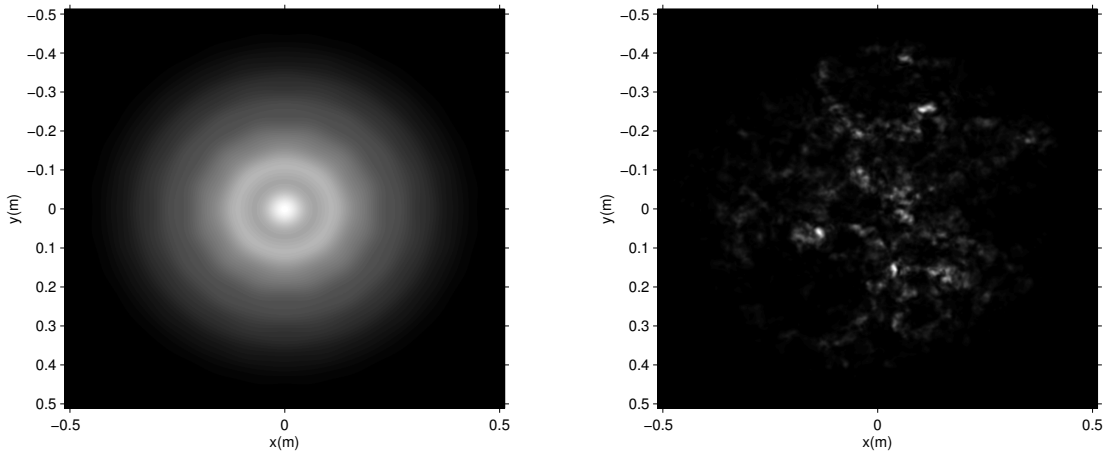

(a) (b)

Figure 4.2 — Received intensity for an FSO link at a distance of 1.5 km; (a) in vacuum; (b) in the presence of turbulence with $C_n^2 = 6.5 \times 10^{-14}\ \mathrm{m}^{-2/3}$ and the inner and outer scales of turbulence of 6.1 mm and 1.3 m, respectively. Transmitter uses a divergent Gaussian beam operating at $\lambda =$ 1550 nm with the beam waist = 1.59 cm and a beam divergence of $\theta_{\mathrm{div}} = 0.46$ mrad.

(SI) is frequently used in the literature. It is defined as:

$$\sigma_I^2 = \mathrm{E}\{I^2\}/\mathrm{E}\{I\}^2 - 1, \tag{4.1}$$

where I is the intensity of the received optical wave. In addition, the Rytov variance is widely used as a measure of the strength of atmospheric turbulence, which is defined for the case of plane wave propagation as [93]:

$$\sigma_R^2 = 1.23 C_n^2 k^{7/6} L^{11/6}, \tag{4.2}$$

where k and L are the optical wave number and link distance, respectively, and C_n^2 is the index of refraction structure parameter (see Subsection 4.2.2.2). Typically, the turbulence is classified into three regimes of weak, moderate, and strong turbulence, which correspond to $\sigma_R^2 \ll 1$, $\sigma_R^2 \sim 1$, and $\sigma_R^2 \gg 1$, respectively [93].

Several statistical channel models have been proposed for the distribution of turbulence-induced fading in FSO systems so far. Especially, there have been significant effort to establish a universal model that is applicable to any type of turbulence conditions. These efforts mainly relied on the use of doubly stochastic theory of scintillation in which the large- and small-scale turbulence eddies are supposed to induce refractive and diffractive effects on the light beam, respectively [93]. A popular model is the Gamma-Gamma ($\Gamma\Gamma$) distribution which has gained wide acceptance in the current literature. By this model, the received intensity I is considered as the product of two independent Gamma random variables X and Y, which represent the irradiance fluctuations arising from large- and small-scale turbulence, respectively. The PDF of I is [93]:

$$p(I) = \frac{2(ab)^{(a+b)/2}}{\Gamma(a)\,\Gamma(b)} I^{(a+b)/2-1} K_{a-b}(2\sqrt{abI}),\ I > 0, \tag{4.3}$$

where the parameters a and b represent the effective numbers of large- and small-scale turbulence cells, $\Gamma(.)$ is the Gamma function, and $K_m(.)$ is the modified Bessel function of second kind and order m. The SI by this model is given by

$$\sigma_I^2 = \frac{1}{a} + \frac{1}{b} + \frac{1}{ab}. \tag{4.4}$$

Concerning the temporal characterization of turbulence, in most practical cases, the channel fading is very slowly varying and the channel coherence time is typically 0.1 to 10 ms [89]. Since in FSO systems we are concerned with very high transmission rates on the order of several tens of Mpbs to several Gbps, the channel fading coefficient remains constant over thousands up to millions of consecutive bits. Therefore, FSO channels should be considered as quasi-static [96].

- Background noise
  Background radiations, also called background noise or ambient noise, can also degrade the performance of FSO links. It may consist of direct sunlight, reflected sunlight, or scattered

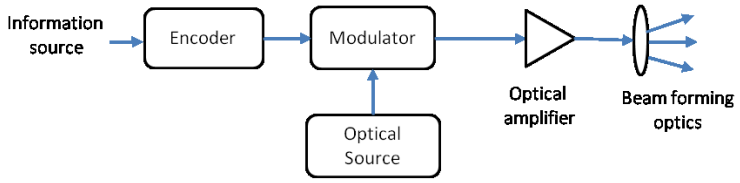

Figure 4.3 — The general block diagram of the FSO Tx.

sunlight from hydrometeor or other objects [18,97,98]. This, in turn, results in a reduced SNR and effective Rx sensitivity [99]. In some circumstances, background radiations can even cause link outages because of the saturation of the Rx [18]. In fixed field-of-view (FOV) receivers, the background noise power is proportional to the Rx pupil area [97]. Experimental measurements indicate that while the received optical signal power is typically about tens to hundreds of μW, the background radiation power is in the range of several μW for scattered sunlight by clouds or fog, about hundreds of μW for reflected sunlight, and up to about 10 mW for direct sunlight [100]. However, this latter case can statistically occur less than 1 hour per year.

4.2.1.2 FSO signal transmission

In an FSO communication system, the information waveforms are modulated onto an optical carrier. The generated optical field is radiated through the atmosphere towards the Rx where the optical field is collected and transformed to an electrical signal by a photo-detector (PD), and then processed to recover the original transmitted information. Current FSO systems typically operate in the near-IR wavelengths. Since certain wavelengths can experience severe absorption due to the presence of different molecules in the atmosphere [98], there are special wavelength windows, located around four specific wavelengths of 850, 1060, 1250, and 1550 nm, where a relatively low attenuation of less than 0.2 dB/km is experienced [101]. Interestingly, the 850 and 1550 nm windows coincide with the standard transmission windows of fiber communication systems. That is why most of commercially available FSO systems operate at these two windows so as to use the corresponding available off-the-shelf components.

- Transmitter
  As we have illustrated in Fig. 4.3, the Tx consists of an optical source, an encoder, a modulator, probably an optical amplifier, and beam forming optics. The modulated laser beam is passed through the optical amplifier to boost the optical intensity. The light beam is collected and refocused by means of beam forming optics before being transmitted. The typical optical source in FSO systems is a semiconductor laser-diode (LD).

- Receiver
  Although coherent systems offer superior performance in terms of background noise rejection, mitigating turbulence-induced fading, and higher Rx sensitivity [89], non-coherent sys-

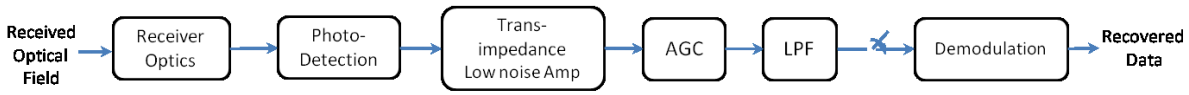

Figure 4.4 — IM/DD FSO Rx block diagram.

tems are commonly used in terrestrial FSO links due to their simplicity and low cost. Due to this reason, I have focused on non-coherent systems so far. These systems are also known as intensity-modulation direct-detection (IM/DD) where the intensity of the emitted light is employed to convey the information, as shown in Fig. 4.4.

At the Rx side, optical filters and a lens are typically used to collect and focus the received beam onto the PD. The PD output current is next converted to a voltage by means of a trans-impedance (TIZ) circuit, usually a low-noise Op-Amp with a load resistor. This latter is determined based on the transmission rate, the dynamic range of the converted electrical signal, the generated Rx thermal noise, and impedance matching with the other Rx parts. The output of the TIZ is then low-pass filtered in order to limit the thermal and background noise levels. The solid state PD can be a P-i-N (PIN) diode or an avalanche photo-diode (APD). PIN diodes are usually used for FSO systems working at ranges up to a few kilometers. The main drawback of PIN PDs is that the Rx performance becomes very limited by the thermal noise. For long distance links, APDs are mostly used which provide a current gain thanks to the process of impact ionization. The drawback of APDs, in turn, is the excess noise at their output, which models the random phenomenon behind the generation of secondary photo-electrons. Due to this reason, the APD gain is usually optimized with respect to the received signal power in order to maximize the received SNR [102]. The advantage of APD comes at the expense of increased implementation complexity and the Rx power consumption, however.

- Intensity modulation
  The most commonly used IM technique due to its implementation simplicity is on-off keying (OOK), which is a binary level modulation scheme. In OOK signaling, modulated data is represented by the presence (“on”) or absence (“off”) of a light pulse in each symbol interval. At the Rx, for optimal signal detection, we need to know the instantaneous channel fading coefficient to perform dynamic thresholding. The CSI can be estimated with good accuracy by using a few pilot symbols in practice [11]. In addition to the need to dynamic thresholding at the Rx, OOK has relatively poor energy and spectral efficiency.
  Several other IM schemes have been proposed to overcome some disadvantages of OOK. Pulse position modulation (PPM) is a powerful solution from the point of view of energy efficiency. For a classic optical channel under peak and average power constraints, PPM can attain the near-optimum channel capacity [97]. When performing hard signal detection at the Rx, PPM has the advantage that, in contrast to OOK, it does not require dynamic thresholding for optimal detection [19, 103].
  In comparison to PPM, multipulse PPM (MPPM) brings the further advantages of having a

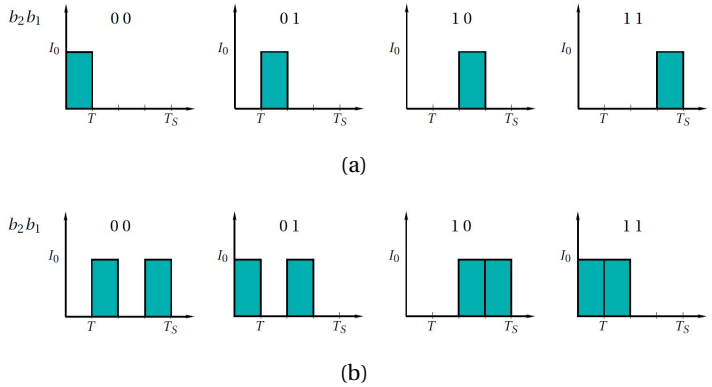

Figure 4.5 — Examples of PPM and MPPM symbols. (a) Bit/symbol mapping for 4-PPM; (b) Bit/symbol mapping for 2-4PPM. I_0 stands for the transmitted light intensity in an "on" slot. T and T_s denote slot and symbol durations, respectively.

reduced peak-to-average power ratio (PAPR) and a higher spectral efficiency [104] while it has an increased demodulation complexity [19] (examples of bit/symbol mapping are shown in Fig. 4.5 for 4-PPM and 2-4PPM modulation schemes). Note that, although there is a large bandwidth available in the optical band, spectral efficiency is still an important design consideration since it is directly related to the required speed of the electronic circuitry in an FSO system from a practical point of view.

4.2.1.3 Diversity techniques

An efficient way of reducing the effect of atmospheric turbulence is to employ diversity techniques. The simplest solution is that of aperture averaging, which is considered as "inherent" receive diversity, and consists in using a relatively large lens at the Rx to average over intensity fluctuations. This technique is efficient when the Rx lens aperture is larger than the (spatial) fading correlation length $\sqrt{\lambda L}$, with λ and L denoting the wavelength and link distance, respectively [105]. Fading reduction by aperture averaging is usually quantified by considering the so-called aperture averaging factor, which is defined as:

$$A = \sigma_I^2(D)/\sigma_I^2(0), \tag{4.5}$$

where $\sigma_I^2(D)$ and $\sigma_I^2(0)$ denote the scintillation indexes for a Rx lens of diameter D and a point Rx (of diameter $D \approx 0$), respectively. Figure 4.6 shows an example of wave-optics simulations that illustrates the interest of aperture averaging in reducing the turbulence effect at the Rx.

Another solution is to employ time diversity by using channel coding and bit-interleaving [11, 106]. However, the main drawback of this solution is that it imposes long delay latencies and requires relatively large memories for storing long data frames.

The most practical and widely used solution to mitigate the atmospheric turbulence is spatial diversity, which can be realized by employing multiple beams at the Tx, multiple apertures at

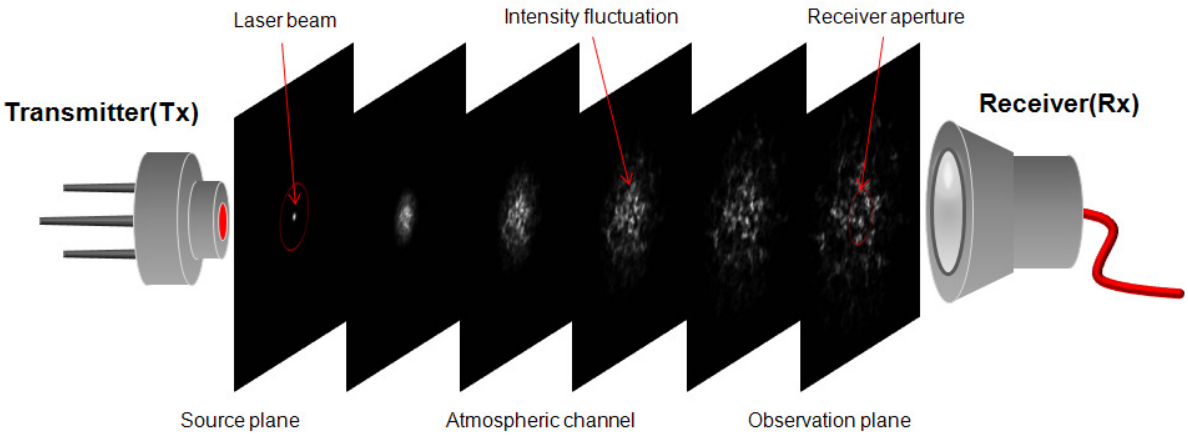

Figure 4.6 — Illustrating the aperture averaging technique. Same conditions as in Fig. 4.2.

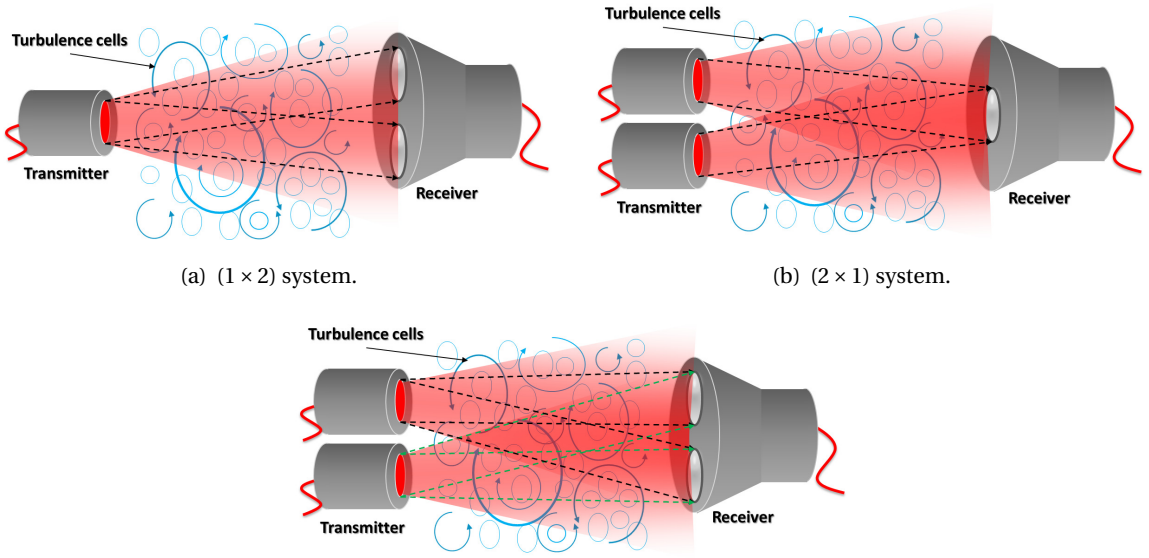

(a) (1 × 2) system.

(b) (2 × 1) system.

(c) (2 × 2) system.

Figure 4.7 — Schematic of SIMO, MISO, and MIMO FSO systems with two apertures at the Rx or/and at the Tx.

the Rx, or a combination of them [93, 107–109]. In contrast to the classical single-beam single-aperture configuration that we will call SISO (standing for Single-Input Single-Output), these configurations are usually referred to as SIMO, MISO, and MIMO, respectively. This technique has also been adopted in several commercial products [110]. We have illustrated space-diversity systems with two apertures at the Rx or/and at the Tx in Fig. 4.7.

For SIMO systems, usually equal-gain combining (EGC) is performed at the Rx, which provides performance close to the optimal maximal-ratio combining (MRC) while having the advantage

of lower implementation complexity [107, 111]. For a MISO FSO system, the simplest signaling scheme is to send the same signal on the different beams; what is usually referred to as repetition coding (RC).
MIMO systems are mostly proposed to reduce the turbulence-induced fading effect by employing RC at the Tx. Nevertheless, an interesting point is to use ST coding at Tx in order to optimize the system performance. A fundamental difference between the ST codes for RF and IM/DD-based FSO communications is that the latter employs nonnegative (unipolar) real signals rather than complex signals [112]. Indeed, most of the proposed ST schemes for RF applications use phase rotation and amplitude weighting, requiring at least bipolar signaling when applied to the FSO context. In general, the ST schemes optimized for RF systems provide full diversity in FSO systems but are not optimized concerning the coding gain [113].
Most of the OSTBC schemes proposed for RF systems can be modified in order to adapt to IM/DD FSO systems by introducing a DC bias to overcome the constraint of unipolar signaling. Due to this DC bias, OSTBC schemes suffer from a degradation in the system performance, compared with the low-complexity RC scheme. Although both RC and OSTBC provide full diversity, RC is quasi-optimum [114]. As a non-orthogonal scheme, we can use spatial multiplexing (the SMux scheme) by simply multiplexing the information bearing signals at the Tx, or to use the so-called optical spatial modulation (OSM) by which only one “on” slot is transmitted from the multiple beams at a given channel-use in order to avoid inter-channel interference [115]. At the Rx, optimal maximum likelihood detection (MLD) can be used to estimate the transmitted bits.

4.2.1.4 Hybrid RF/FSO systems

The performance of FSO links can seriously be affected due to several factors such as severe turbulence in long-span links, strong attenuation in dense fog, misalignment and pointing errors in mobile links, etc. These factors can result in frequent link failures, and hence, there is an important need to increase the reliability of such links. One efficient solution is to use an RF link in parallel with the FSO link so as to serve as back-up in the case of FSO link outage. Although the corresponding data rate in the RF channel can be less than the main FSO link, it can ensure connectivity when the FSO channel becomes inoperative. In effect, such an RF link is less subject to atmospheric turbulence and pointing errors [116], and furthermore is much less affected by fog. As a matter of fact, fog and rain drastically affect FSO and RF links, respectively, but they rarely occur simultaneously. Therefore, concerning these meteorological phenomena, the two links can operate in a complementary manner. Some commercially available hybrid RF/FSO products (see Fig. 4.8) use an RF link as a back-up channel. The RF link is usually designed in the unlicensed X and Ku bands or millimeter waves (MMW) around 60 GHz. For hybrid RF/FSO long-span links, the RF link can also be used for beam acquisition and pointing as well as for the purposes of link control in hybrid automatic-repeat-request (HARQ) scenarios due to its higher reliability [117].

Figure 4.8 — Pictures of hybrid RF/FSO products (Courtesy BridgeWave and LightPointe).

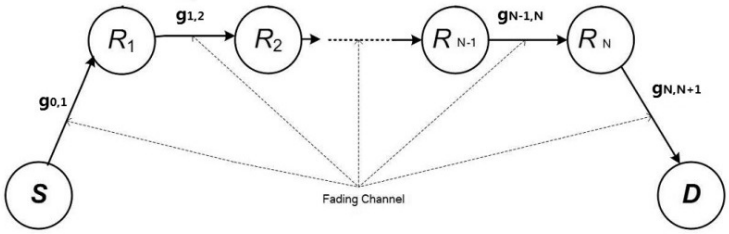

Figure 4.9 — Serial FSO relaying configuration, S, R_i and D represent the source, the i^{th} relay node, and the destination, respectively. $g_{i,i-1}$ is the channel gain between $(i-1)^{\text{th}}$ and i^{th} relay nodes.

4.2.1.5 Cooperative FSO systems

Similar to the context of RF wireless communications, cooperative or relay-assisted transmission is a useful way to broaden the network's coverage area and also to mitigate channel fading. Serial relaying or multi-hop FSO transmission takes advantage of shorter hops and provides significant performance improvements since fading variance is distance-dependent in FSO systems. This is rather different from the RF case where multi-hop transmission is used to extend range but does not provide any fading reduction advantage. On the other hand, parallel relaying can be implemented through the use of multiple Tx apertures directed to the relay nodes. Note that the broadcast nature of wireless RF transmission (i.e., the cost-free possibility of the transmitted signals being received by other than destination nodes) is not present in FSO transmission which is based on LOS transmission through directional beams. This fact makes parallel relays of limited interest in FSO links. Figure 4.9 illustrates the typical scheme of a serial FSO relay system.

Inspired by the ideas in the well-known RF counterparts, several signaling strategies have been proposed for relay-assisted FSO links. The classical approaches consider AF, DF, and detect-and-forward (DetF) protocols [118, 119].

4.2.2 Contributions

In collaboration with our colleagues of Özyeğin University at Istanbul, we have recently published a comprehensive survey of the research works accomplished so far on FSO systems from a communication theory point of view in [10]. This paper presents, in particular, a general overview of OWC, the applications and pros and cons of the FSO technology, as well as different research topics on FSO systems. A sample of this paper is provided in the appendix. My specific research contributions are described in the following.

4.2.2.1 Receiver noise modeling

We have investigated comprehensive noise modeling in FSO receivers, which consist of the PD dark current, the Tx noise, thermal noise, and the photo-current shot-noise (which arises from input signal and/or background radiations) [97, 120, 121]. The PD dark current can be neglected in most practical cases. The Tx noise arises from the instability of the laser intensity and the resulting fluctuations of the photo-current at the Rx, which are modeled by considering the so-called laser relative intensity noise (RIN) [120]. However, RIN has usually a negligible effect on the Rx performance [121]. Thermal noise originates from the Rx electronic circuitry, mainly the load resistor, and is modeled as a zero-mean Gaussian random process. On the other hand, shot noise, also called the quantum noise, arises from random fluctuations of the current flowing through the PD and is modeled by a Poisson process. In the case of using a PIN PD, if the mean number of absorbed photons is relatively large, the shot noise can be approximately modeled by a Gaussian process [120]. In most FSO applications, the received photon flux is high enough to allow this approximation. In the case of using an APD, the distribution of the number of generated electrons can also be approximated by a Gaussian [121, 122]. Notice that this is also true when background radiations cannot be neglected. We have verified that if the background illumination level is negligible, the two main noise sources affecting the Rx are thermal and shot noises. PIN-based receivers are usually thermal-noise limited whereas APD-based receivers are usually shot-noise-limited except for relatively small values of the load resistor where the thermal noise also affects the performance [121].

It is worth mentioning that we consider usually the electrical SNR at the Rx in order to determine the system performance. Lets P denote the transmit optical power, η the PD quantum efficiency, H the channel fading coefficient, and n the Gaussian-modeled Rx noise of zero mean and variance σ_n^2. The average electrical SNR per bit at the Rx is considered as $\left((\eta P)^2 \mathrm{E}\{H\}^2\right)/(4\sigma_n^2)$.

4.2.2.2 Channel modeling for FSO

Atmospheric turbulence is mainly characterized by three parameters: the inner and the outer scales of turbulence denoted respectively by l_0 and L_0, and the index of refraction structure parameter C_n^2, sometimes called the turbulence strength [94]. According to the Kolmogorov theory, L_0 is

the largest cell size before the energy is injected into a region and l_0 is associated with the smallest cell size before energy is dissipated into heat [93]. Usually, the outer scale is approximated as $L_0 \to \infty$ since it has a negligible impact on turbulence in practice [94]. We have investigated the effect of the inner scale l_0, and have shown that it has a significant impact on the turbulence [12]. In particular, larger values of l_0 result in a higher irradiance variance in the strong turbulence regime.

4.2.2.3 Mitigating misalignment loss

When no tracking mechanism is used at the Rx side, which is typically the case for entry model FSO links with a range of several hundred meters, the misalignment loss can be alleviated by increasing the beam divergence at the Tx. In collaborations with OCRG lab researchers, we have proposed the use of spatially partially coherent Gaussian beams to mitigate the misalignment-induced pointing errors. We have investigated the optimization of the beamwidth and the spatial coherence length with respect to the variance of pointing errors and the turbulence strength [17, 123].

4.2.2.4 Mitigating background noise

We have firstly considered background noise modeling. Background noise can be statistically modeled by a Poisson random process [18, 120]. When the background radiation level is relatively high, the average number of the corresponding received photons is large enough to allow the approximation of the Poisson distribution by a Gaussian distribution [120]. Since the mean value of the background noise is rejected by the ac-coupled Rx circuitry, the noise has zero mean. Furthermore, we have shown in [121] that the contributions from the interaction of the signal with background radiations due to the non-linear characteristic of the photo-detector can practically be neglected, and as a result, a signal-independent Gaussian model can be used.

The effect of background noise can be reduced by means of narrow spectral bandpass and spatial filtering prior to photo-detection. Nevertheless, a non-negligible background noise may fall within the spatial and frequency ranges of the detector that can limit the system performance by causing a variable offset in the converted electrical signal. As a more efficient technique, we proposed in [18] to work with two laser wavelengths and to perform signal detection at the Rx in a differential manner. We called this method differential signaling for which the block diagram of the Rx front-end is shown in Fig. 4.10. At the Tx, we send the signal on two wavelengths λ_1 and λ_2 which have a difference of about tens of nanometers. This way, we can consider almost the same channel fading coefficient corresponding to the two wavelengths. For instance, when using OOK modulation, the signals sent on the two wavelengths are complementary. At the Rx, we use equal-bandwidth narrow optical bandpass filters (BPFs) on λ_1 and λ_2 to separate the signals of the two lasers and then perform signal detection in a differential mode. This way, we can practically reject the background noise whereas the thermal noise variance will increase by a factor of 2 due to differential signaling, which is a quite negligible price to pay.

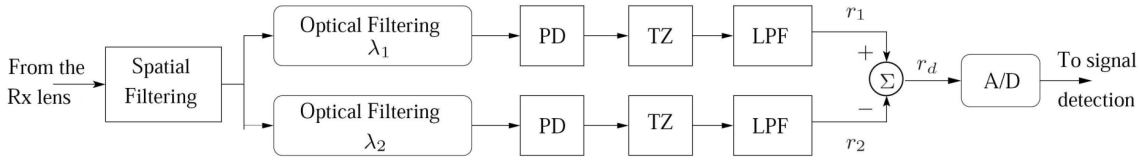

Figure 4.10 — Block diagram of the Rx front-end when performing differential signaling. PD: photo-detector and bias circuit, TZ: trans-impedance circuitry, LPF: low-pass filter, A/D: analog-to-digital converter.

4.2.2.5 FSO channel capacity

Since FSO channels are subject to atmospheric turbulence, the channel capacity should be considered as a random variable due to the randomness of the channel fading coefficient [27]. As the channel coherence time is relatively large, the outage capacity becomes more meaningful here [12]. Considering the ΓΓ turbulence model, we have studied in [12] the outage capacity of FSO systems when employing aperture averaging or spatial diversity techniques to reduce fading effect. For instance, we have shown in Fig. 4.11 curves of C_{out} versus the Rx lens diameter D for the case of strong turbulence with Rytov variance of 19.18, background-noise-limited Rx, uncoded OOK modulation, an outage probability of 10^{-9}, and a moderate average received SNR of 15 dB. From Fig. 4.11(a), corresponding to a SISO system, we notice that C_{out} increases from 0.05 to 0.86 bit/symbol by increasing D from 20 to 100 mm [12]. Also, from Fig. 4.11(b), for a four-aperture FSO system of apertures' diameter 10 and 50 mm (with the same total Rx aperture size as for the SISO case), C_{out} equals 0.61 and ~ 1 bit/symbol, respectively.

4.2.2.6 Channel coding and time diversity

One potential solution for mitigating fading in FSO channels is channel coding. Investigating the efficacy of channel coding in FSO systems, we have shown that it is particularly useful under weak turbulence conditions [12]. It is also efficient in moderate and strong turbulence regimes provided that the impact of turbulence can be first significantly reduced, for example, by means of other fading-mitigation techniques such as aperture averaging, diversity techniques, or adaptive optics.

On the other hand, time diversity can be exploited through the use of channel coding and interleaving. However, as explained previously, the FSO channel coherence time is about 0.1-10 ms. Therefore, fading remains constant over hundreds of thousand up to millions of consecutive bits for typical transmission rates. For atmospheric channels with such long coherence times, exploiting time diversity necessitates long delay latencies and the use of large memories for storing long data frames (see the system block diagram in Fig. 4.12). In addition, since the duration of the fades is random, no single maximum interleaving depth can be used to render the channel completely memoryless. Furthermore, when aperture averaging is employed at the Rx, exploiting time diversity through channel coding becomes more difficult and even practically infeasible [12]. Because,

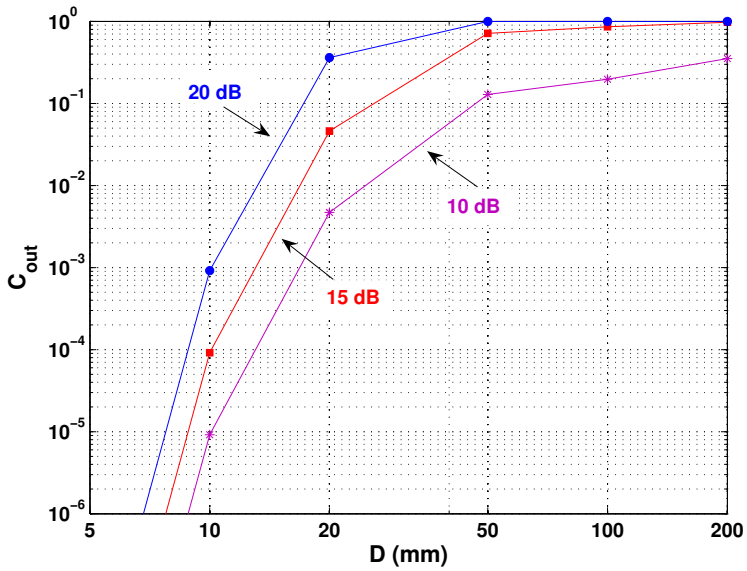

(a) SISO

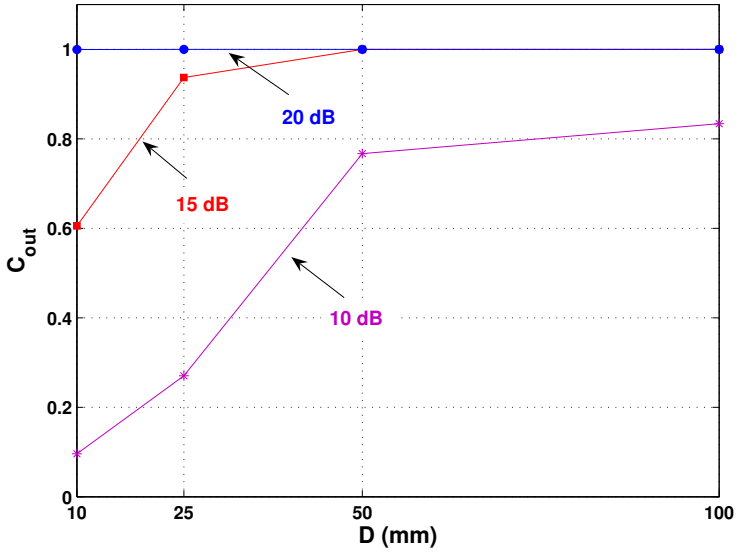

(b) SIMO

Figure 4.11 — Outage capacity C_{out} (in bits per channel-use) versus Rx lens diameter D for strong turbulence regime with $\sigma_R^2 = 19.18$. $P_{\text{out}} = 10^{-9}$, OOK modulation, plane wave propagation, $l_0 = 0$, Gaussian beam with the same parameters as in Fig. 4.2. (a) SISO configuration; (b) (1×4) SIMO configuration.

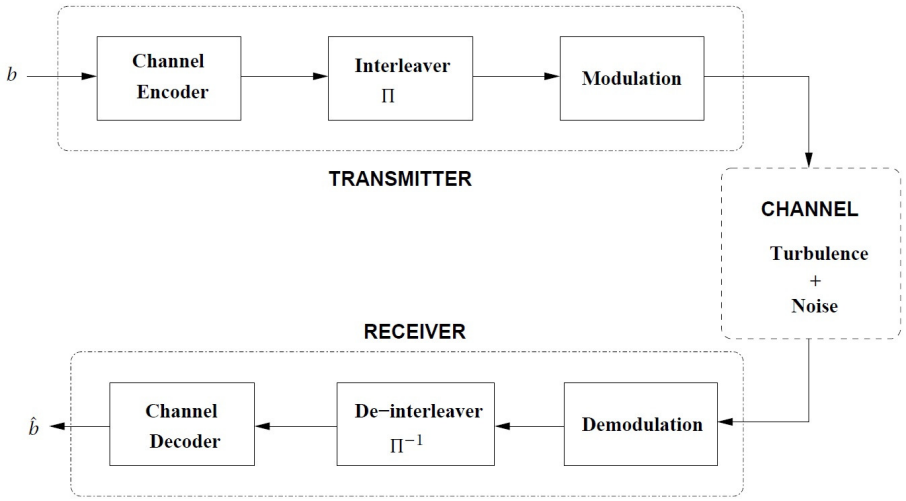

Figure 4.12 — System block diagram for time-diversity using channel coding.

under the assumption that the channel time variations are mostly due to the transversal wind (with respect to the optical axis), the use of a relatively large aperture size results in a large channel coherence time. Regardless of the interleaver size issues, we investigated the use of interleaved convolutional codes, turbo-codes, and concatenated Reed-Solomon (RS) and convolutional codes in [11], where we concluded that convolutional codes may be a suitable choice under any turbulence regime as they make a good compromise between complexity and performance.

Apart from the problem of atmospheric turbulence, channel coding is usually used in order to mitigate the effect of background and Rx noises. Most of the existing works on coded FSO systems assume binary modulation. In order to perform efficient error correction in the case of non-binary modulations, we should either use non-binary codes, or adapt the binary codes to these modulations. Use of non-binary codes necessitates a considerable decoding computational complexity [97] that can be prohibitively large for a practical implementation in a high rate FSO system. Whereas RS coding is a relatively low-complexity solution for PPM-based modulations[1], it cannot provide satisfying performance improvement, in particular, due to hard decoding that is usually performed at the Rx. As another solution, we proposed in [19] to use a classical binary convolutional code and to do iterative soft demodulation and decoding at the Rx. We called this scheme BCID, standing for Binary Convolutional encoding with Iterative Detection. The general block diagram of the Rx is shown in Fig. 4.13. We provided a detailed analysis of this approach in [125] and further extended it to the case of MPPM modulation in [19]. We showed that this solution is quite efficient and suitable for not too-high transmission rates, so that iterative signal detection can be performed in real time.

[1] For example, a (n,k) RS code is matched to Q-ary PPM for $n = Q-1$ [124].

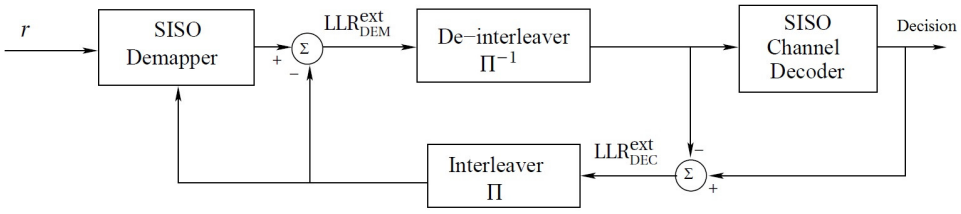

Figure 4.13 — Block diagram of the iterative receiver in BCID transmission scheme. $\mathrm{LLR}^{\mathrm{ext}}_{\mathrm{DEM}}$ and $\mathrm{LLR}^{\mathrm{ext}}_{\mathrm{DEC}}$ denote the extrinsic soft-values at the demapper and the channel decoder, respectively.

4.2.2.7 Spatial diversity

- **Aperture averaging**

  In collaboration with our colleagues at ONERA-Châtillon, we firstly revisited the effect of aperture averaging from a communication theory point of view by investigating its real impact on the system BER and outage capacity under different turbulence conditions [12] . We showed that a substantial scintillation reduction can be obtained by this technique, especially in the case of moderate-to-strong turbulence. For instance, considering OOK modulation, $\Gamma\Gamma$ fading under moderate turbulence conditions with Rytov variance of 2.56, and a target BER of 10^{-5}, the SNR gain with respect to a point Rx is about 30, 47, and 60 dB for Rx lens diameters of 20, 50, and 200 mm, respectively [12]. We have also shown in [12, 126] that the performance improvement by aperture averaging is most significant for plane wave and Gaussian-beam propagation models, and also when more complex modulation schemes (e.g. PPM) are used. Another important point is the change in fade statistics when using aperture averaging. In fact, since averaging is specially performed over small-scale irradiance fluctuations, the PDF of the channel fades shifts toward that of large-scale fluctuations [108]. We have verified that the received signal is well described by a log-normal distribution for about $D > 6\rho_0$ [126]. Here, ρ_0 is the spatial coherence radius, defined as follows in the case of plane wave propagation:

$$\rho_0 = (1.46\, C_n^2\, k^2\, L)^{-3/5}. \tag{4.6}$$

- **Space diversity**

  Instead of using a large aperture, we can use several smaller apertures at the Rx, and this way, benefit from some degree of aperture averaging as well as spatial diversity after combining the signals of the different apertures. Assuming uncorrelated fading on the different apertures' signals, we have shown that the multiple aperture solution provides a better performance than the solution of using a large aperture if we consider the same total effective aperture area in the two cases [12]. For instance, considering background-noise-limited receivers, OOK modulation, $\Gamma\Gamma$ fading with Rytov variance of 19.18, and a target BER of 10^{-5}, we have an SNR gain of about 7 dB by using four apertures of 50 mm diameter each, compared to using a single aperture of 100 mm diameter [12].

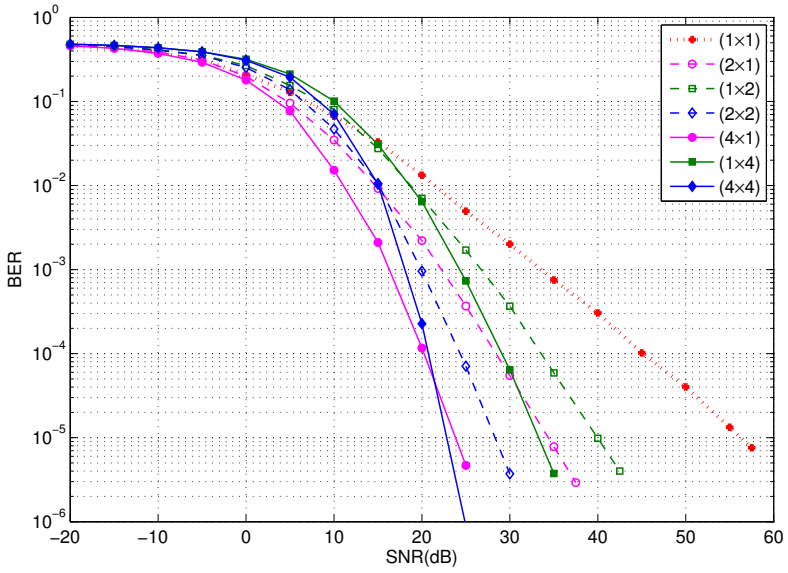

Figure 4.14 — Contrasting BER performance of MISO, SIMO, and MIMO FSO systems with RC and EGC. $L = 5\,\text{km}$, $D_R = 50\,\text{mm}$ for the SISO system. Uncoded OOK, thermal noise limited Rx. Other conditions are the same as in Fig. 4.2.

It should also be noted that, from a practical point of view, the use of a too large lens necessitates a PD with a large active area as well, in order to capture the received photons on the lens focal plane. This will, in turn, impose severe constraints on the system data rate because such a PD will have a relatively large parasitic capacitance.

As another example, we have contrasted in Fig. 4.14 the BER plots for SISO, SIMO, MISO, and MIMO configurations, where RC is used in multiple beam systems to have the same transmission rate for all configurations and EGC is used for multiple aperture configurations. Also, we set the same total Rx aperture size for the four systems. We notice that the MISO system outperforms SIMO, which is because the former benefits from more aperture averaging and also suffers from less noise at the Rx. For instance, at a target BER of 10^{-5}, we have a SNR gain of 9.5 dB for the (4×1) system, compared to the (1×4) system. We notice also that MIMO systems outperform MISO for relatively high SNR. For instance, the (4×4) system provides a better performance than the (4×1) system for SNR larger than about 21 dB.

- **MIMO FSO systems**

  We have investigated the appropriateness of different ST schemes for MIMO FSO systems. Our aim has been to verify the quasi-optimality of RC with respect to non-orthogonal ST schemes. In particular, we fixed the information transmission rate as well as the average transmit optical power for different ST schemes and contrasted their performance assuming no bandwidth constraint. In other words, we wanted to see if we are not limited by practical

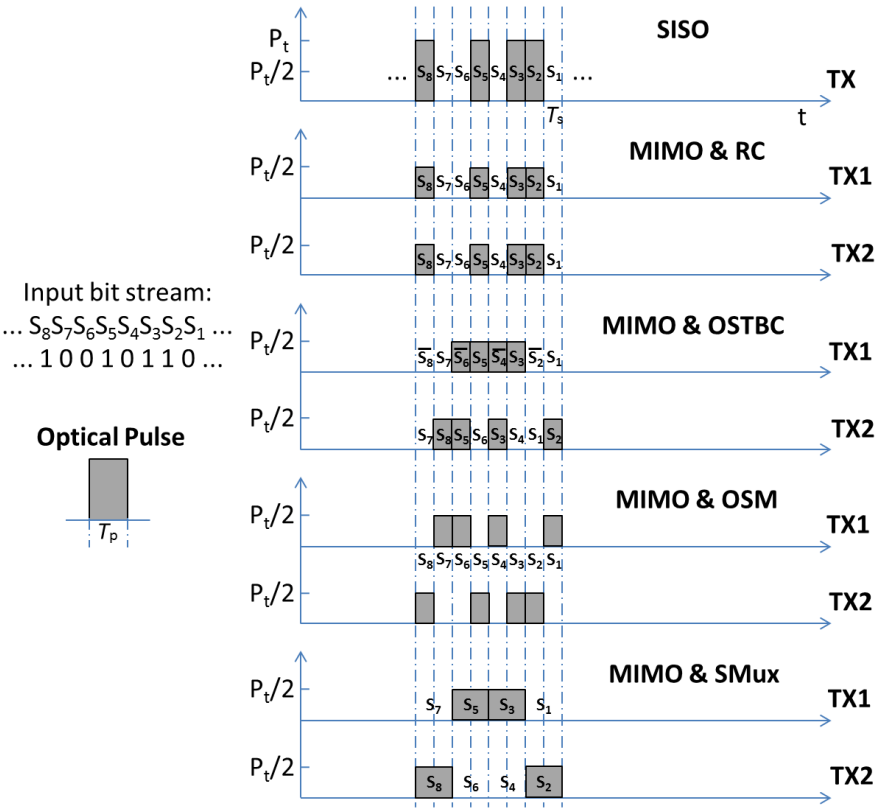

Figure 4.15 — Symbol mapping for different ST schemes in a (2 × 2) MIMO system. Overall transmission data rate and average optical transmit power are fixed for different ST schemes.

implementation considerations such as time synchronization and electronic circuitry speed, whether or not there is an interest to use non-orthogonal ST schemes. As an example, Fig. 4.15 shows an example of the symbol mapping for RC, OSTBC, OSM, and SMux ST schemes for a (2 × 2) system [95]. We showed in [127] that instead of using non-orthogonal ST schemes, we can alternatively use the simple RC with shorter pulse durations while having a better system performance. However, it should be noted that practical limitations on the bandwidth can impose constraints on the minimum pulse width, in which case, the higher-rate ST schemes could become preferable to RC.

For example, consider a link distance of 5 km, ΓΓ fading with Rytov variance of 24.7, a total Rx aperture diameter of 200 mm, a target BER of 10^{-5}, uncoded OOK modulation, and MLD detection at the Rx. Fixing the average transmit power as well as the effective transmission data rate for different ST schemes, we modify the pulse duration for each scheme accordingly. Then, for a MIMO structure of two transmit and two receive apertures, the RC scheme outperforms OSTBC, SMux, and OSM in the average received SNR by 2, 31.5, and 37 dB, respectively [95, 128].

- **Fading correlation effect**

  Evaluating fading correlation for space-diversity FSO systems under practical conditions and

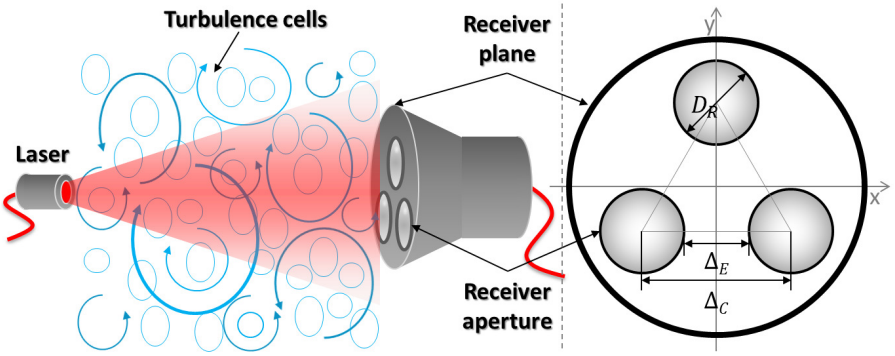

Figure 4.16 — Schematic of an FSO link with a triple-aperture Rx with the Rx geometry depicted on the right.

its effect on the system performance has been another research axis on which we have been collaborating with our colleagues at ORCG lab. As a matter of fact, diversity techniques are most efficient under the conditions of uncorrelated fading on the underlying sub-channels. In practice, however, the performance of spatial diversity systems is impaired by fading correlation. This is because it is not always practically feasible to satisfy the required spacing between the apertures at the Rx and/or between laser beams at the Tx to ensure uncorrelated fading. Under weak turbulence conditions, the required aperture edge separation Δ_E equals the correlation length $\sqrt{\lambda L}$, which is in fact the typical size of scintillation speckles [12]. In the relatively strong turbulence regime, the spatial correlation arises mainly from large-scale fluctuations, where larger aperture spacings are required. For the case of plane wave propagation, we have $\Delta_E = \lambda L / r_0$, where r_0 is the Fried parameter. As an example, assuming the wavelength $\lambda = 1550\,\text{nm}$ and the index of the refraction structure parameter $C_n^2 = 4.58 \times 10^{-13}\,\text{m}^{-2/3}$, we have $\Delta_E \approx 6.4\,\text{cm}$ for $L = 500\,\text{m}$ (moderate turbulence regime), and $\Delta_E \approx 37\,\text{cm}$ for the case of $L = 1500\,\text{m}$ (strong turbulence regime) [12]. Indeed, if the required spacing is more or less reasonable under moderate turbulence conditions, it becomes too large for the strong turbulence regime.

We have quantified the spatial fading correlation in different system configurations using wave-optics simulations based on the split-step Fourier-transform algorithm, where the effect of atmospheric turbulence is taken into account by considering a set of random phase screens [95]. This way, we studied the effect of different system parameters on the fading correlation.

For example, consider a triple-aperture (SIMO) FSO configuration as shown in Fig. 4.16. We have presented in Fig. 4.17 the curves of the average correlation coefficient ρ as a function of aperture spacing Δ_C for aperture diameter $D_R = 50\,\text{mm}$ and different link spans L. We have also shown on each calculated point the error bar corresponding to one standard deviation of the estimation error [95]. Logically, it is seen that the correlation decreases by increasing the aperture spacing. However, it increases for increased link distance because more atmosphere

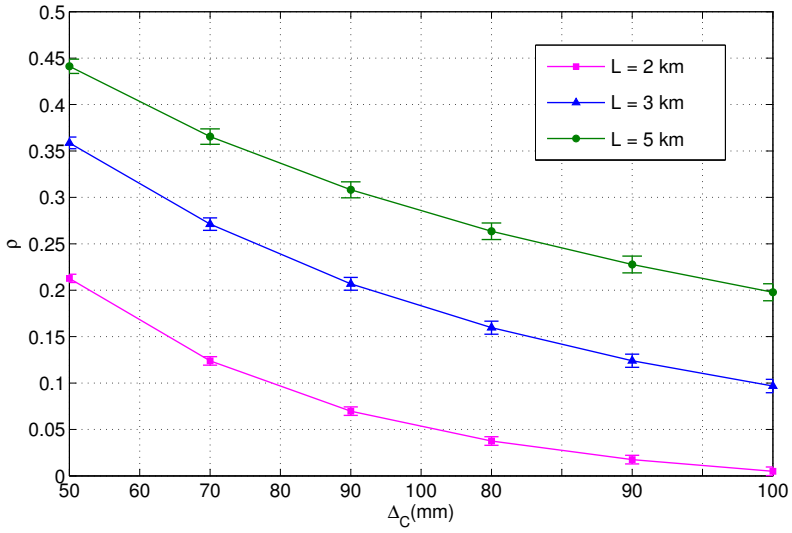

Figure 4.17 — Average correlation coefficient versus aperture spacing in a triple-aperture FSO system for different link distances. $D_R = 50$ mm.

eddies affect the different Rx apertures at the same time. For the same reason, correlation increases by increased Rx aperture size [15, 95]. Also, we have shown that at relatively large link distances where the scattering disk (defined as $L/k\rho_0$) is much larger than the Rx aperture size, the fading correlation coefficient is almost independent of the apertures' diameter and depends only on the apertures' edge separation [15]. When using a doubly-statistic fading model considering separately small- and large-scale fading effects, we showed in [14] that in most practical cases, we can effectively assume uncorrelated small-scale fading and assign the correlation to the large-scale fading component.

Another important question is to see how fading correlation affects the FSO system performance, compared to the uncorrelated fading case. For this purpose, it is necessary to develop an appropriate statistical model. In [13], for a SIMO system with two receive apertures, we approximated the sum of correlated $\Gamma\Gamma$ random variables by an α-μ distribution in order to evaluate the BER performance of the Rx.[2] We then generalized this idea to the case of multiple diversity in [15, 130]. Also, we proposed in [16] the Padé approximation method [131, 132] to obtain the PDF of sum of correlated $\Gamma\Gamma$ random variables from their moment generating function (MGF), that we then used to evaluate the system performance analytically.[3] How-

[2] The α-μ distribution (also called *generalized Gamma*) is a flexible distribution that can be reduced to several distributions such as Gamma, Nakagami-m, exponential, and Rayleigh [129].

[3] More specifically, we first derived in [16] a general expression for the calculation of the n^{th}-order joint moments of arbitrarily-correlated large-scale turbulence Gamma random variables from the corresponding MGF. Next, we obtained an infinite series representation for the MGF of the sum of correlated $\Gamma\Gamma$ random variables that we approximated by Padé approximants in terms of a simple rational function. Then, we obtained the PDF of the sum of $\Gamma\Gamma$ random variables by taking the inverse Laplace transform of the Padé approximant via the residue theory. We evaluated the system performance in terms of the average BER and the outage probability based on the resulting PDF.

ever, due to the limitation of Padé approximation, this method cannot be used for very low BERs, i.e., lower than 10^{-8}.

4.2.2.8 Hybrid RF/FSO solutions

Since a special application of the FSO technology is to provide back-haul for cellular networks, with our colleagues of OCRG lab we have proposed in [133, 134] a new concept for hybrid base-transceiver-station architectures. The hybrid FSO/RF system is integrated at the macro-cell tier, in order to enable high-capacity and power-efficient wireless back-hauling. This solution can be quite interesting in developing "green" metropolitan areas. Meanwhile, we proposed a resource prioritization mechanism to maintain optimal on-demand resource allocation, and to establish sustainable back-haul link availability via switching between the FSO and RF sub-systems [133].

Furthermore, we have recently investigated the viability of using a hybrid RF/FSO link through an experimental study at OCRG lab using a dedicated laboratory chamber to emulate the fog scenario encountered in an outdoor environment (see Paragraph 4.2.2.10). We used an RMS power detector to monitor the signal quality of the primary FSO link and to decide on hard switching between FSO and RF links upon the change in the link visibility. We showed that effective switching between the links depends on the transmission data rate and the target BER [135].

With our colleagues at OCRG lab and Czech Technical University at Prague we are currently investigating a hybrid RF/FSO link scheme that can offer very high link availability. This will obviously be at the cost of additional switching and buffering when using the lower-rate RF link.

4.2.2.9 Relay-assisted FSO links

In collaboration with our colleagues at Özyeğin University and OCRG lab, we have recently studied the performance of a serial FSO relaying system employing DF or AF signaling at the relays. In particular, for the case of DF signaling, we have derived analytical expressions for the outage probability considering an aggregate channel model that takes into account both path loss and ΓΓ turbulence-induced fading. For the case of AF signaling, we have obtained a closed-form expression by assuming perfect available CSI at each relay [136, 137]. We are currently working on this subject with our colleagues at OCRG lab.

4.2.2.10 Experimental works

In addition to the theoretical studies that I have conducted during the past years, I had the opportunity to carry out some experimental results in a controlled atmospheric chamber, emulating an FSO transmission link, at OCRG lab in Northumbria University. These experiments could be realized thanks to the collaboration between Institut Fresnel and the OCRG lab via the Opticwise COST Action IC1101, and the financial support of Institut Carnot-STAR at Aix-Marseille University (concerning my visiting of OCRG lab in April 2013).

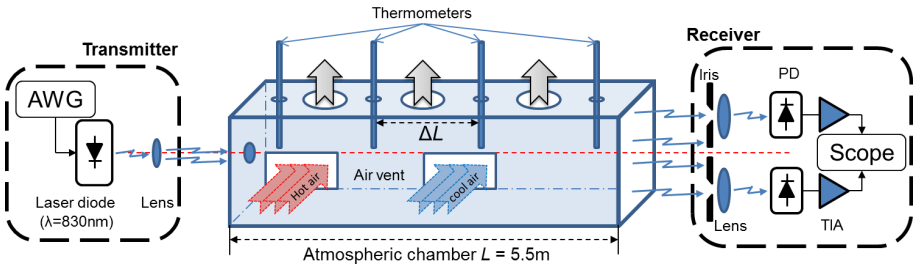

(a)

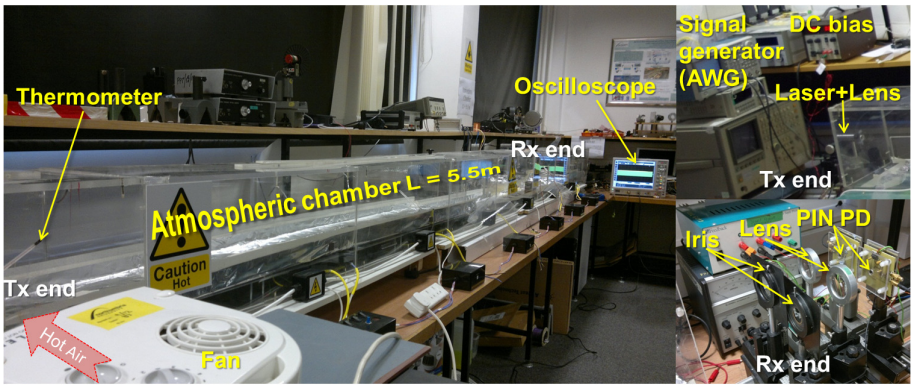

(b)

Figure 4.18 — Atmospheric chamber used in OCRG lab to emulate an FSO link subject to turbulence, fog, and smoke. (a) Block diagram of the experiment setup; (b) Snapshots of the Tx end, the atmospheric chamber, and the Rx end.

The schematic diagram of the experiment setup of a single-laser dual-aperture FSO system is shown in Fig. 4.18(a). At the Tx (as shown at the right top of Fig. 4.18(b)), a laser diode and a collimated lens are used. The collimating lens at the Tx can be adjusted to launch the laser beam with an appropriate divergence angle so that the two collecting lenses at the Rx side can be illuminated totally. The transmit signal is generated by using an arbitrary waveform generator (AWG) with different modulation schemes and directly modulates the emitted laser intensity. A DC bias is added to the signal to let the laser work in the linear region of optical power versus injection current characteristic curve. The laser beam propagates through the atmospheric chamber of dimension $550 \times 30 \times 30\,\text{cm}^3$ (see Fig. 4.18(b), left). Within the chamber, to generate a controlled level of turbulence, independent fans that blow hot or cool air are used to produce a wind perpendicular to the light beam and to maintain a temperature gradient between the Tx and the Rx. At the Rx, two apertures are used, each one consisting of an iris diaphragm, a collecting lens and a PIN PD. The electrical signal at the output of each PD is amplified by a TIZ. A high-frequency digital oscilloscope is used to capture the output signal from TIZs and to carry out some analysis on the received signal, such as calculating the Q-factor, defined as [138]:

$$Q = \frac{\upsilon_H - \upsilon_L}{\sigma_H + \sigma_L}, \tag{4.7}$$

where v_H and σ_H denote the mean value and the standard deviation of the received voltage for a bit '1' in OOK modulation, and v_L and σ_L correspond to a bit '0'. Indeed, the Q-factor is usually used in experimental works to evaluate the system performance instead of measuring the BER which is highly time-consuming. In fact, a higher Q-factor signifies a lower BER as the "high" and "low" states for a received OOK symbol are more distinguishable.

In addition to performing several experiments in the designed FSO-simulating chamber that allowed me to understand better the practical limitations behind implementing an FSO link and also to validate a part of my theoretical studies, we realized a longer transmission link in an amphitheater and generated the conditions of strong turbulence by using several fans and heaters along the path.

4.3 Underwater Optical Communications

4.3.1 Technology overview

Demands for underwater communication systems are increasing due to the on-going expansion of human activities in underwater environments such as environmental monitoring, underwater exploration, offshore oil field exploration/monitoring, port security and tactical surveillance. As such, there is a serious requirement to improve the performance of underwater communication systems in order to effectively use the equipments and the resources. The high cost, lack of flexibility and operational disadvantages of wire-line (particularly optical fiber) systems to provide real-time communication in underwater applications become restrictive for many cases. This triggers the growing demand for underwater wireless links. While acoustic communication suffers from a very small bandwidth available, very low celerity, and large latencies due to the low propagation speed, UWOC which is able to achieve data rates of hundreds of Mbps (and even up to Gbps) for short ranges (typically several tens of meters), appears as an attractive alternative (or as a complementary solution) to long range acoustic communications. In fact, water is relatively transparent to light in the visible band of the spectrum and absorption takes its minimum value in the blue/green spectral range (450 nm-550 nm) [21, 139].

A few UWOC units of limited application have been commercialized very recently. For instance, Ambalux [140] has introduced a commercial UWOC system with a maximum data rate of 20 Mbps over ranges up to 40 m. Also, Sonardyne [141] has commercialized the BlueComm UWOC system, claimed to operate over distances of up to 200 m with a maximum rate of 20 Mbps. Nevertheless, in many respects, this technology still requires further research efforts to overcome several major technical challenges before its wide-scale deployment. Most of current researches are being done in North American organizations such as North Carolina [142], Woods Hole Oceanographic Institution (WHOI) [143], Naval Air Warfare Center [144], and MIT [145].

4.3.1.1 Channel modeling for UWOC systems

The study of feasibility and reliability of an underwater optical link necessitates accurate channel modeling by taking into account the seawater optical properties. The propagation of light underwater is typically modeled by the radiative transfer equation (RTE) [146] which involves integro-differential equation of time and space that characterizes a light field traversing a scattering medium. Different analytical and numerical methods can be used to solve the RTE. The main drawback of the analytical methods is their mathematical complexity. Numerical methods based on Monte Carlo simulations are interesting alternative solutions to RTE and provide a powerful tool that can adequately model light propagation within a scattering medium even if its inherent optical properties (IOPs) vary in space and time [147].

4.3.1.2 Beam misalignment

In a typical UWOC system, angle scattering is highly peaked in the forward direction. Therefore, the optical beam has a high directivity, which turns out to be problematic from the point of view of system implementation. In fact, link misalignments are unavoidable in underwater systems, especially when communicating with a remotely-operated vehicle (ROV). In fact, due to stringent constraints on energy consumption, precise localization and tracking mechanisms may not be feasible to employ. Misalignment errors can seriously impact the performance and reliability of the communication link. This is specially the case for small FOV receivers. As a matter of fact, inserting a lens in front of the PD has the advantage of increasing the received optical intensity but it seriously limits the Rx FOV and, hence, increases the sensitivity to link misalignment [148]. This problem is slightly alleviated in high turbidity waters where we can paradoxically benefit from beam spatial dispersion which helps reduce the sensitivity to link misalignments [144].

An efficient solution may be to use an array of LEDs at the Tx and/or an array of PDs at the Rx. For instance, compact arrays of seven LEDs and seven PDs in the form of truncated hexagonal pyramid structures were used in [142] to achieve quasi-omnidirectional patterns. This allows a large overall Rx FOV and substantial Tx-Rx alignment simplification in practice. The further advantage of such arrays is that we can estimate the angle of arrival of the optical signal at the Rx in order to correct the Rx position/direction or to perform beam steering at the Tx electronically toward the best direction in order to optimize the energy consumption.

4.3.2 Contributions

I describe in the following my contributions and research results on UWOC systems. Most of these works have been accomplished thanks to tight collaborations with our colleagues at IFERMER La-Seyne-sur-Mer. It is worth mentioning that we have recently presented a state-of-the-art of the most recent works on UWOC including theoretical studies and experimental works on channel modeling and transmission schemes, as well as some of the remaining challenges in an invited

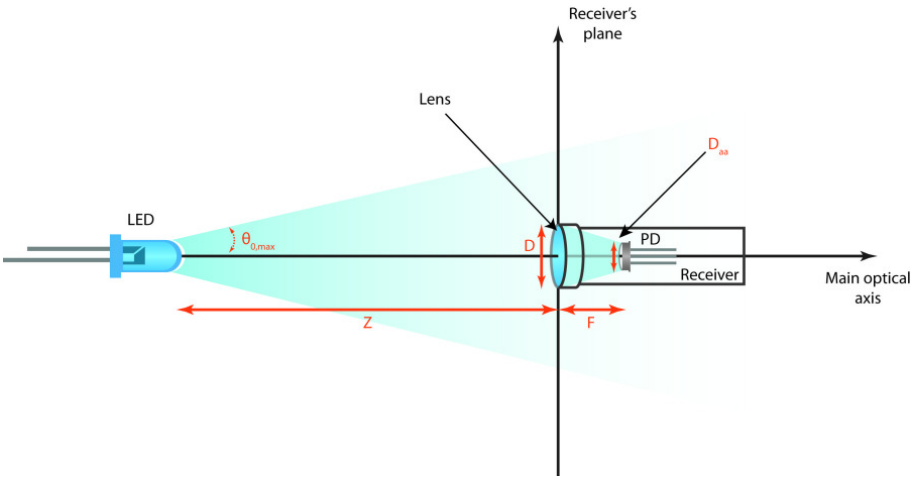

Figure 4.19 — Schematic of an optical wireless underwater link with distance Z, Tx divergence angle $\theta_{0,\max}$, and Rx aperture diameter D.

paper in ICTON 2014 conference [20].

4.3.2.1 Channel characterization and modeling

Modeling and characterization of the underwater optical channel is the key step for an efficient, reliable, and robust UWOC system design. We have investigated the underwater optical channel by characterizing the channel impulse response (CIR) via Monte Carlo simulations of the trajectory of photons launched from the Tx until arriving on the Rx PD active area (if not lost meanwhile) [21, 149]. We considered the two-term Henyey-Greenstein (TTHG) model [150, 151] for the volume scattering function (VSF), which is the main IOP that characterizes light scattering in water. For modeling the channel, we took into account the interaction of photons with water molecules as well as with particles in water. Upon interaction with the in-suspension/solution particles, a propagating light beam is deviated from its initial direction through the scattering process, and a part of its intensity is absorbed and converted into other forms of energy. We considered the so-called Case 1 waters where organic particles and phytoplankton are dominant. For this water type, the channel is characterized mainly by the Chlorophyll concentration [152], which determines the scattering and absorption properties and depends highly on the water type, depth, temperature, etc. Also, we took into account different system parameters such as the Tx beamwidth and beam divergence, wavelength, water type and turbidity, link distance, and the receiver's FOV and aperture size. Figure 4.19 shows a simplified schematic of the typical UWOC link we considered in our study.

We quantified the channel time dispersion, especially for different link distances, Tx beam divergences, and Rx lens aperture sizes. We showed that, except for highly turbid waters, the channel time dispersion can be neglected when working over moderate distances. For instance, we have shown in Fig. 4.20 the CIR for different water types, where the abscissa represents the absolute propagation time from the Tx to the Rx. In this figure, Z represents the link distance and c is the

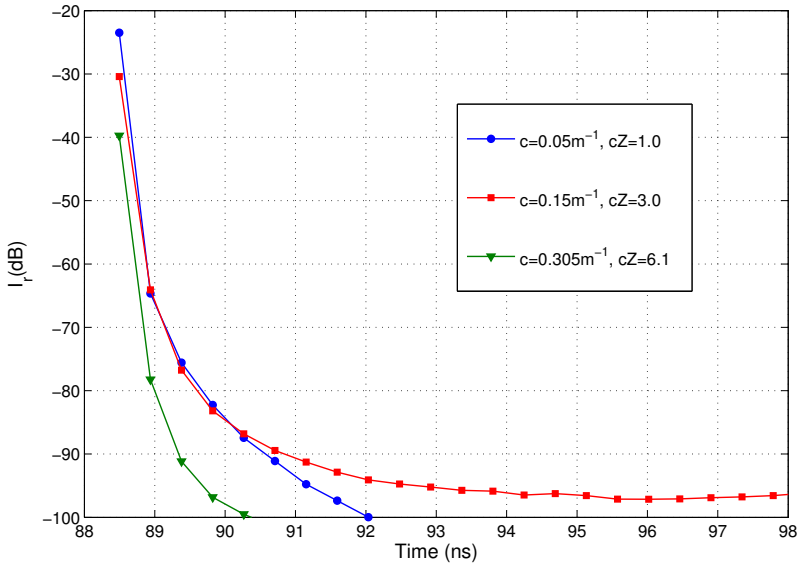

Figure 4.20 — CIR (received intensity as a function of time) for pure sea, clean ocean, and coastal waters. I_r denotes the received optical intensity on the PD active area. Z =20 m, Rx lens diameter D =20 cm and FOV = 180°, Tx divergence angle and beam width $\theta_{0,\max}$ =20° and w_0 =0.3 cm (see Fig. 4.19).

attenuation (also called extinction) coefficient which is set to 0.05, 0.15, and 0.305 m^{-1} for the three cases of pure sea, clean ocean, and coastal waters, respectively. These c values correspond to Chlorophyll concentrations of 0.005, 0.31, and 0.83 mg/m^3, respectively [21, 153].

4.3.2.2 Signal modulation

Most current UWOC works consider uncoded intensity-based modulation although some recent works have also considered channel coding. One critical issue is the Tx power consumption that should be minimized through the judiciously chosen hardware along with the proper selection of data transmission techniques. We have contrasted in [154] the performances of different modulation techniques from the point of view of energy efficiency, considering realistic system parameters and when a PIN PD or an APD was used at the Rx. Meanwhile, we took into consideration the bandwidth efficiency and the Rx implementation complexity and focused on IM/DD techniques due to the transceiver cost and complexity concerns.

For instance, we have presented in Fig. 4.21 plots of BER as a function of link span for OOK, PPM, and digital pulse interval modulation (DPIM)[4] schemes. Although PPM remains the most

[4]By DPIM, for each symbol, a pulse is sent followed by a number of empty slots, depending on the input bits. An additional guard slot is also usually added to avoid sending consecutive "on" pulses. DPIM is an asynchronous modulation scheme with variable symbol length, and does not require symbol synchronization [155]. In addition, it is more spectrally efficient than PPM, because it does not need to wait the end of a fixed symbol period before sending the next

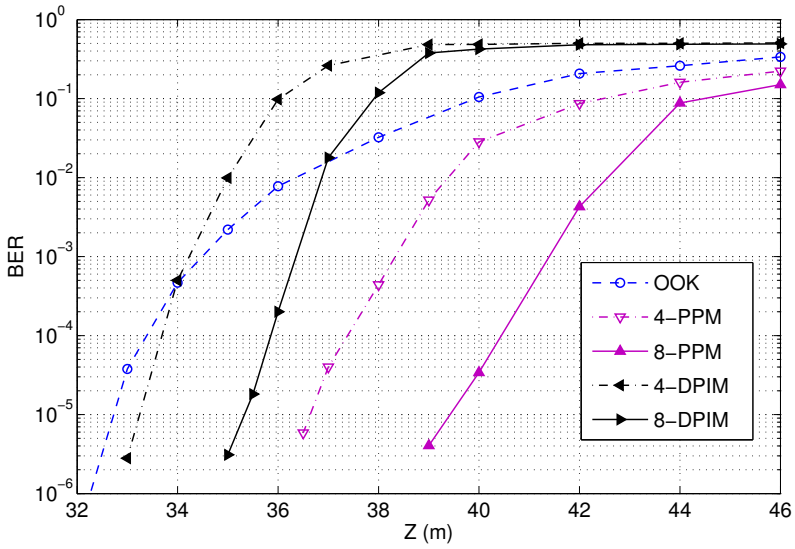

Figure 4.21 **—** Contrasting BER performance for OOK, PPM, and DPIM modulations. Transmit power P_t = 0.1 W, data rate R_b =100 Mbps. Rx parameters: lens diameter and focal distance D =20 cm and F =25 cm, FOV =0.69°, PIN PD with cut-off frequency f_c =300 MHz and quantum efficiency η =0.82.

energy efficient modulation scheme, DPIM may be considered as a more suitable choice as it is an asynchronous modulation and also has a lower PAPR. However, the improved bandwidth efficiency of DPIM is obtained at the expense of more computationally complex demodulation.

4.3.2.3 Experimental test and measurements

We have further evaluated the performance of an UWOC link through experimental measurements [153]. The experimental set-up consisted of a simplex point-to-point link that was developed in a pool of 4 m length at IFREMER site in La-Seyne-sur-Mer (see Fig. 4.22). The Tx was put inside a waterproof titanium cylindrical frame and submerged in the pool. The Rx was installed outside the pool behind a 40 cm diameter side-window. In addition, a rail system installed above the pool was used to install and position the Tx module inside it. Figure 4.23 (a) shows the Tx (submerged in pool) and the Rx modules in our set-up. The block diagram of the set-up is shown in Fig. 4.24. We studied, in particular, the intensity loss in the channel, the impact of Tx-Rx misalignment, and have compared the performances of different modulation schemes [153].

symbol. The main potential problem with DPIM is the possibility of error propagation in signal demodulation at the Rx. In fact, if an "off" slot is detected erroneously as "on," all the succeeding symbols in the frame will be decoded with error.

Figure 4.22 — General view of the pool with the rail system above (Courtesy IFERMER La-Seyne-sur-Mer).

4.3.2.4 Effect of beam misalignment

Taking into account the Tx beam parameters and the Rx optics, we have investigated the effect of Tx-Rx misalignment on the performance of a point-to-point underwater optical link [148]. Using the set-up described above and a metric bench plate with mounting threads spaced by 2.5 cm, we investigated the effect of beam misalignment on the received signal by shifting the Rx away from the optical axis. Figures 4.23 (b) and (c) show the beam spot at the Rx side for Rx lateral displacements of $\Delta = 2.5$ and 12.5 cm with respect to the optical axis. The degradation of the received signal with misalignment is illustrated in Fig 4.25 where the Rx FOV is around 10° (given the photo-diode active area and the collimating lens parameters). We notice a considerable sensitivity of the link performance to beam misalignment.

4.4 Indoor Visible-Light Communications

4.4.1 Technology overview

The VLC technology consists in exploiting LED luminaries for simultaneous illumination and broadband data transmission [156, 157]. LEDs are expected to be the primary illumination source in the future thanks to the advances in incoherent solid-state lighting and because this allows to reduce significantly energy consumption and to easily control intensity and color of illuminated spaces [158]. The most relevant case is that of white light illumination for which there are two methods in LED-based luminaries. The “classical” approach is to use separate red-green-blue (RGB) emitters and to combine them to produce white light. However, this approach is of lim-

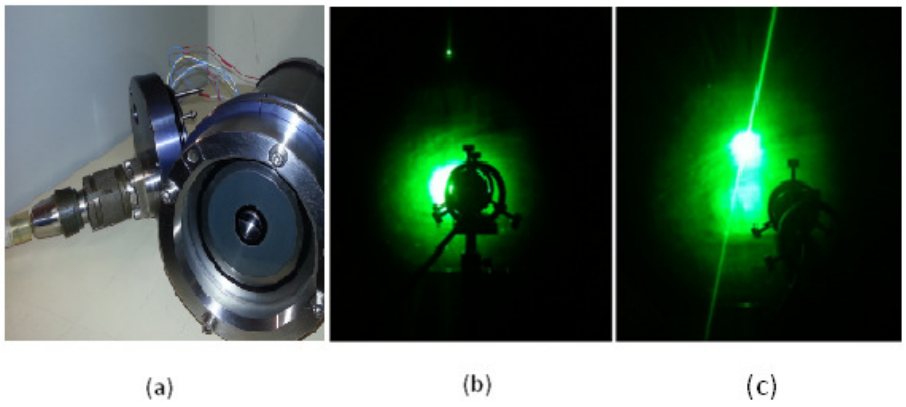

Figure 4.23 — Transmitter and Rx in the experimental set-up. (a) LED placed within titanium waterproof housing; (b) Spot shape of the received beam on the Rx plane with a displacement of $\Delta = 2.5$ cm; (c) Spot shape of the received beam on the Rx plane with a displacement of $\Delta = 12.5$ cm (Courtesy IFERMER La-Seyne-sur-Mer).

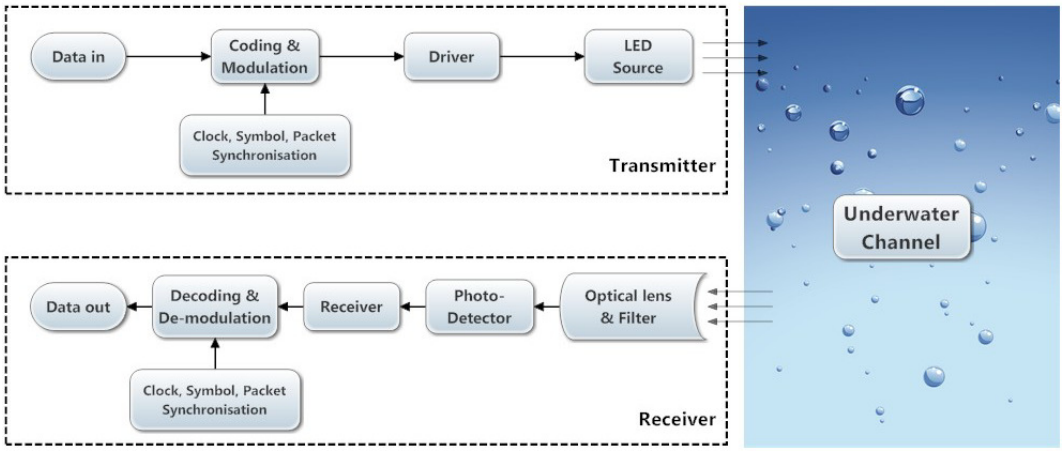

Figure 4.24 — Block diagram of the Tx and the Rx for the experimental set-up.

ited use and is phasing out in lighting industry due to difficulties in RGB balancing and high cost, although it provides devices of relatively high bandwidth (a few hundred MHz) and gives the possibility of color mixing [159]. A popular alternative to RGB lighting is to use the so-called white LEDs, where a blue LED is used together with yellowish phosphor coating to emit broad spectrum white light. These devices are preferred over the RGB option due to the reduced production cost since a single diode is needed instead of three [160, 161]. Several proof-of-concept examples have been realized recently showing the possibility of using LEDs for both illumination and communication, where most of them concerned indoor and automotive applications. Some application scenario examples are shown in Fig. 4.26.

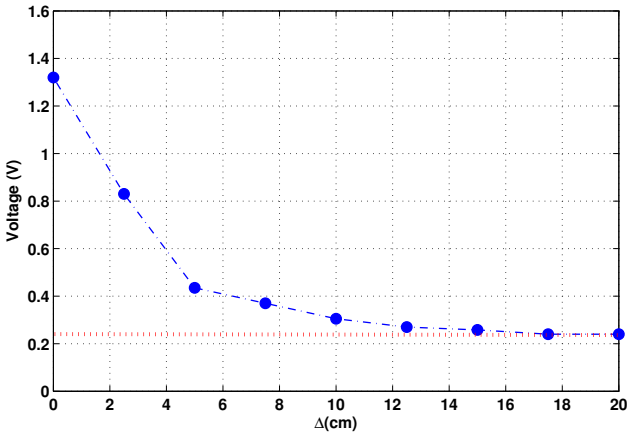

Figure 4.25 — Measured voltage of the received signal after TIZ as a function of Δ. Receiver FOV = 10.8°, Tx beam half-angle = 10°, 3.5 m link, water attenuation coefficient $c = 0.43\,\mathrm{m}^{-1}$. The red dotted line corresponds to the measured noise level.

Figure 4.26 — Illustration of some potential applications of the VLC technology.

4.4.1.1 Challenges

One of the challenges in the development of commercial VLC systems is the slow modulation response of commercial white LEDs, which is due to the slow response time of the phosphorous. This limits the modulation bandwidth of the device to a few MHz. One proposed solution is to use a blue filter at the Rx to remove this slow component from the modulated signal. By this method, the modulation bandwidth can be increased up to 20 MHz [162]. The application of the blue filter causes an intensity loss on the order of 10 dB, but this is not a problem in practice as we have in general a sufficiently high SNR (that can exceed 70 dB) at the Rx due to the illumination level recommended by the European lighting standard [161]. Other proposed solutions are pre- or post-equalization, high-order modulation/multiplexing based on subcarrier intensity modulation (SIM) with OFDM, and spatial multiplexing by parallel data transmission [157]. The peak reported data rates (laboratory set-ups) are around 1 Gbps for the case of white LEDs and about 3 Gbps for the case of RGB LEDs over a range of several tens of centimeters typically [161]. Very recently, researchers have considered the use of GaN-based micron-size LEDs (commonly called μLEDs) that have the advantage of very large modulation bandwidths (typically a 3-dB bandwidth

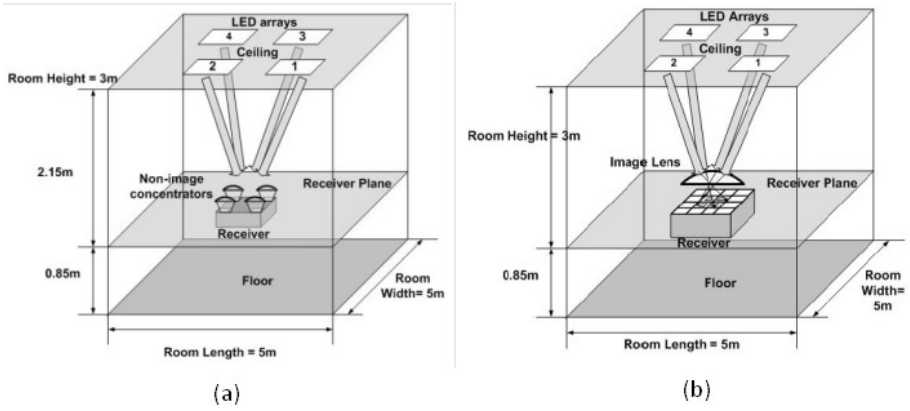

Figure 4.27 — Examples of schematics of (a) non-imaging and (b) imaging VLC MIMO systems (Reproduced from [165]).

of 60 MHz) for VLC applications [163].

Other challenges with VLC technology include: establishing the uplink, mitigating the ambient noise and interference from fluorescent lighting, dimming control, and dealing with nonlinear LED characteristics.

4.4.1.2 MIMO VLC systems

Since in most indoor VLC applications we have usually a very high SNR available and at the same time are concerned with low bandwidth devices, this appeals for the use of MIMO technology with SMux or OSM ST schemes to boost the transmission data rate. The design of MIMO techniques is somehow different from RF and FSO applications. As a matter of fact, the indoor VLC channel does not exhibit channel fading [164]. So, in contrast to RF or FSO counterparts, where MIMO systems are used to increase link reliability by providing spatial diversity gain, in VLC systems we are concerned with a deterministic channel, and hence, the only interest of MIMO architectures is for increasing the data throughput.

Two approaches of non-imaging and imaging receivers have been considered for MIMO VLC systems so far. The simpler one is the non-imaging system where at the Rx side, non-imaging lenses are used for collecting the transmitted intensity. Figure 4.27(a) shows an example of such a system where the LEDs and receivers are arranged in a 2×2 array. Unfortunately, the condition of full rank channel matrix is not always satisfied or it can become ill-conditioned, in which cases there will not be the possibility of spatial multiplexing at Tx, in particular. To circumvent the problem of rank-deficient or ill-conditioned channel matrix, an imaging lens system can be used at the Rx. Figure 4.27(b) illustrates the imaging MIMO structure, where the LED arrays are "imaged" to the Rx plane via the imaging lens [165]. This requires a large enough Rx area so that the images of the LED arrays fall on the detectors for all possible Rx positions inside the room. This technique is quite efficient but the Rx imaging lens is bulky and introduces additional expense and complexity.

4.4.1.3 Organic LEDs

Organic LEDs (OLEDs) have recently attracted a great attention as a flexible panel light source for displays, e.g. high-definition television displays. This is because OLEDs can be of variable wavelength, and hence, do not require color filtering or a back-light and hence are more efficient that liquid crystal displays. Other advantages of OLEDs include wide FOV, low power consumption, fast response, and flexibility. OLEDs have also been considered for illumination and, naturally, are under study for VLC communications. As a matter of fact, OLEDs have most of the properties of standard LEDs, but instead of using in-organic materials, they consist of a thin film of organic material laid between two electrodes [166]. However, compared to standard LEDs, OLEDs suffer from lower bandwidth as their typical bandwidth is about hundreds of kHz only. This is an important challenge for OLEDs to be used as Tx in high-data-rate VLC systems [167].

4.4.2 Contributions

I have started working on the VLC topic since end of 2012 to acquire the state-of-the-art on this technology and to identify the challenges and the related proposed solutions. Also, thanks to the Opticwise COST Action support, I had the opportunity to visit several highly-qualified research labs (Institute of Communication Information and Perception Technologies at Scuola Superiore Sant'Anna in Pisa, OCRG lab at Northumbria University in Newcastle, and Digital Communication lab at the University of Edinburgh) and to witness the most recent progresses and the related developed set-ups on different aspects of the VLC technology. Having this solid background, we have entered the active research phase in our research team, while continuing to collaborate with other laboratories specialized on this topic.

4.4.2.1 Channel modeling

An important step in the design of a VLC system is to comprehend the limitations arising from the optical channel. Accurate channel characterization is an important prerequisite to set the system parameters appropriately in order to establish a high quality link since it permits to better exploit the available energy and spectral resources in view of optimizing the system design. An accurate channel model is also necessary to predict precisely the performance of a VLC system.

We have started our studies by investigating channel characterization for indoor VLC systems. There, the link distance is relatively short (typically less than 3 meters) and multipath dispersion seems to be insignificant in small-size rooms [162]. In relatively large rooms or conference halls, however, multipath dispersion may result in channel frequency selectivity and ISI at the Rx. So, we intended to quantify the channel delay dispersion to check the limitations arising from signal propagation in the VLC channel on the data rate. It should be noted that it is generally believed that the data rate constraint in VLC systems is principally arising from bandwidth limitation of components (i.e. LEDs). Our objective has been to see if any practical limitation can arise from the

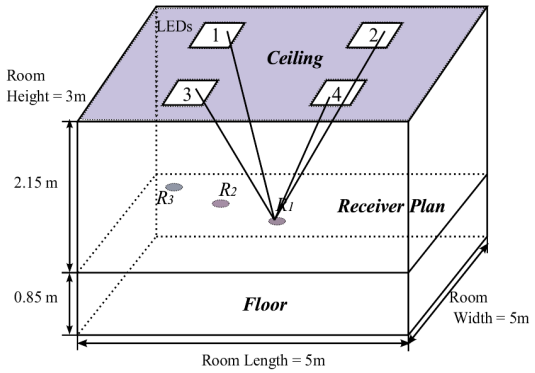

Figure 4.28 — Schematic of a typical indoor VLC transmission system.

channel (by excluding the case of OFDM signaling). For this purpose, for a classical VLC channel, we have obtained via simulations the impulse response of the aggregate channel including LOS and diffuse components using the iterative site-based method [168]. Then, considering a typical scenario depicted in Fig. 4.28, we analyzed the channel RMS delay spread, its 3-dB bandwidth, and the signal-to-interference ratio [169]. We verified that the usually-considered assumption of flat channel is almost true, even when considering relatively large room sizes. For instance, the normalized CIRs for three different positions of the Rx, identified by R_1, R_2, and R_3 in Fig. 4.28 are shown in Fig. 4.29. Here, we have a higher LOS contribution at position R_2 where the Rx is just beneath the LED 1. The RMS delay spread for the three Rx positions of R_1, R_2, and R_3, are 0.35, 0.92, and 1.08 ns, respectively.

4.4.2.2 Efficient transmission schemes

We are currently working on spectrally efficient transmission schemes to further increase the data rate in VLC systems. In particular, we are considering MIMO configurations with OFDM modulation and investigating solutions to deal with dimming and non-ideal component characteristics. Of special importance is the nonlinear LED characteristics.

At the same time, we are working on alternative solutions to OFDM that allow high data rate transmission with simplified hardware at the Tx side. As a matter of fact, optical OFDM is a robust solution to the limited bandwidth of the LEDs and at the same time to channel delay dispersion. However, although OFDM has become very popular for indoor VLC systems, its optimality is rather questionable, in particular from the points of view of spectral and energy efficiency. For instance, it does not effectively exploit half of the subcarriers due to the constraint of unipolar signaling (related to intensity modulation), and cyclic prefix insertion reduces further the spectral efficiency. Moreover, it suffers from high PAPR, especially for large constellation sizes, and this worsens the system performance due to nonlinearity of the LEDs and the clipping noise.

Some other modulation schemes have recently been under investigation such as pulse-

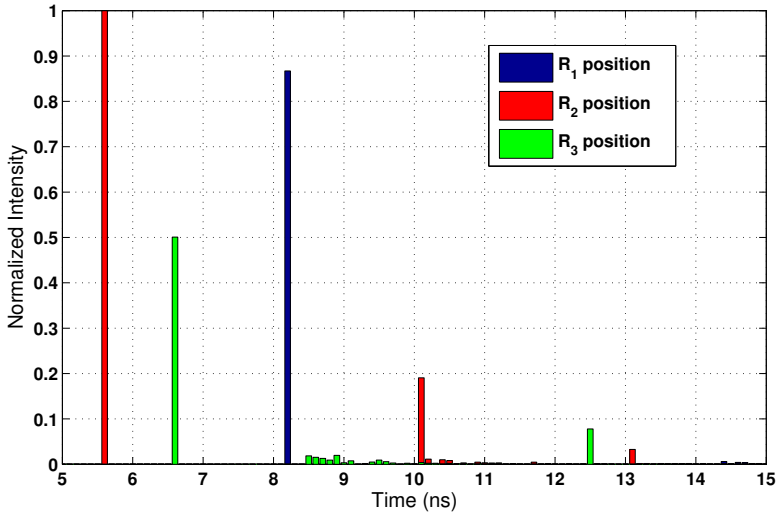

Figure 4.29 — CIR for a medium size room (of dimension $5 \times 5 \times 3\,\mathrm{m}^3$) for the three Rx positions shown in Fig. 4.28. The received intensities are normalized with respect to the peak intensity received from LOS at R_2 position (notice that R_2 is just beneath LED #1. Time resolution is 0.1 ns. PD active area $1\,\mathrm{cm}^2$, Tx semi-angle 60°, Rx FOV 70°, ceiling reflectivity 0.38, floor reflectivity 0.61, wall reflectivity 0.74.

amplitude modulation (PAM) and carrierless amplitude and phase (CAP) modulation. The disadvantage of PAM or CAP is the necessity of channel equalization at the Rx at comparable data-rates with OFDM. In some aspects, these modulation schemes have the advantage of reduced Tx complexity but would suffer from a more complex hardware at the Rx.

4.5 Concluding Remarks

Extending my research activities to the field of OWC necessitated at first a considerable time and effort in order to become familiar with the particular aspects of optical communication and to understand the practical considerations and the limitations arising from the optical channel and components, which are very different from the RF communication field. At the present time, I have established several national and international collaborations with academic and industrial institutions and am involved in the supervision of three PhD students. To these reasons, I feel really pleased to work on this area and I have developed my research perspectives, presented in the next chapter, mainly on the OWC domain.

Chapter 5

Conclusions and Perspectives for Future Research

Contents

5.1 General Conclusions

In the past decade, world has witnessed a dramatic increase in the traffic and demand for high-speed Internet services such as HDTV, video calls, and cloud-computing. This has strengthened the need for further innovation and research and development (R&D) in new emerging wireless technologies capable of delivering high transmission rates. In this view, my contributions have firstly concerned RF communication and the solutions allowing to attain high spectral efficiencies such as the MIMO technology. I have mainly investigated issues related to the practical implementation of these systems and have been interested in the development of methods of reduced computational complexity. My main research contributions since my PhD in 2002 include iterative signal detection and channel estimation for single- and multi-carrier MIMO systems as well as for WRNs.

Later, as OWC systems were demonstrated as a powerful alternative in some special applications to RF transmission systems by offering a number of technical and operational advantages, I devoted a significant part of my time to work on this area. At the beginning, I was particularly interested in the FSO technology, which has numerous advantages over RF transmission in a variety of applications. The widespread deployment and use of this technology has been slowed down, however, by its relatively low link reliability due to the sensitivity to weather conditions and the atmospheric turbulence-induced fading. During the last nine years or so, I have been working on this topic to address these major technical challenges. In addition to investigating channel char-

acterization and turbulence modeling which are very particular to optical signal transmission, I have explored the adequacy of several innovative physical layer concepts, originally introduced in the context of RF systems, such as MIMO structures and cooperative diversity in FSO networks. My other research activities have concerned mitigating link misalignment in FSO systems as well as hybrid RF/FSO links.

Another exciting technology in which I became interested is UWOC that can help considerably progress the underwater exploration and surveillance activities. With the increasing use of robotics in underwater missions and the recent advances in the design and development of automated underwater vehicles (AUVs) and ROVs and the need to communicate with them in various challenging scenarios, the UWOC technology has recently become more promising than ever. My research works on this topic have concerned aquatic channel characterization and modeling, efficient signal modulation, and study of link misalignment effects.

Lastly, I have recently extended my research activities to VLC systems that are a particularly promising solution for providing high-rate data transmission, especially in indoor environments, by using already-installed LED lighting infrastructures. VLC can be considered as a good example of green communication for the next generation of high-speed local area networks. My research works have concerned channel modeling and investigation of high spectrally-efficient transmission schemes.

5.2 Perspectives for Future Research

CONFIDENTIAL

List of Figures

Bibliography

[1] M. A. Khalighi, J.-F. Hélard, S. M. S. Sadough, and S. Bourennane, "Suitable combination of channel coding and space-time schemes for moderate-to-high spectral efficiency MIMO systems," *AEUE International Journal of Electronics and Communications*, vol. 64, no. 7, pp. 595–606, July 2010.

[2] M. A. Khalighi, J. J. Boutros, and J.-F. Hélard, "Data-aided channel estimation for turbo-PIC MIMO detectors," *IEEE Communications Letters*, vol. 10, no. 5, pp. 350–352, May 2006.

[3] M. A. Khalighi and J. J. Boutros, "Semi-blind channel estimation using EM algorithm in iterative MIMO APP detectors," *IEEE Transactions on Wireless Communications*, vol. 5, no. 11, pp. 3165–3173, Nov. 2006.

[4] M. A. Khalighi and S. Bourennane, "Semi-blind single-carrier MIMO channel estimation using overlay pilots," *IEEE Transactions on Vehicular Technology*, vol. 57, no. 3, pp. 1951–1956, May 2008.

[5] S. M. S. Sadough, M. A. Khalighi, and P. Duhamel, "Improved iterative MIMO signal detection accounting for channel-estimation errors," *IEEE Transactions on Vehicular Technology*, vol. 58, no. 7, pp. 3154–3167, Sept. 2009.

[6] E. P. Simon and M. A. Khalighi, "Iterative soft-Kalman channel estimation for fast time-varying MIMO-OFDM channels," *IEEE Wireless Communications Letters*, vol. 2, no. 6, pp. 599–602, Dec. 2013.

[7] Yi Zhang, M. A. Khalighi, and S. Bourennane, "Iterative channel estimation and data detection for amplify-and-forward relay networks," *IEEE Communications Letters*, vol. 16, no. 5, pp. 710–713, May 2012.

[8] Y. Zhang, M. A. Khalighi, S. M. S. Sadough, and S. Bourennane, "Semi-blind channel estimation for amplify-and-forward cooperative relay networks," *Mediterranean Journal of Computers and Networks, Special Issue on Wireless Networks*, vol. 10, no. 1, pp. 212–222, Jan. 2014.

[9] Yi Zhang, M. A. Khalighi, S. M. S. Sadough, and S. Bourennane, "Improved MAP signal detection for amplify-and-forward relay networks with imperfect channel state information," *IET Communications*, accepted.

[10] M. A. Khalighi and M. Uysal, "Survey on free space optical communication: A communication theory perspective," *IEEE Communications Surveys & Tutorials*, accepted.

[11] F. Xu, M. A. Khalighi, P. Caussé, and S. Bourennane, "Channel coding and time-diversity for optical wireless links," *Optics Express*, vol. 17, no. 2, pp. 872–887, Jan. 2009.

[12] M. A. Khalighi, N. Schwartz, N. Aitamer, and S. Bourennane, "Fading reduction by aperture averaging and spatial diversity in optical wireless systems," *IEEE/OSA Journal of Optical Communications and Networking*, vol. 1, no. 6, pp. 580–593, Nov. 2009.

[13] G. Yang, M. A. Khalighi, S. Bourennane, and Z. Ghassemlooy, "Approximation to the sum of two correlated Gamma-Gamma variates and its applications in free-space optical communications," *IEEE Wireless Communications Letters*, vol. 1, no. 6, pp. 621–624, Dec. 2012.

[14] G. Yang, M. A. Khalighi, Z. Ghassemlooy, and S. Bourennane, "Performance evaluation of receive-diversity free-space optical communications over correlated Gamma-Gamma fading channels," *Applied Optics*, vol. 52, no. 24, pp. 5903–5911, Aug. 2013.

[15] G. Yang, M. A. Khalighi, S. Bourennane, and Z. Ghassemlooy, "Fading correlation and analytical performance evaluation of the space-diversity free-space optical communications system," *IOP Journal of Optics*, vol. 16, no. 3, pp. 1–10, Feb. 2014.

[16] G. Yang, M. A. Khalighi, Z. Ghassemlooy, and S. Bourennane, "Performance analysis of space-diversity FSO systems over the correlated Gamma-Gamma fading channel using Padé approximation method," *IET Communications*, vol. 8, no. 13, pp. 2246–2255, Sept. 2014.

[17] I. E. Lee, Z. Ghassemlooy, W. P. Ng, and M. A. Khalighi, "Joint optimization of a partially coherent Gaussian beam for free-space optical communication over turbulent channels with pointing errors," *Optics Letters*, vol. 38, no. 3, pp. 350–352, Feb. 2013.

[18] M. A. Khalighi, F. Xu, Y. Jaafar, and S. Bourennane, "Double-laser differential signaling for reducing the effect of background radiation in free-space optical systems," *IEEE/OSA Journal of Optical Communications and Networking*, vol. 3, no. 2, pp. 145–154, Feb. 2011.

[19] F. Xu, M. A. Khalighi, and S. Bourennane, "Coded PPM and multipulse PPM and iterative detection for Free-Space optical links," *IEEE/OSA Journal of Optical Communications and Networking*, vol. 1, no. 5, pp. 404–415, Oct. 2009.

[20] M. A. Khalighi, C. Gabriel, T. Hamza, S. Bourennane, P. Léon, and V. Rigaud, "Underwater wireless optical communication; recent advances and remaining challenges," *IEEE International Conference on Transparent Optical Networks (ICTON)*, pp. 1–4, July 2014, Invited paper, Graz, Austria.

[21] C. Gabriel, M. A. Khalighi, S. Bourennane, P. Léon, and V. Rigaud, "Monte-carlo-based channel characterization for underwater optical communication systems," *IEEE/OSA Journal of Optical Communications and Networking*, vol. 5, no. 1, pp. 1–12, Jan. 2013.

[22] Z. Ghassemlooy, D. Wu, M.A. Khalighi, and X. Tang, "Indoor non-directed optical wireless communications - optimization of the Lambertian order," *Journal of Electrical and Computer Engineering Innovations*, vol. 1, no. 1, pp. 1–9, May 2013.

[23] E. Telatar, "Capacity of multi-antenna Gaussian channels," *European Transactions on Telecommunications*, vol. 10, no. 6, pp. 585–595, Nov.-Dec. 1999.

[24] G. J. Foschini, "Layered space-time architecture for wireless communication in a fading environment when using multi-element antennas," *Bell Labs Technical Journal*, vol. 1, no. 2, pp. 41–59, Autumn 1996.

[25] G. J. Foschini and M. J. Gans, "On limits of wireless communications in a fading environment when using multiple antennas," *Wireless Personal Communications*, vol. 6, no. 3, pp. 311–335, Mar. 1998.

[26] G. D. Golden, G. J. Foschini, R. A. Valenzuela, and P. W. Wolniansky, "Detection algorithm and initial laboratory results using the V-BLAST space-time communication architecture," *Electronics Letters*, vol. 35, no. 1, pp. 14–15, Jan. 1999.

[27] E. M. Biglieri, J. Proakis, and S. Shamai (Shitz), "Fading channels: information-theoretic and communications aspects," *IEEE Transactions on Information Theory*, vol. 44, no. 6, pp. 2619–2692, Oct. 1998.

[28] M. A. Khalighi, *Study of Multiple Antenna Communication Systems; Channel Capacity and Iterative Detection*, Ph.D. thesis, Institut National Polytechnique de Grenoble (INPG), Grenoble, Oct. 2002, in French.

[29] M. A. Khalighi, K. Raoof, and G. Jourdain, "Capacity of wireless communication systems employing antenna arrays, a tutorial study," *Wireless Personal Communications*, vol. 23, no. 3, pp. 321–352, 2002.

[30] B. Vucetic and J. Yuan, *Space-Time Coding*, Wiley, 2003.

[31] V. Tarokh, H. J. Jafarkhani, and A. R. Calderbank, "Space-time block codes from orthogonal designs," *IEEE Transactions on Information Theory*, vol. 45, no. 5, pp. 1456–1467, July 1999.

[32] S. M. Alamouti, "A simple transmit diversity technique for wireless communications," *IEEE Journal on Selected Areas in Communications*, vol. 16, no. 8, pp. 1451–1458, Oct. 1998.

[33] B. Hassibi and B. M. Hochwald, "High-rate codes that are linear in space and time," *IEEE Transactions on Information Theory*, vol. 48, no. 7, pp. 1804–1824, July 2002.

[34] S. M. S. Sadough and M. A. Khalighi, *Radio Communication*, chapter Recent Developments in Channel Estimation and Detection for MIMO Systems, IN-TECH Press, Apr. 2010.

[35] B. Hassibi and B. M. Hochwald, "How much training is needed in multiple-antenna wireless links?," *IEEE Transactions on Information Theory*, vol. 49, no. 4, pp. 951–963, Apr. 2003.

[36] H. Zhu, B. Farhang-Boroujeny, and C. Schlegel, "Pilot embedding for joint channel estimation and data detection in MIMO communication systems," *IEEE Communications Letters*, vol. 7, no. 1, pp. 30–32, Jan. 2003.

[37] M. A. Khalighi, J. M. Brossier, G. Jourdain, and K. Raoof, "Water filling capacity of Rayleigh MIMO channels," *IEEE International Symposium on Personal, Indoor and Mobile Radio Communications (PIMRC)*, vol. A, pp. 155–158, Sept.-Oct. 2001, San Diego, CA.

[38] K. Raoof, M. A. Khalighi, and N. Prayongpun, *Adaptive Signal Processing For Wireless Communications*, chapter MIMO Systems: Principles, Iterative Techniques and Advance Polarization, CRC Press, Aug. 2008.

[39] M. A. Khalighi, J. M. Brossier, G. Jourdain, and K. Raoof, "On capacity of Ricean MIMO channels," *IEEE International Symposium on Personal, Indoor and Mobile Radio Communications (PIMRC)*, vol. A, pp. 150–154, Sept.-Oct. 2001, San Diego, CA.

[40] E. Viterbo and J. J. Boutros, "A universal lattice code decoder for fading channels," *IEEE Transactions on Information Theory*, vol. 45, no. 5, pp. 1639–1642, July 1999.

[41] M. Sellathurai and S. Haykin, "Turbo-BLAST for wireless communications: theory and experiments," *IEEE Transactions on Signal Processing*, vol. 50, no. 10, pp. 2538– 2546, Oct. 2002.

[42] G. Caire, G. Taricco, and E. Biglieri, "Bit-interleaved coded modulation," *IEEE Transactions on Information Theory*, vol. 44, no. 3, pp. 927–946, May 1998.

[43] P. Robertson, P. Hoeher, and E. Villebrun, "Optimal and sub-optimal maximum a posteriori algorithms suitable for turbo decoding," *European Transactions on Telecommunications*, vol. 8, no. 2, pp. 119–125, Mar. 1997.

[44] M. A. Khalighi and J.-F. Hélard, "Should MIMO orthogonal space-time coding be preferred to non-orthogonal coding with iterative detection?," *IEEE Symposium on Signal Processing and Information Technology (ISSPIT)*, pp. 340–345, Dec. 2005, Athens, Greece.

[45] M. A. Khalighi, J.-F. Hélard, and S. Bourennane, "Choice of appropriate space-time coding scheme for MIMO systems employing channel coding under BICM," *IEEE International Workshop on Signal Processing Advances for Wireless Communications (SPAWC)*, July 2006, Cannes, France.

[46] M. A. Khalighi, J.-F. Hélard, and S. Bourennane, "Contrasting orthogonal and non-orthogonal space-time schemes for perfectly-known and estimated MIMO channels," *IEEE International Conference on Communication Systems (ICCS)*, Oct.-Nov. 2006, Singapore.

[47] J.-C. Belfiore, G. Rekaya, and E. Viterbo, "The golden code: a 2×2 full-rate space-time code with nonvanishing determinants," *IEEE Transactions on Information Theory*, vol. 51, no. 4, pp. 1432–1436, Apr. 2005.

[48] M. A. Khalighi and J. J. Boutros, "Modified unbiased EM-based channel estimation for MIMO turbo receivers," *IEEE Symposium on Signal Processing and Information Technology (ISSPIT)*, pp. 127–131, Dec. 2004, Rome, Italy.

[49] M. A. Khalighi and J. J. Boutros, "Channel estimation in Turbo-BLAST detectors using EM algorithm," *International Conference on Acoustics, Speech, and Signal Processing (ICASSP)*, vol. III, pp. 1037–1040, Mar. 2005, Philadelphia, PA.

[50] T. K. Moon and W. C. Stirling, *Mathematical Methods and Algorithms for Signal Processing*, Upper Saddle River, NJ: Prentice Hall, 2000.

[51] M. A. Khalighi, L. Berriche, and J.-F. Hélard, "Overlaid or time-multiplexed pilots for channel estimation in iterative MIMO receivers," *International Symposium on Signal Processing and its Applications (ISSPA)*, pp. 483–486, Sept. 2005, Sydney, Australia.

[52] M. A. Khalighi and S. Bourennane, "Semi-blind channel estimation based on superimposed pilots for single-carrier MIMO systems," *IEEE Vehicular Technology Conference (VTC-Spring)*, pp. 1480–1484, Apr. 2007, Dublin, Ireland.

[53] S. M. S. Sadough and M. A. Khalighi, "Optimal Turbo-BLAST detection of MIMO-OFDM systems with imperfect channel estimation," *IEEE International Symposium on Personal, Indoor and Mobile Radio Communications (PIMRC)*, Sept. 2007, Athens, Greece.

[54] S. ten Brink, "Designing iterative decoding schemes with the extrinsic information transfer charts," *AEÜE International Journal of Electronics and Communications*, vol. 54, no. 6, pp. 389–398, Nov. 2000.

[55] A. Swami, Q. Zhao, Y. W. Hong, and L. Tong, *Wireless Sensor Networks: Signal Processing and Communication Perspectives*, Wiley, 2007.

[56] C. Y. Chong and S. P. Kumar, "Sensor networks: Evolution, opportunities and chanllenges," *Proceedings of IEEE*, vol. 91, no. 8, pp. 1247–1256, Aug. 2003.

[57] J. L. Hill, *System Architecture for Wireless Sensor Networks*, Ph.D. thesis, University of California, Berkeley, CA, 2003.

[58] I. F. Akyildiz, W. Su, Y. Sankarasubramaniam, and E. Cayirci, "A survey on sensor networks," *IEEE Communications Magazine*, vol. 40, no. 8, pp. 102–114, Aug. 2002.

[59] T. Q. S. Quek, D. Dardari, and M. Z. Win, "Energy efficiency of dense wireless sensor networks: To cooperate or not to cooperate," *IEEE Journal on Selected Areas in Communications*, vol. 25, no. 2, pp. 459–470, Feb. 2007.

[60] X. Y. Li, *Wireless Ad Hoc and Sensor Networks: Theory and Applications*, Cambrige University Press, 2008.

[61] A. Nosratinia, T. E. Hunter, and A. Hedayat, "Cooperative communication in wireless networks," *IEEE Communications Magazine*, vol. 42, no. 10, pp. 74–80, Oct. 2004.

[62] J. N. Laneman, D. N. C. Tse, and G. W. Wornell, "Cooperative diversity in wireless networks: Efficient protocols and outage behavior," *IEEE Transactions on Information Theory*, vol. 50, no. 12, pp. 3062–3080, Dec. 2004.

[63] M. Gastpar and M. Vetterli, "On the capacity of large Gaussian relay networks," *IEEE Transactions on Information Theory*, vol. 51, no. 3, pp. 765–779, Mar. 2005.

[64] C. T. K. Ng and A. J. Goldsmith, "The impact of CSI and power allocation on relay channel capacity and cooperation strategies," *IEEE Transactions on Wireless Communications*, vol. 7, no. 12, pp. 5380–5389, Dec. 2008.

[65] Y. Jing and H. Jafarkhani, "Distributed differential space-time coding for wireless relay networks," *IEEE Transactions on Communications*, vol. 56, no. 7, pp. 1092–1100, July 2008.

[66] Y. Jing and B. Hassibi, "Distributed space-time coding in wireless relay networks," *IEEE Transactions on Wireless Communications*, vol. 5, no. 12, pp. 3524–3536, Dec. 2006.

[67] J. N. Laneman and G. W. Wornell, "Distributed space-time-coded protocols for exploiting cooperative diversity in wireless networks," *IEEE Transactions on Information Theory*, vol. 49, no. 10, pp. 2415–2425, Oct. 2003.

[68] A. Chowdhery and R. K. Mallik, "Linear detection for the nonorthogonal amplify and forward protocol," *IEEE Transactions on Wireless Communications*, vol. 8, no. 2, pp. 826–835, Feb. 2009.

[69] A. Sendonaris, E. Erkip, and B. Aazhang, "User cooperation diversity - Part I: system description," *IEEE Transactions on Communications*, vol. 51, no. 11, pp. 1927–1938, Nov. 2003.

[70] Y. Gong, C. Luo, and Z. Chen, "Two-path successive relaying with hybrid demodulated and forward," *IEEE Transactions on Vehicular Technology*, vol. 61, no. 5, pp. 2044–2053, June 2012.

[71] Yi Zhang, *Channel Estimation for Wireless Relay Networks Using Cooperative Diversity Techniques*, Ph.D. thesis, École Centrale Marseille, Nov. 2012.

[72] G. S. Rajan and B. S. Rajan, "Leveraging coherent distributed space-time codes for noncoherent communication in relay networks via training," *IEEE Transactions on Wireless Communications*, vol. 8, no. 2, pp. 683–688, Feb. 2009.

[73] S. Cui, A. J. Goldsmith, and A. Bahai, "Energy-efficiency of MIMO and cooperative MIMO techniques in sensor networks," *IEEE Journal on Selected Areas in Communications*, vol. 22, no. 6, pp. 1089–1098, Aug. 2004.

[74] S. K. Jayaweera, "Virtual MIMO-based cooperative communication for energy-constrained wireless sensor networks," *IEEE Transactions on Wireless Communications*, vol. 5, no. 5, pp. 984–989, May 2006.

[75] Yi Zhang, M. A. Khalighi, and S. Bourennane, "EM-based channel estimation for cooperative relay networks," *IEEE International Conference on Telecommunications (ConTEL)*, pp. 279–286, June 2011, Graz, Austria.

[76] Yi Zhang, M. A. Khalighi, and S. Bourennane, "Iterative channel estimation and data detection for amplify-and-forward relay networks," *IEEE Communications Letters*, vol. 16, no. 5, pp. 710–713, May 2011.

[77] Yi Zhang, M. A. Khalighi, S. M. S. Sadough, and S. Bourennane, "Signal detection for amplify-and-forward relay networks with imperfect channel estimation," *IEEE International Symposium on Communication Systems, Networks and Digital Signal Processing (CSNDSP)*, pp. 1–5, July 2012, Poznań, Poland.

[78] Y. Huang and J. A. Ritcey, "Optimal constellation labeling for iteratively decoded bit-interleaved space-time coded modulation," *IEEE Transactions on Information Theory*, vol. 51, no. 5, pp. 1865–1871, May 2005.

[79] S. Haykin, "Cognitive radio: brain-empowered wireless communications," *IEEE Journal on Selected Areas in Communications*, vol. 23, no. 2, pp. 201–220, Feb. 2005.

[80] A. Goldsmith, S. A. Jafar, I. Maric, and S. Srinivasa, "Breaking spectrum gridlock with cognitive radios: An information theoretic perspective," *Proceedings of the IEEE*, vol. 97, no. 5, pp. 894–914, May 2009.

[81] E. Hossain, D. Niyato, and Z. Han, *Dynamic Spectrum Access and Management in Cognitive Radio Networks*, Cambridge University Press, 2009.

[82] J. Lee, H. Wang, J. G. Andrews, and D. Hong, "Outage probability of cognitive relay networks with interference constraints," *IEEE Transactions on Wireless Communications*, vol. 10, no. 2, pp. 390–395, Feb. 2011.

[83] "Visible light communication (VLC) - a potential solution to the global wireless spectrum shortage," *GBI Research*, 2011, http://www.gbiresearch.com/Report.aspx?ID=Visible-

Light-Communication-(VLC)-A-Potential-Solution-to-the-Global-Wireless-Spectrum-Shortage&ReportType=Industry_Report.

[84] N. Cardona (Ed.), "Scientific challenges towards 5G mobile communications," COST Action IC1004 White Paper, Dec. 2013.

[85] K. David, S. Dixit, and N. Jefferies, "2020 vision," *IEEE Vehicular Technology Magazine*, vol. 5, no. 3, pp. 22–29, Sept. 2010.

[86] E. Larsson, O. Edfors, F. Tufvesson, and T. Marzetta, "Massive MIMO for next generation wireless systems," *IEEE Communications Magazine*, vol. 52, no. 2, pp. 186–195, Feb. 2014.

[87] D. Rodewald, "MRV introduces industry's first 10G Ethernet wireless point-to-point system," MRV Communications, Inc., 2008, http://www.mrv.com/newsroom/press-releases/view/288.

[88] H. A. Willebrand and B. S. Ghuman, "Fiber optics without fiber," *IEEE Spectrum*, vol. 40, no. 8, pp. 41–45, Aug. 2001.

[89] V. W. S. Chan, "Free-space optical communications," *IEEE/OSA Journal of Lightwave Technology*, vol. 24, no. 12, pp. 4750–4762, Dec. 2006.

[90] H. Willebrand and B. S. Ghuman, *Free Space Optics: Enabling Optical Connectivity in Today's Networks*, Sams Publishing, 2001.

[91] Z. Ghassemlooy, W. Popoola, and S. Rajbhandari, *Optical Wireless Communications: System and Channel Modelling with* MATLAB, CRC Press, 2013.

[92] M. Grabner and V. Kvicera, "Multiple scattering in rain and fog on free-space optical links," *IEEE/OSA Journal of Lightwave Technology*, vol. 32, no. 3, pp. 513–520, Feb. 2014.

[93] L. C. Andrews and R. L. Phillips, *Laser Beam Propagation Through Random Media*, SPIE Press, 2nd edition, 2005.

[94] L. C. Andrews, R. L. Phillips, and C. Y. Hopen, *Laser Beam Scintillation with Applications*, SPIE Press, Bellingham, Washington, 2001.

[95] G. Yang, *Space-Diversity Free-Space Optical Systems: Performance Analysis under Correlated Fading Conditions*, Ph.D. thesis, École Centrale de Marseille, Sept. 2013.

[96] J. G. Proakis and M. Salehi, *Digital Communications*, McGraw-Hill, New York, 5th edition, 2007.

[97] R. M. Gagliardi and S. Karp, *Optical Communications*, John Wiley & Sons, 2nd edition, 1995.

[98] S. Bloom, E. Korevaar, J. Schuster, and H. Willebrand, "Understanding the performance of free-space optics," *Journal of Optical Networking*, vol. 2, no. 6, pp. 178–200, June 2003.

[99] D. Rollins, J. Baars, D. Bajorins, C. Cornish, K. Fischer, and T. Wiltsey, "Background light environment for free-space optical terrestrial communications links," *Proceedings of SPIE, Optical Wireless Communications V*, vol. 4873, pp. 99–110, Dec. 2002.

[100] V. G. Sidorovich, "Solar background effects in wireless optical communications," *Proceedings of SPIE, Optical Wireless Communications V*, vol. 4873, pp. 133–142, Dec. 2002.

[101] "A comparison of FSO wavelength system designs," *LightPointe White Paper*, 2002, http://www.lightpointe.com/home.cfm.

[102] K. Kiasaleh, "Performance of APD-based, PPM free-space optical communication systems in atmospheric turbulence," *IEEE Transactions on Communications*, vol. 53, no. 9, pp. 1455–1461, Sept. 2005.

[103] S. G. Wilson, M. Brandt-Pearce, Q. Cao, and J. H. Leveque, "Free-space optical MIMO transmission with Q-ary PPM," *IEEE Transactions on Communications*, vol. 53, no. 8, pp. 1402–1412, Aug. 2005.

[104] B. Moision and J. Hamkins, "Multipulse PPM on discrete memoryless channels," *IPN Progress Report*, vol. 42-160, Feb. 2005, Jet Propulsion Laboratory.

[105] F. S. Vetelino, C. Young, L. C. Andrews, and J. Recolons, "Aperture averaging effects on the probability density of irradiance fluctuations in moderate-to-strong turbulence," *Applied Optics*, vol. 46, no. 11, pp. 2099–2108, Apr. 2007.

[106] F. Xu, *Development of Transmission Methods for a High Data-Rate Free-Space Optical Communication System*, Ph.D. thesis, Paul-Cézanne (AIX-MARSEILLE III) University, Marseille, July 2010.

[107] E. J. Lee and V. W. Chan, "Part 1: optical communication over the clear turbulent atmospheric channel using diversity," *IEEE Journal on Selected Areas in Communications*, vol. 22, no. 9, pp. 1896–1906, Nov. 2004.

[108] J. A. Anguita, M. A. Neifeld, and B. V. Vasic, "Spatial correlation and irradiance statistics in a multiple-beam terrestrial free-space optical communication link," *Applied Optics*, vol. 46, no. 26, pp. 6561–6571, Sept. 2007.

[109] S. G. Wilson, M. Brandt-Pearce, Q. L. Cao, and M. Baedke, "Optical repetition MIMO transmission with multipulse PPM," *IEEE Journal on Selected Areas in Communications*, vol. 23, no. 9, pp. 1901– 1910, Sept. 2005.

[110] *MRV website, Terescope product series*, http://www.mrv.com.

[111] S. M. Navidpour, M. Uysal, and M. Kavehrad, "BER performance of free-space optical transmission with spatial diversity," *IEEE Transactions on Wireless Communications*, vol. 6, no. 8, pp. 2813–2819, Aug. 2007.

[112] M. K. Simon and V. A. Vilnrotter, "Alamouti-type space-time coding for free-space optical communication with direct detection," *IEEE Transactions on Wireless Communications*, vol. 4, no. 1, pp. 35–39, Jan. 2005.

[113] E. Bayaki and R. Schober, "On space-time coding for free-space optical systems," *IEEE Transactions on Communications*, vol. 58, no. 1, pp. 58–62, Jan. 2010.

[114] M. Safari and M. Uysal, "Do we really need OSTBCs for free-space optical communication with direct detection?," *IEEE Transactions on Wireless Communications*, vol. 7, no. 11, pp. 4445–4448, Nov. 2008.

[115] R. Mesleh, H. Elgala, and H. Haas, "Optical spatial modulation," *IEEE/OSA Journal of Optical Communications and Networking*, vol. 3, no. 3, pp. 234–244, Mar. 2011.

[116] S. Arnon, J. R. Barry, G. K. Karagiannidis, R. Schober, and M. Uysal, Eds., *Advanced Optical Wireless Communication Systems*, Cambridge University Press, 2012.

[117] L. B. Stotts, L. C. Andrews, P. C. Cherry, J. J. Foshee, P. J. Kolodzy, W. K. Mcintire, M. Northcott, R. L. Phillips, H. A. Pike, B. Stadler, and D. W. Young, "Hybrid optical RF airborne communications," *Proceedings of the IEEE*, vol. 97, no. 6, pp. 1109–1127, June 2009.

[118] M. Safari and M. Uysal, "Relay-assisted free-space optical communication," *IEEE Transactions on Wireless Communications*, vol. 7, no. 12, pp. 5441–5449, Dec. 2008.

[119] M. Karimi and N. Nasiri-Kenari, "BER analysis of cooperative systems in free-space optical networks," *IEEE/OSA Journal of Lightwave Technology*, vol. 27, no. 12, pp. 5639–5647, Dec. 2009.

[120] B. E. A. Saleh and M. C. Teich, *Fundamentals of Photonics*, John Wiley & Sons, 1991.

[121] F. Xu, M. A. Khalighi, and S. Bourennane, "Impact of different noise sources on the performance of PIN- and APD-based FSO receivers," *COST IC0802 Workshop, IEEE ConTEL Conference*, pp. 211–218, June 2011, Graz, Austria.

[122] F. M. Davidson and X. Sun, "Gaussian approximation versus nearly exact performance analysis of optical communication systems with PPM signaling and APD receivers," *IEEE Transactions on Communications*, vol. 36, no. 11, pp. 1185–1192, Nov. 1988.

[123] I. E. Lee, Z. Ghassemlooy, W.P. Ng, M. A. Khalighi, and M. Uysal, "Capacity analysis of free-space optical links for a partially coherent Gaussian beam over a turbulent channel with pointing errors," *European Conference on Network and Optical Communications (NOC)*, pp. 281–286, July 2013, Graz, Austria.

[124] D. Divsalar, R. M. Gagliardi, and J. H. Yuen, "PPM performance for Reed-Solomon decoding over an optical-RF relay link," *IEEE Transactions on Communications*, vol. 32, no. 3, pp. 302–305, Mar. 1984.

[125] F. Xu, M. A. Khalighi, and S. Bourennane, "Pulse position modulation for FSO systems: Capacity and channel coding," *International Conference on Telecommunications (ConTEL)*, pp. 31–38, June 2009, Zagreb, Croatia.

[126] M. A. Khalighi, N. Aitamer, N. Schwartz, and S. Bourennane, "Turbulence mitigation by aperture averaging in wireless optical systems," *International Conference on Telecommunications (ConTEL)*, pp. 59–66, June 2009, Zagreb, Croatia.

[127] G. Yang, M. A. Khalighi, T. Virieux, S. Bourennane, and Z. Ghassemlooy, "Contrasting space-time schemes for MIMO FSO systems with non-coherent modulation," *International Workshop on Optical Wireless Communications (IWOW)*, Oct. 2012, Pisa, Italy.

[128] G. Yang, M. A. Khalighi, and S. Bourennane, "Performance of receive diversity FSO systems under realistic beam propagation conditions," *IEEE/IET International Symposium on Communication Systems, Networks and Digital Signal Processing (CSNDSP)*, pp. 1–5, July 2012, Poznań, Poland.

[129] M. D. Yacoub, "The α-μ distribution: a physical fading model for the Stacy distribution," *IEEE Transactions on Vehicular Technology*, vol. 56, no. 1, pp. 27–34, Jan. 2007.

[130] G. Yang, M. A. Khalighi, Z. Ghassemlooy, and S. Bourennane, "Performance evaluation of correlated-fading space-diversity FSO links," *International Workshop on Optical Wireless Communications (IWOW)*, pp. 71–73, Oct. 2013, Newcastle upon Tyne, UK.

[131] G. A. Baker and P. Graves-Morris, *Padé Approximants*, Cambridge University Press, Cambridge, UK, 2nd edition, Jan. 1996.

[132] G. K. Karagiannidis, "Moments-based approach to the performance analysis of equal gain diversity in Nakagami-m fading," *IEEE Transactions on Communications*, vol. 52, no. 5, pp. 685–690, May 2004.

[133] I.E. Lee, Z. Ghassemlooy, W.P. Ng, and M. A. Khalighi, "Green-inspired hybrid FSO/RF wireless backhauling and basic access signalling for next generation metrozones," *International Symposium on Environment-Friendly Energies and Applications (EFEA)*, pp. 230–236, June 2012, Newcastle upon Tyne, UK.

[134] I. E. Lee, Z. Ghassemlooy, W. P. Ng, and M. A. Khalighi, *Green Networking and Communication, ICT for Sustainability*, chapter Green-Inspired Hybrid Base Transceiver Station Architecture with Joint FSO/RF Wireless Backhauling and Basic Access Signaling for Next Generation Metrozones, CRC Press, Oct. 2013.

[135] I. E. Lee, Z. Ghassemlooy, W. P. Ng, V. Gourdel, M. A. Khalighi, S. Zvanovec, and M. Uysal, "Practical implementation and performance study of a hard-switched hybrid FSO/RF link under controlled fog environment," *IEEE/IET International Symposium on Communication*

Systems, Networks and Digital Signal Processing (CSNDSP), pp. 388–393, July 2014, Manchester, UK.

[136] S. Long, "Improving the robustness of wireless optical transmission systems against adverse channel effects," *M.Sc. thesis*, July 2013, École Centrale Marseille, Marseille, France.

[137] S. Long, M. A. Khalighi, M. Uysal, Z. Ghassemlooy, and S. Bourennane, "Performance analysis of serial-relay FSO links over Gamma-Gamma fading channels," Opticwise COST Action IC1101 Input Document, Oct. 2013, Newcastle upon Tyne, UK.

[138] Z. Ghassemlooy, H. Le Minh, S. Rajbhandari, J. Perez, and M. Ijaz, "Performance analysis of ethernet/fast-ethernet free space optical communications in a controlled weak turbulence condition," *IEEE/OSA Journal of Lightwave Technology*, vol. 30, no. 13, pp. 2188–2194, July 2012.

[139] F. Hanson and S. Radic, "High bandwidth underwater optical communication," *Applied Optics*, vol. 47, no. 2, pp. 277–283, Jan. 2008.

[140] *Ambalux High Bandwidth Underwater Transceivers*, http://www.ambalux.com/underwater-transceivers.html.

[141] *Sonardyne product: BlueComm Underwater Optical Modem*, http://www.sonardyne.com/products/all-products/instruments/1148-bluecomm-underwater-optical-modem.html.

[142] J. A. Simpson, B. L. Hughes, and J. F. Muth, "Smart transmitters and receivers for underwater free-space optical communication," *IEEE Journal on Selected Areas in Communications*, vol. 30, no. 5, pp. 964–974, June 2012.

[143] N.E. Farr, A.D. Bowen, J.D. Ware, C. Pontbriand, and M.A. Tivey, "An integrated, underwater optical/acoustic communications system," in *IEEE OCEANS Conference*, May. 2010, pp. 1–6, Sydney.

[144] B. Cochenour, L. Mullen, and J. Muth, "Temporal response of the underwater optical channel for high-bandwidth wireless laser communications," *IEEE Journal of Oceanic Engineering*, vol. 38, no. 4, pp. 730–742, Oct. 2013.

[145] M. Doniec, M. Angermann, and D. Rus, "An end-to-end signal strength model for underwater optical communications," *IEEE Journal of Oceanic Engineering*, vol. 38, no. 4, pp. 743–757, Oct. 2013.

[146] C.F. Bohren and D.R. Huffman, Eds., *Absorption and Scattering of Light by Small Particles*, Wiley-VCH, Apr. 2012.

[147] G. N. Plass and G. W. Kattawar, "Radiative transfer in an atmosphere-ocean system," *Applied Optics*, vol. 8, no. 2, pp. 455–466, Feb. 1969.

[148] C. Gabriel, M. A. Khalighi, S. Bourennane, P. Léon, and V. Rigaud, "Misalignment considerations on point-to-point underwater wireless optical links," *IEEE Oceans Conference*, June 2013, Bergen, Norway.

[149] C. Gabriel, M. A. Khalighi, S. Bourennane, P. Léon, and V. Rigaud, "Channel modeling for underwater optical communication," *IEEE Workshop on Optical Wireless Communications, Global Communication Conference*, pp. 833–837, Dec. 2011, Houston, TX.

[150] V.I. Haltrin, "Two-term Henyey-Greenstein light scattering phase function for seawater," in *IEEE International Geoscience and Remote Sensing Symposium (IGARSS)*, June-July 1999, vol. 2, pp. 1423–1425, Hamburg, Germany.

[151] V. Haltrin, "One-parameter two-term Henyey-Greenstein phase function for light scattering in seawater," *Applied Optics*, vol. 41, no. 6, pp. 1022–1028, Feb. 2002.

[152] C.D. Mobley, *Light and Water: Radiative Transfer in Natural Waters*, Academic Press, May 1994.

[153] C. Gabriel, *Channel Characterization and Performance Analysis for an Underwater Optical Transmission System*, Ph.D. thesis, École Centrale de Marseille, May 2013.

[154] C. Gabriel, M. A. Khalighi, S. Bourennane, P. Léon, and V. Rigaud, "Investigation of suitable modulation techniques for underwater wireless optical communication," in *International Workshop on Optical Wireless Communications (IWOW)*, Oct. 2012, pp. 1–3, Pisa, Italy.

[155] Z. Ghassemlooy, A. R. Hayes, N. L. Seed, and E. D. Kaluarachchi, "Digital pulse interval modulation for optical communications," *IEEE Communications Magazine*, vol. 36, no. 12, pp. 95–99, Dec. 1998.

[156] T. Komine and M. Nakagawa, "Fundamental analysis for visible-light communication system using LED lights," *IEEE Transactions on Consumer Electronics*, vol. 50, no. 1, pp. 100–107, Feb. 2004.

[157] D. K. Borah, A. C. Boucouvalas, C. C. Davis, S. Hranilovic, and K. Yiannopoulos, "A review of communication-oriented optical wireless systems," *EURASIP Journal on Wireless Communications and Networking*, vol. 2012:91, pp. 1–28, Mar. 2012.

[158] H. Elgala, R. Mesleh, and H. Haas, "Indoor optical wireless communication: Potential and state-of-the-art," *IEEE Communications Magazine*, vol. 49, no. 9, pp. 56–62, Sept. 2011.

[159] Z. Ghassemlooy, H. Le Minh, P. A. Haigh, and A. Burton, "Development of visible light communications: emerging technology and integration aspects," *Optics and Photonics Taiwan International Conference (OPTIC)*, Dec. 2012, Taipei, Taiwan.

[160] A. Jovicic, J. Li, and T. Richardson, "Visible light communication: opportunities, challenges and the path to market," *IEEE Communications Magazine*, vol. 51, no. 12, pp. 26–32, Dec. 2013.

[161] L. Grobe, A. Paraskevopoulos, J. Hilt, D. Schulz, F. Lassak, F. Hartlieb, C. Kottke, V. Jungnickel, and K.-D. Langer, "High-speed visible light communication systems," *IEEE Communications Magazine*, vol. 51, no. 12, pp. 60–66, Dec. 2013.

[162] J. Grubor, S. Randel, K.-D. D. Langer, and J.W. Walewski, "Broadband information broadcasting using LED-based interior lighting," *IEEE/OSA Journal of Lightwave Technology*, vol. 26, no. 24, pp. 3883–3892, Dec. 2008.

[163] S. Zhang, S. Watson, J. J. D. McKendry, D. Massoubre, A. Cogman, E. Gu, R. K. Henderson, A. E. Kelly, and M. D. Dawson, "1.5 Gbit/s multi-channel visible light communications using CMOS-controlled GaN-based LEDs," *Journal of Lightwave Technology*, vol. 31, no. 8, pp. 1211–1216, Apr. 2013.

[164] J. M. Kahn and J. R. Barry, "Wireless infrared communications," *Proceedings of the IEEE*, vol. 85, no. 2, pp. 265–298, Feb. 1997.

[165] L. Zeng, D. C. O'Brien, H. Le Minh, G. E. Faulkner, K. Lee, D. Jung, Y. J. Oh, and " E. T. Won, "High data rate multiple input multiple output (MIMO) optical wireless communications using white LED lighting," *IEEE Journal on Selected Areas in Communications*, vol. 27, no. 9, pp. 1654–1662, Dec. 2009.

[166] P. A. Haigh, Z. Ghassemlooy, and I. Papakonstantinou, "1.4 Mb/s white organic LED transmission system using discrete multi-tone modulation," *IEEE Photonics Technology Letters*, vol. 25, no. 6, pp. 615–618, Mar. 2013.

[167] P. A. Haigh, Z. Ghassemlooy, S. Rajbhandari, and I. Papakonstantinou, "Visible light communications using organic light emitting diodes," *IEEE Communications Magazine*, vol. 51, no. 8, pp. 148–154, Aug. 2013.

[168] J. B. Carruthers and P. Kannan, "Iterative site-based modeling for wireless infrared channels," *IEEE Transactions on Antennas and Propagation*, vol. 50, no. 5, pp. 759–765, May 2002.

[169] S. Long, M. A. Khalighi, M. Wolf, S. Bourennane, and Z. Ghassemlooy, "Channel characterization for indoor visible light communications," *IEEE International Workshop on Optical Wireless communications (IWOW)*, Sept. 2014, Madeira, Portugal, accepted.